Ministry of Science and Higher Education
Federal State Autonomus Educational Institution of Higher Education
Kazan Federal University (KFU)

A. Farhadian, M. A. Varfolomeev

ENVIRONMENTALLY FRIENDLY KINETIC GAS HYDRATE INHIBITORS FOR FLOW ASSURANCE APPLICATION

Study Guide

Kazan
2025

UDC 620.193.4

LBC 34.66 i73

A. Farhadian, M. A. Varfolomeev

Environmentally friendly kinetic gas hydrate inhibitors for flow assurance application: A Study Guide. A. Farhadian, M. A. Varfolomeev.; Ministry of Science and Higher Education. Kazan Federal University. Kazan: KFU Publishing, 2020. 103 p.

This book considers the issues related to the corrosion inhibition strategies for flow assurance in oil and gas transportation pipelines

This study guide is intended for students in master's program 21.04.01 – Petroleum Engineering, discipline "Flow assurance" and full-time bachelor's program 21.03.01 "Petroleum Engineering".

The book was developed and edited at the Department of Petroleum Engineering in collaboration with the PJSC Tatneft.

Printed by the resolution of the Editorial Advisory Board of Kazan Federal University.

Reviewed by:

Authors

Dr. Abdolreza Farhadian and Dr. Mikhail A. Varfolomeev
Department of Petroleum Engineering, Institute of Geology and Petroleum Technologies, Kazan Federal University

Contents

1. Introduction

The clathrate hydrate formation (gas hydrates), pipeline corrosion, scale formation, asphaltene and wax deposition, naphthenate, and carboxylate fouling are the main challenges in the oil and gas industry [104, 246]. Among them, the gas hydrate formation in the presence of light hydrocarbons, such as methane, ethane, and propane as well as non-hydrocarbon gases like hydrogen sulfide (H_2S) and carbon dioxide (CO_2) are considered a serious problem for flow assurance in the oil and gas pipelines because of their faster formation period [246].

Natural gas hydrates are crystalline compounds consisting of hydrogen-bonded molecules of water and hydrate-forming gases trapped in the water structure cavities [60, 185, 190]. Gas hydrates are non-stoichiometric substances and can potentially store a large amount of gases inside their cavities (up to 160-180 m^3 of gas can be accommodated in 1 m^3 of gas hydrate) [26, 49, 57, 63, 219, 223]. In addition, abundant natural methane sources significantly widens the challenges and opportunities connected to the sustainable energy supply and climate change problems [123]. Moreover, this problem is becoming increasingly important because the attention of many countries is focused now on the development of hydrocarbon resources in the Arctic, where natural conditions favour the gas hydrate formation [246]. Therefore, unforeseen costs for ensuring the stability of the flow, environmental risks, and large quantities of chemicals should be supplied to inhibit the hydrate formation process. Generally, low temperature, high pressure, presence of water, and hydrate former (mostly hydrocarbon gases) are critical conditions for gas hydrate formation [103, 125]. Besides, turbulent flow and crystallization centres (e.g., some defects in the pipelines, sand particles, and mud particles) can increase the chance of hydrate formation. Hence, when these conditions are met in the oil and gas pipelines, gas hydrates can form a plug in the multiphase flow, which blocks the flow in the pipe and lead to serious technical and environmental issues [188].

Currently, there are several ways to manage hydrate formation risk, but none of them is ideal. These include depressurization of the pipe after forming the gas

hydrate, increasing the temperature, dehydration of pipelines, altering the gas phase with another gas, and utilizing the gas hydrate inhibitors [52, 106, 160, 188]. The use of inhibitors has been considered the most effective method in recent years, which can change the thermodynamic equilibrium, delay the formation of first hydrate particles, and decrease the rate of hydrate formation [50, 58, 59, 61, 125, 180, 259, 307]. Gas hydrate inhibitors are classified into thermodynamic hydrates inhibitors (THIs) and low-dosage hydrate inhibitors (LDHIs), depending on their mechanism of action [41, 62, 109, 305]. THIs shifts the phase equilibrium conditions toward the zones of higher pressure and/or lower temperatures [69, 112, 152, 228]. There is a wide range of THIs, but methanol and monoethylene glycol are the most popular in the petroleum industry [104]. The minimum concentration of THIs to reduce the risk of hydrate formation could be as high as 20-50 wt % of the water mass which makes the costs for exploitation of the pipelines sufficiently expensive operation [172]. Besides, storage equipment is required to store a large amount of methanol or ethylene glycol on the site, adversely affecting the quality of transported oil (in gas-rich oil pipelines) [104]. Furthermore, methanol is a highly toxic substance, therefore is environmentally dangerous because its solubility in water is high and it can pollute big areas in case of spills [52, 104]. Another drawback of the THIs usage is their incompatibility with the corrosion inhibitors. It has been reported that methanol significantly reduces the inhibition efficiency of corrosion inhibitors during their co-injection into the pipelines [21, 58, 124]. The natural conditions would be more favorable for the gas hydrate formation; hence the utilization of these chemicals is becoming more difficult. Therefore, implementing LDHIs, which could be efficient at lower concentrations (0.5-3 wt %), has received much attention in recent years due to environmental concerns and economic calculations [260, 284].

LDHIs are two classes of chemicals, kinetic hydrate inhibitors (KHIs) and anti-agglomerants (AAs) [40, 150, 306, 308]. KHIs are mostly amphiphilic polymers that contain amide groups and short alkyl chains [97, 107, 188]. KHIs do not affect the equilibrium conditions of hydrate formation, but they can delay the nucleation

process of gas hydrates and decrease the hydrate growth rate [127, 145, 178, 311]. Polymers based on N-vinylpyrrolidone (VP), N-isopropylmethacrylamide (NIPMAm) or N-vinyl caprolactam (VCap) monomers, and hyperbranched poly(ester amide)s (HPEAs) are examples of commercial KHIs [108, 262, 284, 294]. AAs, such as quaternary ammonium and phosphonium salts, are generally surfactants that allow stable water-in-oil emulsions to be formed [310]. AAs do not prevent hydrate formation, but they inhibit the aggregation of the formed hydrate particles [43, 146, 236, 237]. The mechanism of AAs performance is based on reducing the chances of hydrate particles to interact with each other and minimizing of aggregation forces; therefore, hydrates can be transported as a slurry in an oil phase [85, 177, 283]. It is worth to mention that AAs can be used at a wider range of subcooling temperature and some of them can also demonstrate kinetic inhibitory activity [104]. The main drawback of AAs is their poor performance if the water cut reaches 50 % or higher [52].

However, the vast majority of KHIs and AAs show poor biodegradability [97]. In recent years, scientists have made great efforts to develop greener KHIs due to strict environmental regulations [51, 53, 105]. Ionic liquids, carbohydrate polymers, vegetable oils, amino acids, protein, and peptides are the main natural resources used to synthesize biodegradable KHIs [105, 263]. This study reviews recent developments in bio-based KHIs that showed acceptable efficiency. An in-depth description of the structural properties of KHIs, experiment conditions, and the main findings are presented. It should be mentioned that some natural resources, such as amino acids and ionic liquids, show significant THI activity in gas hydrate formation, which were also discussed.

2. Carbohydrate polymers

Carbohydrate polymers (CPs) as products of biochemical processes in living organisms have been used for various applications such as drug delivery, binders, coatings, and corrosion inhibitors [229]. They are the most abundant natural

compounds on earth and monosaccharides (e.g., glucose and fructose) are their building blocks. Cellulose, chitin, chitosan, starch, hyaluronic acid, dextrin and cyclodextrin, and various gums are the most common CPs in nature. CPs are chemically stable, biodegradable, and relatively high molecular mass macromolecules with several functional groups, such as amine, hydroxyl, cyclic rings, and carboxylic acid. Recently, hydrate scientists have developed natural gas hydrate inhibitors based on cellulose, chitosan, starch, and pectin as the conventional KHIs are toxic in nature [190, 297]. The idea of using natural compounds to synthesize gas hydrate inhibitors is that their functional groups significantly interact with water found in gas hydrate and free water in the system.

Sloan et al. [247] reported the first application of hydroxyethyl cellulose (HEC) as a low toxic and environmentally friendly additive for preventing gas hydrate formation. They revealed that six-membered and five-membered cyclic chemical rings in the HEC structure affected the hydrate inhibition process. They claimed a combination of poly(N-vinyl-2-pyrrolidone) and HEC showed reasonable inhibition efficiency. Lee et al. [42] investigated the potential of several cationic starches, namely tapioca, Raisabond, Raisamyl, and Raifix starches as KHIs for methane-ethane, methane-propane, and methane (CH_4) hydrates. All samples exhibited a poor inhibition effect except tapioca starch which delayed the induction time by order of magnitude. Moreover, they showed that the performance of all starches improved by adding 0.0025 wt % of polyethylene oxide (PEO). Besides, the memory effect was suppressed in the solution containing tapioca starch and PEO. They suggested that the inhibition mechanism of starch is similar to the hydrophilic pendant lactam group by fitting its anhydroglucose unit into the hydrate structure. On the other hand, due to the hydrophilic nature of cationic starches, they have a remarkable capacity to make hydrogen bonds with water molecules to disrupt the hydrate formation process. The uncertainties of pressure and temperature measurements were 0.07 MPa and 0.1 ºC, respectively. A new hydrate inhibitor was proposed based on a combination of PEO and cationic starch (from a high amylose

carbohydrate source) by Kannan et al [100]. Chemical structure of cationic starch is shown in Fig. 1. The inhibitor significantly prevented the formation of gas hydrate and retarded the induction time beyond 20 h at 0.1 wt %. They showed that the inhibitor impedes nucleation of hydrates, delays induction time, eliminates memory effect, and works as antifreeze. They suggested that cationic starch can be used as an inexpensive and environment-friendly inhibitor owing to its abundant availability and simple preparation method.

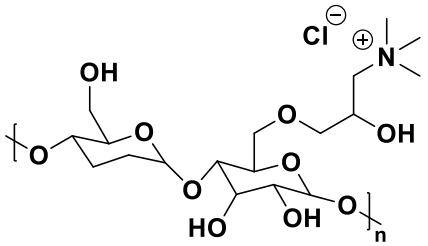

Fig. 1. Chemical structure of cationic starch [3]

For the first time, Xu et al. [290] reported chitosan as KHI to inhibit methane and methane-ethane gas hydrates. Molecular structure of chitosan is displayed in Fig. 2. They showed that the degree of deacetylation (DD) increases the induction time. However, no significant effect was observed in the degree of deacetylation above 80%. In addition, the molecular weight of chitosan and the addition of PEO had a small effect on the induction time. The best inhibition performance of chitosan was obtained at 0.6 wt %. Although the main inhibition effect of chitosan was on the nucleation step, it also lowered the crystal growth rate of hydrates. They suggested that inhibitory activity of chitosan might be related to the hydrophilic nature and the anhydroglucose unit of chitosan. The uncertainty of temperature measurements was 0.1 ºC.

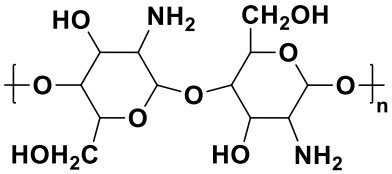

Fig. 2. Chemical structure of chitosan [3]

Li et al. [142] developed a series of green KHIs with different hydrophobicity based on carboxymethyl chitosan and chitosan to investigate the relationship between the molecular structures of the inhibitors and their inhibition efficiency. They showed that KHIs based on chitosan worked better than carboxymethyl chitosan in inhibiting CH_4 hydrate formation with the same functional groups. In addition, the long-branched chains with hydrophobic functional groups were conducive to improve the inhibitory activity of KHIs. They showed that the interfacial resistance of CH_4 molecules was enhanced in presence of chitosan derivatives, decreasing the rate of gas dissolution and retarding the induction time of hydrate formation. The uncertainties of temperature and pressure measurements were 0.1 ºC and 0.01 MPa, respectively. Yánez et al. evaluated *mango* seed extract pectin (*Mangifera indica*) as a green compound to prevent tetrahydrofuran (THF) hydrate using a conductivity technique [292]. Their results revealed that 0.2 wt % of the mango seed extract could provide an inhibition efficiency equal to 20% v/v of methanol. Ivall [92] investigated the inhibition effect of four natural polysaccharides based on the xylomannan sugar found in the Alaskan beetle *Upis ceramboides* on CH_4 hydrate nucleation and growth kinetics. The proposed disaccharide core structure of the xylomannan is depicted in Fig. 3. The results showed that all polysaccharides have poor inhibition power on hydrate nucleation and growth. It has been suggested that low solubility and lack of active functional groups in hydrate inhibition are two main reasons for their weak efficiency. Therefore, it can be concluded that using natural polysaccharides as hydrate inhibitors in pure form is limited, and significant modification is needed to improve their solubilization and inhibition performance.

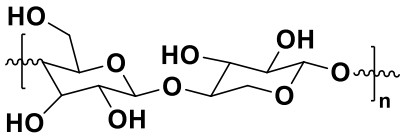

Fig. 3. Chemical structure of xylomannan sugar [3]

Talaghat [256] studied the inhibition activity of modified starch (oxidized starch) as a KHI using a recirculation flow loop filled with a mixture of methane, propane, iso-butane, and carbon dioxide. The results indicated that the modified starch showed higher efficiency than polyvinylpyrrolidone (PVP) as it considerably delayed the induction time at 2 ºC and 4 MPa compared to commercial KHI. The uncertainties of pressure and temperature measurements were 0.05 MPa and 0.1 ºC, respectively. Talaghat [257] also investigated the synergy effect of polypropylene oxide (PPO) and ethylene oxide (PEO) on the inhibition performance of modified starch. Both PEO and PPO enhanced the efficiency of starch; however, the synergism effect of PPO was more pronounced. Jokandan et al. [95] studied the synergy effect of hydroxyethyl cellulose (HEC) on the inhibition performance of PVP for CH_4 hydrate. The molecular structure of HEC is shown in Fig. 4. They observed that adding 0.25 wt % of HEC to the PVP solution improved the inhibition efficiency of the inhibitor so that the induction time was increased 8 times compared to the pure PVP system. The rate of CH_4 hydrate formation also was lowered from 45.28×10^4 (MPa/sec) in the PVP solution to 30.28×10^4 (MPa/sec) in the HEC+PVP solution. The uncertainties of pressure and temperature measurements were 0.05 MPa and 0.1 ºC, respectively.

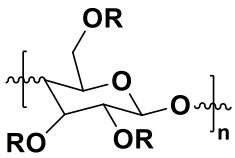

R = H or CH_2CH_2OH

Fig. 4. Chemical structure of HEC [3]

Xu et al. [287] reported a molecular dynamics (MD) simulation study to evaluate CH_4 hydrate growth in a solution containing different concentrations of pectin. The chemical structure of pectin is represented in Fig. 5. Their results implied that pectin has good efficiency and showed higher inhibition effect on CH_4 hydrate growth. Pectin can disturb the growth of hydrate crystals by creating new hydrogen

bonds between its oxygen atoms and hydroxyl groups with hydrogen-oxygen atoms of water, respectively (Fig. 6). Indeed, active groups of pectin have both proton donor and electron acceptor roles. Therefore, it shows a good inhibition effect on the growth of CH_4 hydrate.

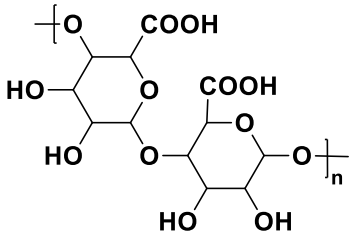

Fig. 5. Chemical structure of pectin [3]

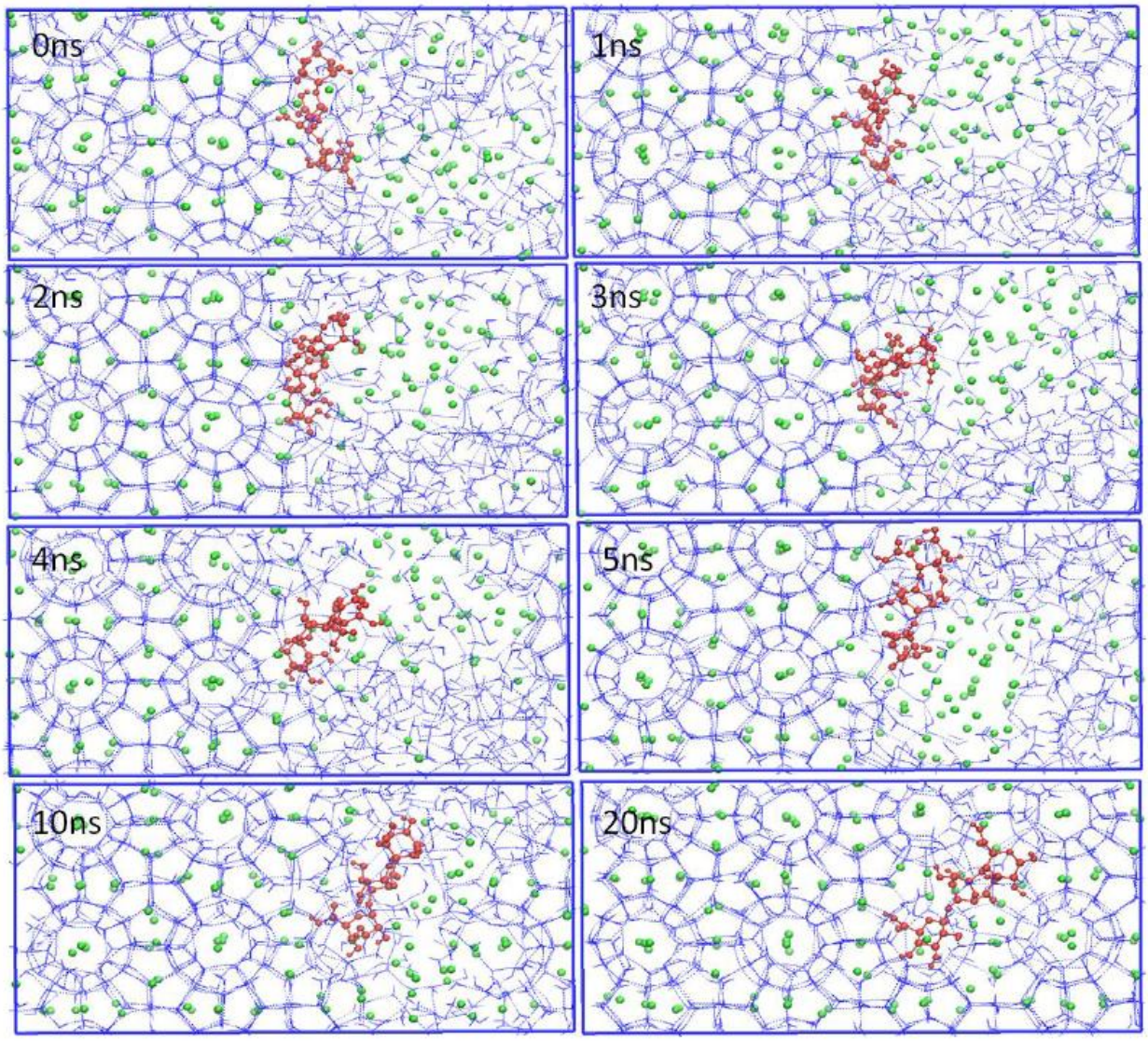

Fig. 6. Snapshot configurations of 3.62 wt % pectin at the liquid-solid interface system at 0, 1, 2, 3, 4, 5, 10, 20 ns [287]

Xu et al. [288] experimentally showed that pectin could be considered a novel eco-friendly KHI to hinder CH_4 hydrate. They used standard induction time and crystal growth inhibition (CGI) techniques to assess the inhibition power of pectin. Their results revealed that pectin effectively inhibited CH_4 hydrate formation at high subcooling temperatures (12.5 ºC), and it significantly lowered the hydrate crystal growth. Moreover, the maximum growth rate of 2.0%/h in presence of pectin was lesser than that of PVCap (5.5%/h) at the same concentration. They suggested that such excellent inhibition efficiency of pectin can be related to its ability to form new hydrogen bonding with water molecules by its carbonyl and oxygen atoms, disrupting the water structure and formation of hydrate cages. Furthermore, pectin can retard hydrate crystal growth by binding its oxygen atoms to the surface of the hydrate crystal. In addition, the results of the biodegradability study confirmed that pectin could be classified as highly biodegradable KHI. Effendi et al. [45] also reported that high-methoxylated pectin worked slightly better than PVCap at 1 wt %. Low-methoxylated pectin offered inhibition efficiency up to three times higher than that of PVCap at 0.5 wt %. In another study, the synergistic effect of pectin, guar gum, and k-carrageenan was assessed on the inhibition efficiency of Luvicap55w, PVCap, PVP, and HIOP for CH_4 hydrate formation by Singh et al [242]. All polysaccharides worked as good synergists with the studied KHIs. The best inhibition synergy was observed for K-carrageenan with all KHIs at 0.25 wt %, which increased induction time by 20−35% and lowered the rate of hydrate growth up to 90%. The main synergistic effect of guar gum was on hydrate growth rates, which reduced by 77-90% for all KHIs. A good synergistic effect of pectin was reported with HIOP, increasing its induction time by 45%. The uncertainties of pressure and temperature measurements were 0.1 MPa and 0.5 ºC, respectively. However, the results of a study by Abrahamsen et al. [1] indicated that pectin citrus and HEC are not good KHIs for both CH_4 and natural gas systems. They used a constant cooling protocol and steel rocking cells to evaluate the inhibition performance of the inhibitors. According to their findings, HEC showed poor KHI

activity even in combination with PVP and polyacrylamide (PAM). In another study, Kelland [105] investigated the inhibition effect of extracted pectin from seeds and mango skins on THF hydrate, CH_4 hydrate, and natural gas hydrate. The results revealed that pectin had no significant inhibition effect in all systems. One possible reason for such dramatic differences in studies of natural polymers as KHI might be related to their different sources, containing other components. To address this issue, Roosta et al. [211] modified HEC and starch and evaluated their effect on the hydrate growth rate of methane-propane hydrate. They prepared a series of modified starches and HECs with acrylamide through graft copolymerization and functionalization. Their results indicated that all samples which were synthesized by ammonium persulfate and ceric ammonium nitrate had inhibition effects on the hydrate growth rate. However, all polymers were synthesized in presence of a mixture of sodium bisulfite and ammonium persulfate and the functionalized samples acted as hydrate promoters in the system. The uncertainties of pressure and temperature measurements were 0.01 MPa and 0.1 ºC, respectively. The inhibition properties of carboxymethylcellulose sodium salt were assessed under a quasi-equilibrium thermodynamic condition by Ishmuratov et al [91]. The results releveled that carboxymethylcellulose sodium salt can be used as an effective inhibitor for gas hydrate formation at low concentrations. They showed that the inhibitor lowers the rate and alters the gas hydrate formation conditions, implying it can work as THI and KHI simultaneously with an efficiency 300 times more than methanol at the same concentration. Wan et al. [279] assessed the inhibition efficiency of several natural polymers, namely starch, gum Arabic, guar gum, sodium alginate, and carboxymethyl chitosan in a methane-water medium using a high-pressure stainless steel cell. The chemical structure of the polysaccharides is depicted in Fig. 7. All carbohydrate polymers improved the subcooling temperature of hydrate formation and prevented hydrate growth. Guar gum showed the best performance among the polysaccharides, and sodium alginate was ranked second. It was proposed that the presence of the side anhydroglucose group in the structure of guar gum has the main

effect on its efficiency. Carboxymethyl chitosan and starch also showed relatively good inhibition performance. However, gum Arabic had poor hydrate inhibition at low subcooling and even enhanced hydrate formation when the subcooling was raised to 6 ºC. The uncertainties of pressure and temperature measurements were 0.02 MPa and 0.01 ºC, respectively.

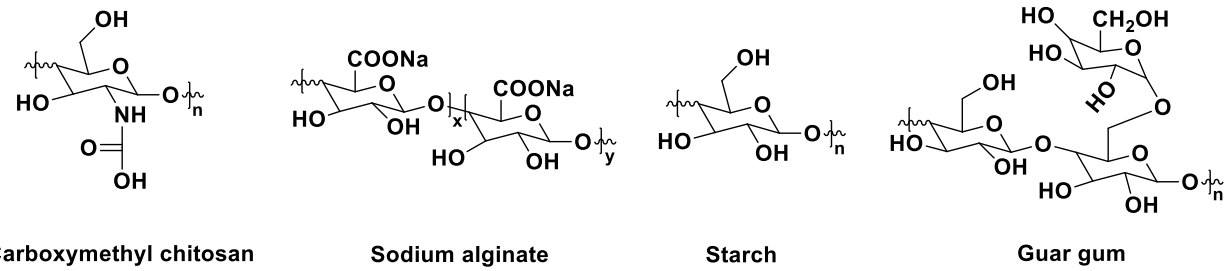

Fig. 7. Molecular structure of carboxymethyl chitosan, sodium alginate, starch, and guar gum [3]

They suggested that the anhydroglucose unit of the natural polymers can bind to the open cavities of the hydrate structure in a similar manner to the lactam groups of PVCap, which hinder the entry of gas molecules into the cavities and thus inhibits further growth of hydrate crystals as shown in Fig. 8. Moreover, the side chain of the polysaccharides can strongly affect their inhibition power. The side anhydroglucose group of guar gum improves its adsorption on the hydrate crystals, showing the best performance among the carbohydrate polymers. Fakhreeva et al. [48] introduced carboxymethylcellulose sodium salt (Na-CMC) as an effective additive to prevent natural gas hydrate formation (Fig. 9). Na-CMC changed the hydrate formation conditions, indicating that it has properties of a thermodynamic inhibitor with efficiency 350 times more than methanol. They also investigated the effect of the molecular weight of Na-CMC (90, 250, and 700 kDa) on the hydrate formation process. They found that the inhibitor with a molecular weight of 90 kDa showed the best performance at concentrations of 0.005, 0.01 and 0.05 wt %. They proposed that the hydrogen bonds and electrostatic interaction of sodium cations and carboxylate ions of Na-CMC with water molecules are responsible for the inhibition properties of Na-CMC.

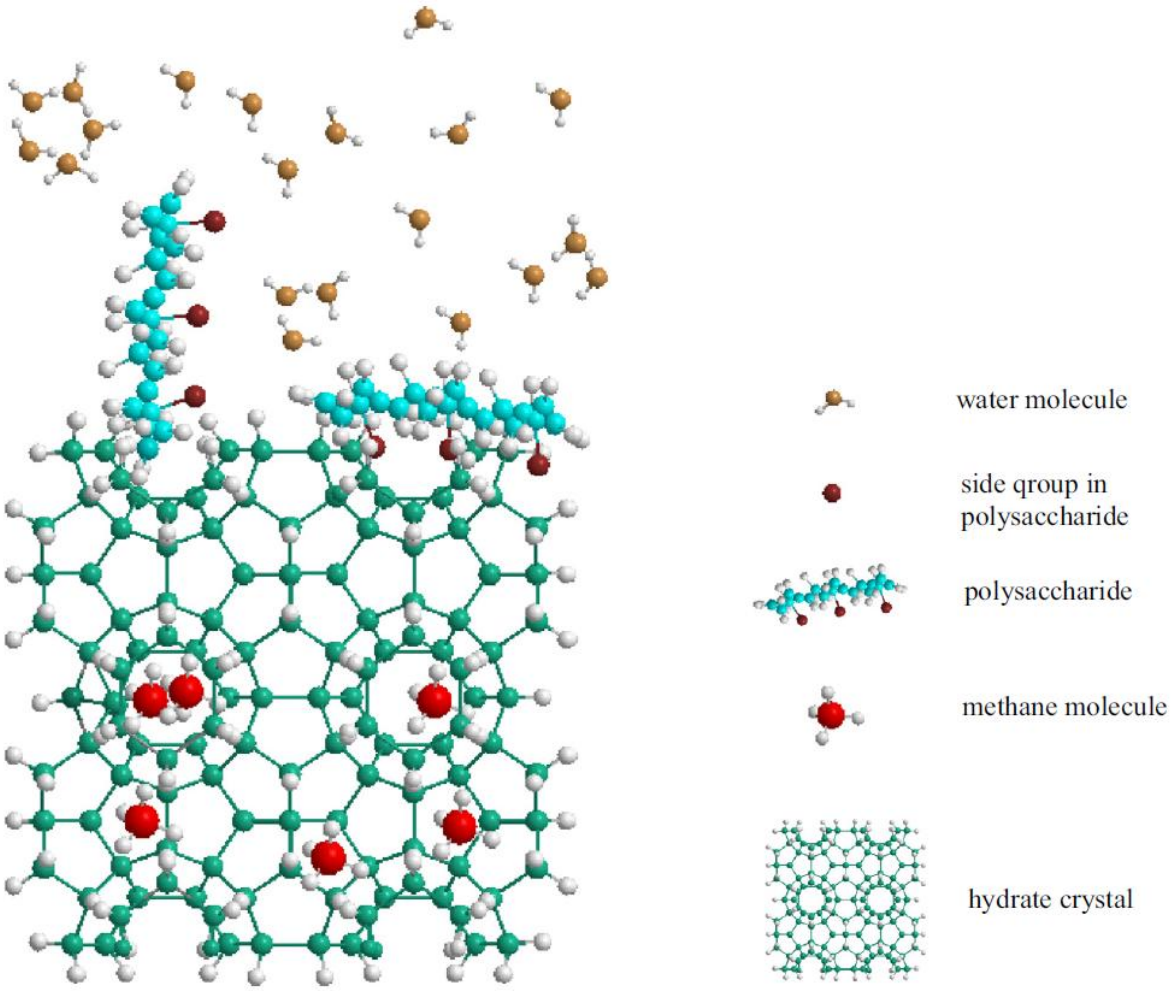

Fig. 8. Schematic of the possible mechanism for inhibition of hydrate growth in the presence of polysaccharides [279]

Yaqub et al. [296] assessed the kinetic inhibition efficiency of several biopolymers (Tapioca starch, dextran, xanthan gum, pectin, and sodium-carboxymethyl cellulose (Na-CMC) on CH_4 hydrate formation at 9.5 MPa and 9-12 ºC subcooling temperatures. Their findings implied that 0.5 wt % of biopolymers effectively inhibited CH_4 hydrate formation. Pectin and Na-CMC showed the best kinetic inhibition among all samples since they retarded the induction time for 78 and 61 minutes, respectively. In addition, Na-CMC, Tapioca starch, and pectin considerably decreased hydrate formation rate and CH_4 consumption. Besides, the interaction energy obtained using the Screening Model for Real Solvents indicated that attractive interactions between water molecules and biopolymers led to prolonging of induction time. Moreover, hydrogen bonding energies were predicted

by the model and showed that the hydroxyl groups of biopolymers create hydrogen bonds with a water molecule, which disrupted the hydrate cage and hindered hydrate formation and growth. A high hydrogen bonding energy (-20 kcal/mol) with maximum induction time was reported for pectin. Furthermore, biopolymers reduced the interfacial properties between aqueous solutions and methane gas. The lowest air-liquid interfacial tension and highest zeta potential is required for excellent inhibition of gas hydrate in the presence of biopolymer-based KHIs. The uncertainties of pressure and temperature measurements were 0.15 MPa and 0.01 ºC, respectively. In another investigation, Shen et al. [234] assessed inhibitory performance of Na-CMC on CO_2 hydrate using an isochoric and isothermal method to measure the mass transfer characteristics of the system. Their results revealed that CMC-Na considerably reduced the formed hydrate at 1 wt %. The performance of CMC-Na was strongly dependent on its concentration so that its KHI activity completely lost at 0.1 wt % or lower concentrations. Moreover, they suggested that mass transfer resistance played a critical role in the inhibition mechanism of CMC-Na. The inhibitor provided the slowest mass transfer rate of CO_2 hydrate compared to PVP and pure water.

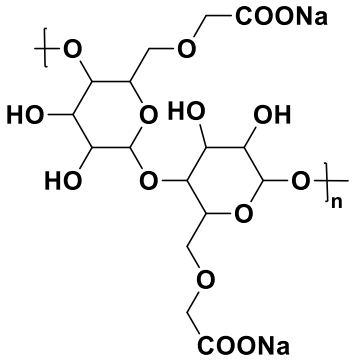

Fig. 9. Molecular structure of Na-CMC [3]

Novel KHIs were developed based on Arabic and guar gums to mitigate CH_4 hydrate formation by Mollashahi Sanatgar et al [225]. The results indicated that guar gum was more efficient than Arabic gum at concentrations lower than 0.05 wt %. The induction time was increased from 28.8 minutes in the blank system to 42.7

minutes in the presence of guar gum. It also raised the total time of gas uptake from 6.48 h in uninhibited solution to 17.6 h in the inhibited system. The uncertainties of pressure and temperature measurements were 0.5 MPa and 0.3 ºC, respectively. Gupta et al. [75] studied the kinetics of formation and dissociation of CH_4 hydrate in presence of guar and xanthan gums. They observed that concentration and molecular weight of polysaccharides played a significant role in gas consumption. Xanthan and guar gums with 640 kDa and 1700 kDa molecular weight also worked well as KHIs at 0.05 wt %. Natural polymers with low molecular weight did not provide better hydrate inhibition than their higher molecular weight. Carbohydrate polymers at higher concentrations were effective in lowering gas consumption and the hydrate growth rate due to improvements in heat and mass transfer limitation because of increment in the concentration of polymer and the adsorption of inhibitor molecules onto the hydrate surface. In addition, the inhibitors effectively delayed the release of gas and retarded the hydrate dissociation process. The uncertainties of pressure and temperature measurements were 0.005 MPa and 0.05 ºC, respectively. Yaqub et al. [295] evaluated KHI and THI effects of pectin, dextran, tapioca starch, and sodium carboxymethyl cellulose on CO_2 hydrates. They observed that dextran provided a maximum thermodynamic promotion effect with an average temperature of 0.36 ºC. Sodium carboxymethyl cellulose and pectin retarded nucleation of CO_2 hydrate for 181 and 423 minutes, respectively. Moreover, sodium carboxymethyl cellulose and pectin decreased the rate of hydrate formation by 32% and 13%, respectively. In addition, they found that a lesser mole of gas was consumed in presence of the larger carbohydrate polymers. Besides, pectin was more efficient than PVP in increasing induction time. However, the rate and mole consumption of the gas hydrate was much lower in the PVP system compared to the studied natural polymers. In another study, Liu et al. [145] evaluated the inhibition activity of apple pectin on gas hydrate formation, growth, and blockage using a fully visual rocking cell. For sII hydrate, a solution containing 0.2 wt % apple pectin showed a similar inhibition effect to that of PVCap; however, its inhibition performance decreased at high concentration due

to its low solubility. Apple pectin retarded gas hydrate formation, but it did not reduce the final conversion of water to hydrates. Farhadian et al. [54] introduced the first dual-function inhibitor based on sulfonated chitosan (SCS) to prevent gas hydrate and corrosion inside the oil and gas pipelines. The chemical structure of SCS is shown in Fig. 10. Low and medium molecular weight SCSs increased the induction time from 2 minutes in a pure water system to 14.3 and 9.6 minutes, respectively. The results of high-pressure micro differential scanning calorimetry (HP-μDSC) experiments indicated that the amount of CH_4 hydrate formed in SCS solutions was much lower than the blank solution. SCSs showed no cloud point up to 100 ºC in 0.5 wt % solutions in deionized water. In addition, weight loss measurements as a standard corrosion test indicated that low molecular weight SCS inhibited mild steel corrosion in the 2M HCl solution by 95.6 % protection at 0.5 wt %. Besides, SCS improved polarization resistance and reduced corrosion current density of the steel. The uncertainties of pressure and temperature measurements were 0.005 MPa and 0.1 ºC, respectively.

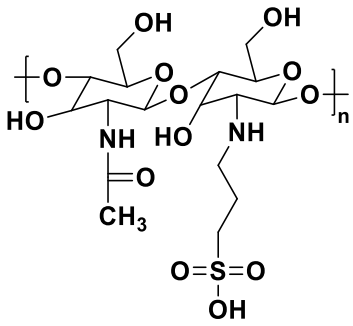

Fig. 10. Molecular structure of SCS [3]

Chitosan-*graft*-polyacrylamide (CS-*g*-PAM) was developed as a novel eco-friendly and high-cloud point KHI to inhibit CH_4 hydrate formation by Farhadian et al [56]. The chemical structure of CS-*g*-PAM is depicted in Fig. 11. No cloud point was observed in both 3.5 wt % NaCl solution and deionized water containing 1 wt % of CS-*g*-PAM up to 100 ºC. According to high-pressure autoclave tests, CS-*g*-PAM increased 13 times the nucleation time of CH_4 hydrate (in 1 wt % sample) in comparison with pure water. Furthermore, the results of HP-μDSC experiments

signified that adding 1 wt % CS-*g*-PAM decreased the onset temperature of the hydrate formation from -12.7 ºC in blank solution to -19.0 ºC. Moreover, a viscous foam-like slurry was obtained in presence of the inhibitor that can easily flow inside the pipelines. The uncertainties of pressure and temperature measurements were 0.005 MPa and 0.1 ºC, respectively.

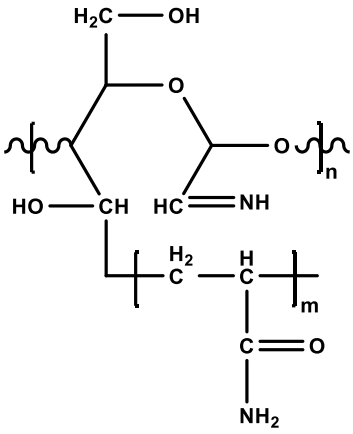

Fig. 11. Molecular structure of CS-*g*-PAM [3]

Fu et al. [66] investigated CH_4 hydrate formation in a water-continuous vertical flow loop in presence of xanthan gum. They suggested that the mass transfer phenomenon controls gas hydrate formation. Xanthan gum concentration and the flow velocity had the main effect on CH_4 hydrate formation, while the effect of subcooling temperature was smaller. Their results denoted that the higher flow velocity accelerates CH_4 hydrate formation in drilling fluid, but increasing the concentration of xanthan gum inhibits the hydrate formation. Shao et al. [230] studied the effects of modified cellulose on the decomposition of CH_4 hydrate experimentally and theoretically. They used aminosilane with different chain lengths as coupling agents to prepare modified cellulose. Their results showed that the inhibitor delayed the dissociation time from 6.8 h to 10 h, and the average dissociation rate was decreased. The MD simulations revealed that the aminosilane chain worked as an adsorption group. In addition, fewer number of intramolecular hydrogen bonds were observed for modified cellulose compared to pure cellulose, which improves the potential of the modified inhibitor for adsorption to the hydrate

surface. Besides, the amino groups strongly interacted with CH_4 hydrate and restricted the free movement of the cellulose chain. Hence, the introduction of amino functional groups to the cellulose structure increased its adsorption capacity on the gas hydrate surface, and improved the inhibition efficiency of the inhibitor. Silva et al. [239] reported sodium alginate (Fig. 12) as a new biodegradable KHI to prevent CH_4 hydrate formation. Alginate is a carbohydrate polymer derived from the brown seaweed *Phaeophyceae* and is produced by some bacteria, such as *Azotobacter* and *Pseudomonas*. They showed that sodium alginate had the best performance as KHI at concentrations of 0.1% (wt/vol). Furthermore, the results revealed that an acidic pH was favorable for the efficiency of the inhibitor because the inhibition power influenced by the degree of protonation of sodium alginate. Their results demonstrated that the inhibitory activity of sodium alginate dropped by increasing its concentration due to the precipitation of the inhibitor.

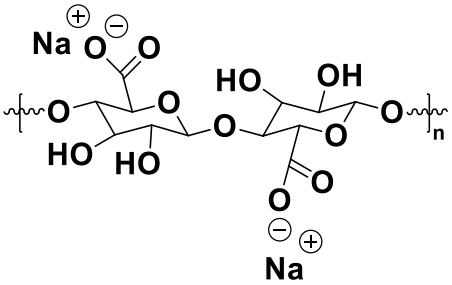

Fig. 12. Molecular structure of sodium alginate [3]

Chigozirim et. al [27] investigated the inhibition potential of starch from Manihot Esculenta on natural gas hydrate formation using the Aspen HYSYS process simulator. Their results showed that starch prevented the formation of gas hydrates at 0.05, 0.1, 0.15, and 0.2 mole fractions, and its optimum concentration was 0.2 mole fraction. The inhibition effect of arabinogalactan, dextran, and sodium salt of carboxymethylcellulose on the thermobaric conditions of natural gas hydrate formation was studied by Dokichev et al [270]. Arabinogalactan is a complex branched polysaccharide containing β-(1→3)-D-galactan backbone with a certain amount of branch points. They found that the investigated polysaccharides can be

considered effective inhibitors for gas hydrate formation at low concentrations (0.005-0.008 wt %). The polysaccharides decreased the rate and changed the conditions of gas hydrate formation, indicating their thermodynamic and kinetic inhibition properties exceeding methanol. Effendi et al. [46] developed polysaccharides from *Tamarindus indica L. polysaccharide* (TSP) as natural KHI in a high subcooling environment. TSP is a highly branched, hydrophilic, and mucoadhesive polysaccharide and contain a high methoxyl content. The KHI activity of TSP was assessed using HP-μDSC at 5 MPa with a subcooling degree of 17.5 ºC. The solubility of TSP increased at high temperatures, which makes a good KHI to inject into hot fluids. Their results showed that the optimum concentration of TSP to effective prevention of gas hydrate formation is 0.25 wt %. The uncertainty of pressure measurements was 0.1 MPa. Zhang et al. [309] synthesized four green KHIs based on chitosan and carboxymethyl chitosan inhibit CH_4 hydrate formation. The molecular structure of the synthesized inhibitors is displayed in Fig. 13.

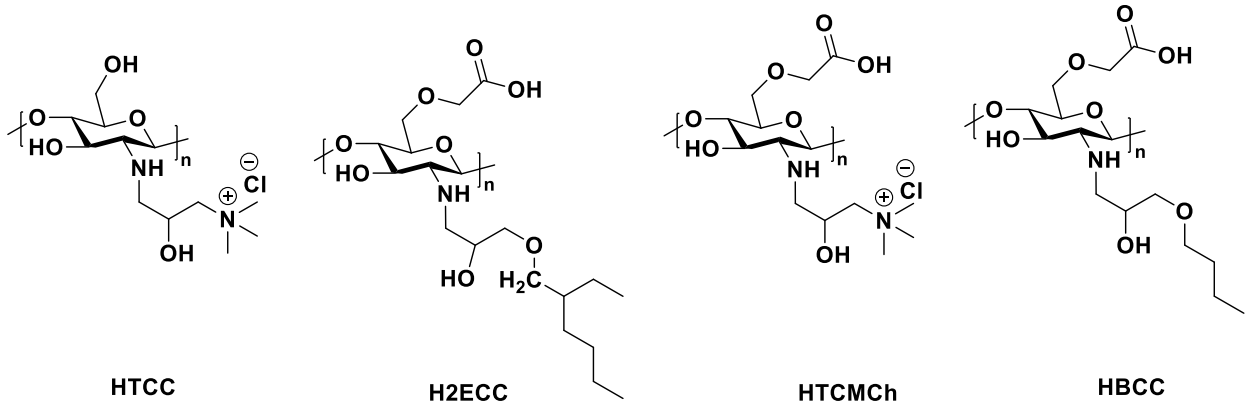

Fig. 13. Molecular structure of various chitosan derivatives [3]

They reported that the hydrophobicity of the inhibitors positively affects their inhibition performance. The effect of methyl groups on the inhibitory activity of the inhibitors was more significant than the length of alkyl groups. The incorporation of N-2-hydroxypropyl-3-isooctyl ether and hydroxypropyl-3-trimethylamine groups into the structure of carboxymethyl chitosan improved its inhibition efficiency. Additionally, the nucleation and growth of CH_4 hydrate were further inhibited in the presence of trimethyl quaternary ammonium group as it raised the ion content of the

solution. In another research, some natural polymers derived from stevia, table sugar, and fruit peels were studied as KHIs by Idress et al [88]. Only sugar showed KHI activity as it increased the induction time of CH_4 hydrate formation from 75 minutes for pure water at 5 MPa to 82 minutes. The uncertainty of pressure measurements was 0.1 MPa. In addition to polysaccharide-based KHIs, literature shows that there are some effective saccharide-additives as KHIs and synergists for gas hydrate inhibitors. For example, Xu et al. [291] reported D-sorbitol as a promising THI for CO_2 and CH_4 hydrate. Fig. 14 shows the molecular structure of D-sorbitol. Thermodynamic inhibition ability of D-sorbitol was assessed based on hydrate dissociation enthalpies (ΔH_{diss}) and equilibrium pressure change (ΔP). They demonstrated that D-sorbitol could be considered an efficient THI as it increased the gas-liquid-hydrate equilibrium (GLHE) pressure in both CH_4 and CO_2 systems. According to ΔP data, D-sorbitol increased the GLHE pressure by 11.6, 25.0, 41.4% for CH_4 hydrate and 10.1, 18.6, 32.7% CO_2 hydrate at concentrations of 1.00, 2.00, 3.00 (mol%), respectively, compared to pure water. Moreover, no participation of D-sorbitol in the hydrate crystal structure was observed in accordance with ΔH_{diss} data. The inhibitor changed the activity of water in the solution through the hydrogen bond action. Therefore, the GLHE condition of gas hydrates was influenced. The uncertainties of pressure and temperature measurements were 0.01 MPa and 0.01 ºC, respectively.

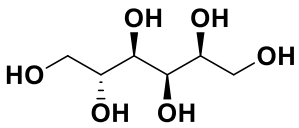

Fig. 14. Molecular structure of D-sorbitol [3]

Farhadian et al. [55] developed novel dual-function synergists based on sucrose and glucose to inhibit corrosion and gas hydrate formation. Fig. 15 represents the molecular structure of sucrose-based (SBS) and glucose-based (GBS) synergists. They reported a modification method for simple carbohydrates by incorporating carboxyl and sulfonate groups into their structures, which can be

applied to prepare effective dual-function inhibitors. The results demonstrated that mixtures of the SBA and GBS with Luvicap EG and Luvicap 55W showed a considerable synergy effect. The onset temperature of hydrate formation was reduced by 3.5 ºC in the presence of 0.1 wt % of synergist and 0.5 wt % of commercial KHIs. Furthermore, SBA and GBS effectively suppressed pipeline steel corrosion in 2M HCl solution by 91% and 88% protection at 0.5 wt %, respectively.

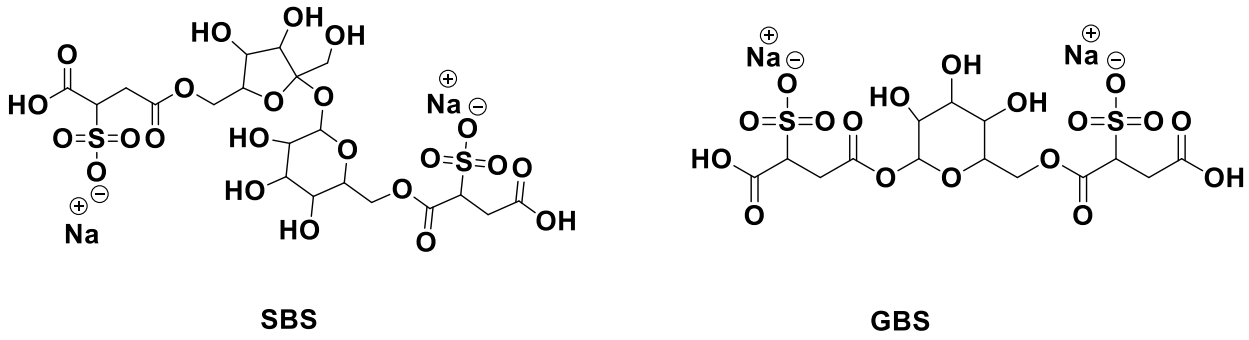

Fig. 15. Molecular structure of SBS and GBS [3]

2.1. Mechanism action of carbohydrate polymers

Carbohydrate polymers contain hydrophilic and hydrophobic functional groups that interact strongly with water to inhibit gas hydrate plugging in pipelines. Their performance depends on active functional groups—hydroxyl, amine, amide, and carboxylic acid—which form hydrogen bonds with water to disrupt water structure and bind to hydrate crystal surfaces, inhibiting nucleation and growth. The anhydroglucose units fill empty hydrate cavities similar to PVCap's lactam ring, while hydroxyl groups facilitate water-polysaccharide interactions. This prevents gas hydrate formers from entering the hydrate structure, suppressing crystal growth and reducing gas consumption. The inhibition effectiveness is significantly influenced by different side chains.

2.2. Challenges of using carbohydrate polymers as KHI

KHIs based on carbohydrate polymers have been reported as green additives to prevent gas hydrate formation in recent years. However, several challenges in their functionalizing and preparation should be considered. Some carbohydrates are

not economical to use on a large scale for industrial applications due to their high price. Moreover, poor solubility in organic solvents and water is one of the main challenges of most carbohydrate polymers. Therefore, there are problems in functionalizing and modifying carbohydrate polymers to enhance their inhibition performance. In addition, the molecular weight of KHIs has a critical effect on their performance, yet determination of their exact molecular weight is impossible by conventional methods. Although carbohydrate polymers contain active groups in inhibiting gas hydrate formation, their high molecular weight is one of the serious problems for good efficiency. Literature reveals that the optimum molecular weight of carbohydrate polymers is lower than 10 kDa. However, the molecular weight of the polysaccharides is higher than 50 kDa. We suggest that hydrolysis of natural polymers to smaller segments may improve their KHI activity. Besides, carbohydrate polymers may contain different components depending on their source; thus, the polymer source should be specified to avoid conflicting results. THI effects of carbohydrate polymers on gas hydrate formation have not been extensively investigated, and therefore more studies are needed to explore their thermodynamic behavior.

3. Amino acids

Amino acids are eco-friendly substances that contain carboxylic acid and amine functional groups. An additional group such as amide, alkyl chain, carboxylic acid, and phenyl, is present in the structure of some amino acids, which determine their nature like hydrophobicity/hydrophilicity or basicity/acidity [10, 153]. Hydrophilic, hydrophobic or charged are the main classes of amino acids according to their additional groups. Amino acids have been studied as potential green hydrate inhibitors because they can interact with water molecules via hydrogen-bonding and electrostatic interactions [105, 138, 172, 190, 261]. The structure and hydrophobicity of typical amino acids which have been reported as THIs and KHIs are shown in Table 1.

Table 1

Chemical structure and hydrophobicity of amino acids [3]

Amino acid	Molecular structure	Hydrophobicity	Amino acid	Molecular structure	Hydrophobicity
Glycine [216]	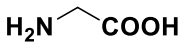	-0.4	Serine [154]	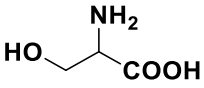	-0.8
Proline [120]	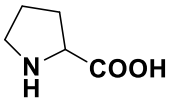	-1.6	Arginine [12]	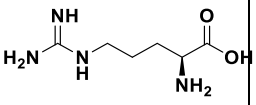	-4.5
Leucine [214]	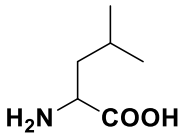	3.8	Glutamine [210]	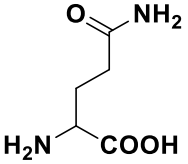	-3.5
Isoleucine [214]	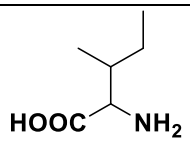	4.5	Threonine [210]	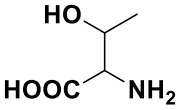	-0.7
Alanine [154]	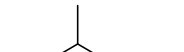	1.8	Proline [210]	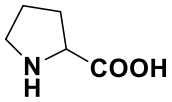	-1.6
Valine [214]	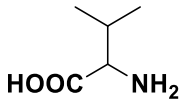	4.2	Asparagine [215]	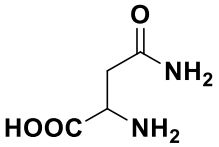	-3.5
Histidine [215]	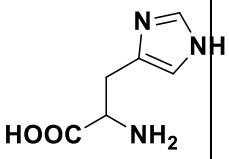	-3.2	Phenylalanine [215]	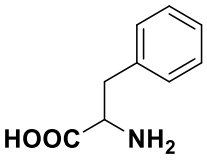	2.8

The amino acid-water interactions as the critical parameter in gas hydrate formation is responsible for their role as THIs. The reorientation dynamic of water molecules rises with an increase in hydrogen bond energy of amino acids, inhibiting gas hydrate formation. Additionally, the concentration, viscosity, solubility, density, and alkyl chain of amino acids strongly affect the thermodynamic phase boundary of hydrate formation. Sa et al. [216] determined the equilibrium conditions of liquid-hydrate-vapor for CO_2 hydrate in solutions containing 0.1-3 mol % of amino acid in the range of 1.41-3.52 MPa and 0-8.3 ºC. They showed the following order of

inhibiting properties for amino acids: L-valine > L-alanine > glycine. Moreover, Sa et al. [218] found that L-proline was an outstanding THI because it reduced the water activity via hydrogen bonds and electrostatic interactions. Sun et al. [253] showed that L-arginine provided higher formation pressure for CH_4 hydrate than pure water at the same temperature so that it could be used as a THI. Bavoh et al. [12] measured the CH_4 hydrate-liquid-vapor equilibrium curve of five amino acid solutions including glycine, alanine, proline, serine, and arginine. It was found that all these amino acids inhibited hydrate formation. Among them, glycine performed best with an average depression temperature of 1.78 ºC at a concentration of 10 wt %. The uncertainties of pressure and temperature measurements were 0.01 MPa and 0.15 ºC, respectively. The study reported by Chen et al. [23] also indicated that L-proline was an effective THI for CH_4 hydrate. The hydrate stability conditions of natural gas, CO_2, and CH_4 hydrates for solutions containing threonine, glycine, proline, phenylalanine, alanine, valine, serine, histidine, arginine, and asparagine was theoretically investigated by Mehrabi et al [159]. They concluded that a higher inhibitory activity can be achieved for amino acids with shorter alkyl chains owing to the stronger hydrogen bonds with water. Although, glycine and alanine performed better than other amino acids, their inhibition power was weaker than ethylene glycol and methanol. In another study, Burla et al. [20] reported that a mixture of L-threonine and L-methionine (80−20 vol %) significantly prevented CH_4 hydrate formation at 0.5 wt %. Bavoh et al. [13] assessed the inhibitory action of arginine, proline, glycine, serine, and alanine on the phase equilibrium conditions of CO_2 hydrate under 2.53–4.0 MPa at 5-20 wt %. Their results revealed that the hydrate phase boundary significantly shifted to region with lower temperatures and higher pressures in presence of the amino acids. The highest temperature shift of 1.83 ºC was achieved for glycine at 10 wt %. They demonstrated that amino acids do not insert in hydrate cavities during hydrate formation. The uncertainties of pressure and temperature measurements were 0.01 MPa and 0.1 ºC, respectively. Mannar et al. [156] reported that lysine could shift the equilibrium phase boundary conditions of

CH_4 and CO_2 hydrates to higher pressure and/or lower temperature regions. A solution containing 10 wt % of lysine provided an average suppression temperature of 1.44 ºC and 1.49 ºC for CH_4 and CO_2 hydrates, respectively. The uncertainties of pressure and temperature measurements were 0.06 MPa and 0.1 ºC, respectively. Kim et al. [120] reported that hydrophilic amino acids like L-serine and L-proline were efficient THIs for CO_2 hydrate because of their hydrophilic side chains, carboxylic acid, and amine groups. In addition, L-proline showed a better THI performance than methanol on a molar concentration basis. Bavoh et al. [14] measured the dissociation temperature of CH_4 hydrate in the presence of arginine and valine at 10 MPa to evaluate their THI activity. A slight inhibition effect (0.5 ºC shift in dissociation temperature) on the CH_4 hydrate phase boundary was observed in concentrations of 0.01 and 0.05 wt % for both amino acids. Another study has investigated [15] THI power of asparagine, threonine, valine, and phenylalanine on CH_4 hydrate formation at 3.52-10.25 MPa. Valine showed the best inhibition impact (0.529 ºC shift in dissociation temperature) at 5 wt %, while phenylalanine was the worst sample. They revealed that the side chain of amino acids is responsible for the variations in their inhibition efficiency. They also examined THI effect of glycine + 1-Ethyl-3-methylimidazolium chloride (EMIM-Cl) mixture on CH_4 hydrate formation at 3-11 MPa [16]. The results demonstrated that glycine + EMIM-Cl mixture has THI activity but its efficiency was slightly lower than pure samples at 10 wt %. Ramos et al. [240] developed new organic salts from L-alanine, L-proline, and L-tyrosine as green THIs for CO_2 hydrate formation as displayed in Fig. 16. They observed that the salts based on L-proline (Fig. 16b) has KHI property for CO_2 hydrates, while L-alanine (Fig. 16a) and L-tyrosine- based (Fig. 16c) salts acted as THIs. Among them, dodecyl L-tyrosine hydrochloride showed the best THI effect. The more hydrophilic organic salts showed THI effects, while the hydrophobic salts worked as KHIs. Moreover, a relationship was detected between the size of the alkyl chain and CO_2 solubility in water, where the organic salts with longer alkyl chains showed poor solubility. This observation can be related to the salting out effect

because adding salt decreases the activity of water and reduces its solubility. Such behavior was also observed in their other work for CO_2 hydrate formation in the presence of synthesized organic salts from L-threonine [241].

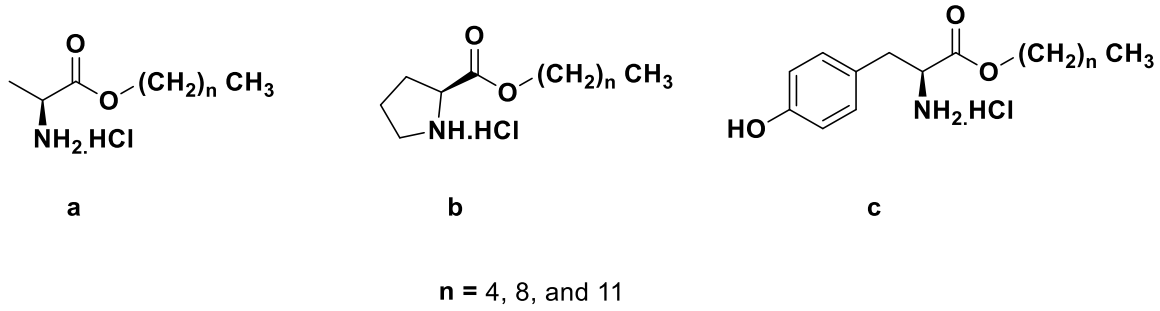

Fig. 16. Chemical structure of synthesized organic salts from amino acids [3]

The KHI power of amino acids can be assessed by determining induction time, rate of hydrate formation, and gas consumption. The side chain length, concentration, and hydrophobicity are the main parameters that affect KHI activity of amino acids. Using a flow mini-loop apparatus, Talaghat [255] found that the presence of L-tyrosine provided lower gas consumption and longer induction time during the formation of CO_2, CH_4, propane, and iso-butane hydrates. The results were approximately three times higher than PVP at 0.02 wt %. Sa et al. [214] investigated natural hydrophobic amino acids as KHIs to hinder CO_2 hydrate formation. Their results signify that glycine and L-alanine with lower hydrophobicity performed better in inhibiting hydrate nucleation and growth of CO_2 hydrate formation through perturbation of water network. In comparison, L-isoleucine, L-leucine, and L-valine with higher hydrophobicity strengthened the local water structure, as shown in Fig. 17. They concluded that the perturbation or disruption of liquid water structure played a vital role in hydrate inhibition. In addition, Sa et al. [217] identified the abnormal incorporation of L-alanine, L-valine, and α-glycine into the CO_2 hydrate crystal lattice, resulting in lattice distortion and expansion as depicted in Fig. 18. The results indicate that sharing the crystal lattice provide a potential for their natural coexistence.

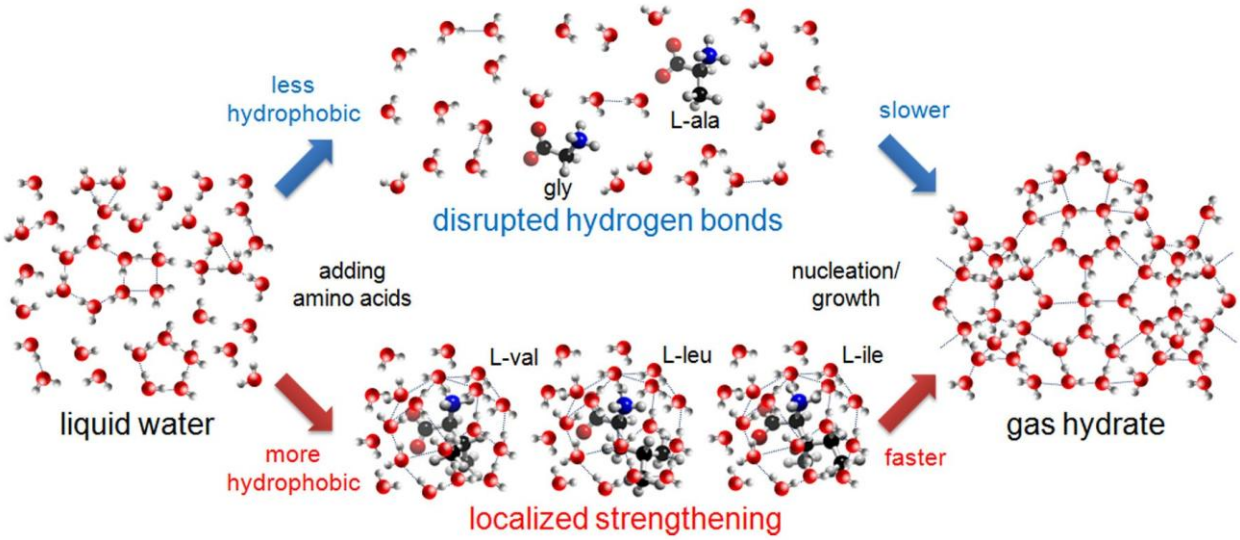

Fig. 17. Effect of different hydrophobic amino acids on CO_2 hydrate formation [214]

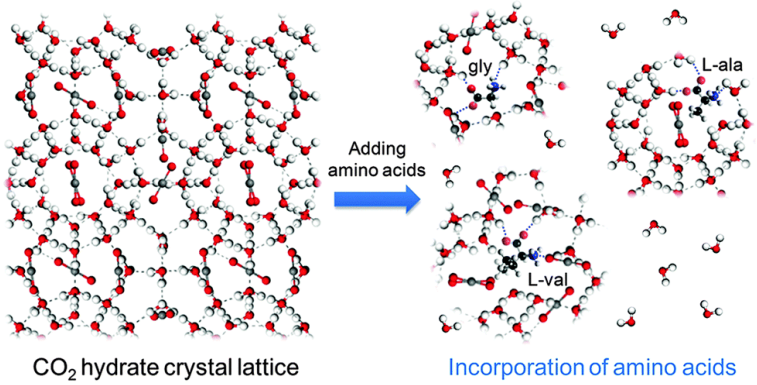

Fig. 18. The lattice distortion and expansion of CO_2 hydrate due to the incorporation of amino acids into the crystal lattice [217]

Naeiji et al. [168] determined the equilibrium temperature and induction time of THF hydrate formation in amino acid solutions. They showed that glycine had better inhibitory performance than L-leucine due to its lower hydrophobicity. Glycine increased the induction time 2.5 times compared to pure water at 1.5 wt %. Rad et al. [195] performed experimental and theoretical investigations on ethane hydrate formation, and their results indicated that amino acids with lower hydrophobicity showed the highest inhibition power than others in delaying the nucleation and slowing the growth of hydrates. Therefore, glycine was a better KHI than L-leucine similar to the previous work [168]. Roosta et al. [210] evaluated KHI

activity of amino acids in an aqueous solution according to their hydrophobicity, the net charge of amino acids, and the electrical charge of the side chain. They ranked the performance of amino acids based on experimental results as follows: L-histidine> glycine > L-proline ≈ L-serine ≈ L-threonine > L-glutamine. In another study, Roosta et al. [212] investigated the dual effect of amino acids on the nucleation and growth rate of methane-propane, ethane, and methane-THF hydrates. The results showed that the hydrophobic/hydrophilic characteristics of amino acids played an important role in inhibiting and promoting hydrate formation when hydrophobic gas molecules are only present in the system. L-serine and glycine as hydrophobic amino acids acted as poor KHIs for ethane and methane-propane hydrates, whereas L-glutamine and L-histidine as hydrophilic amino acids promoted the hydrate formation in these systems. Hu et al. [86] carried out a density functional theory (DFT) study and MD simulation to investigate the inhibitory effect of serine, glycine, and valine on the growth of CH_4 hydrate. The results signified that a more stable adsorption mode was achieved because the hydrogen and nitrogen/oxygen atoms in the hydrophilic groups of the amino acids preferred to simultaneously attach to the hydrogen and oxygen atoms of water molecules in CH_4 hydrate. Among three amino acids, the inhibitory effect of serine is the best owing to the strong interaction with water molecules in CH_4 hydrate. The inhibition power of L-tyrosine on natural gas hydrate formation was evaluated by Saberi et al [220]. They demonstrated that L-tyrosine was not a good inhibitor from the point of the induction time of natural gas hydrate formation. However, it acted well in inhibiting hydrate growth. They suggested that the balance between the effects of hydrophobic side chains and the hydrophilic terminal groups of L-tyrosine on the local water structure determines the inhibition efficiency of the amino acid on hydrate growth step. Das [36] reported that sarcosine exhibited higher induction and agglomeration times than PVCap and PVP in a clay-free water-based drilling fluid in terms of induction time for THF hydrate. Aghajanloo et al. [2] assessed the inhibition effect of L-tyrosine on methane-hydrogen sulfide clathrate hydrate formation at 1-7 ºC and 10 MPa. The

results demonstrated that L-tyrosine at a concentration of less than 2 wt % approximately had no obvious influence on thermodynamic equilibrium conditions but significantly increased the induction time and reduced the gas consumption. The uncertainties of pressure and temperature measurements were 0.5 MPa and 0.1 ºC, respectively. Talaghat [258] studied the inhibition effect of L-histidine as a polar amino acid on the kinetic of methane-propane and methane-isobutane hydrate formation using a mini flow loop. He showed that L-tyrosine worked better than PVP at 0.01 wt % and 0.02 wt %. In addition, the addition of 0.005 wt % or 0.0075 wt % L-tyrosine to PVP prolonged the induction time more than pure PVP. The uncertainties of pressure and temperature measurements were 0.05 MPa and 0.1 ºC, respectively. Longinos and Longinou [151] investigated the inhibition or promotion effect of aspartic acid, valine, arginine, and threonine on methane-propane hydrate formation at 2 ºC and 2.45 MPa. Among the amino acids, aspartic acid and threonine acted as KHIs (aspartic acid > threonine), while valine and arginine worked as gas hydrate promoters (arginine > valine). They suggested that the higher promotion effect of valine compared to arginine may be due to the incorporation of the methyl group of valine into the hydrate cavity as a guest molecule.

3.1. Synergistic inhibition effect of amino acids

Talaghat [255] reported that L-tyrosine exhibited a synergistic effect with PEO and PPO in flow mini-loop tests for CO_2, CH_4, propane, and iso-butane hydrates. A mixture of L-tyrosine and PPO or PEO showed a higher kinetic inhibition effect than PVP. Xu et al. [289] studied the inhibitory power of glycine and its synergistic effect on PVCap. They found that glycine could not prevent CH_4 hydrate formation alone but it enhanced the inhibition efficiency of PVCap on hydrate crystal growth even at 13.5 ºC subcooling. Glycine reduced the crystal growth rate of CH_4 hydrate up to 80% in PVCap solution. The uncertainties of pressure and temperature measurements were 0.01 MPa and 0.1 ºC, respectively. Using a rocking cell apparatus, Altamash et al. [4] observed that L-phenylalanine, glycine, L-alanine, L-

histidine, and L-asparagine had poor thermodynamic and kinetic inhibition properties at a low concentration, but they showed a strong kinetic inhibitory effect when coupled with PEO. A mixture of L-alanine-PEO provided an induction time of 35 h for CH_4 hydrate formation at 5.6 MPa, four times more than the induction time when L-alanine was tested. The uncertainties of pressure and temperature measurements were 0.02 MPa and 0.2 ºC, respectively. Long et al. [149] measured the hydrate-liquid-vapor equilibrium for CH_4 in presence of ethylene glycol and glycine (1:1 mixture). They found that the inhibition performance was improved by mixing glycine and ethylene glycol. Furthermore, they calculated the molar hydrate dissociation enthalpies and concluded that the interaction of ethylene glycol and glycine did not impact the structure of hydrates. The study performed by Bharathi et al. [18] indicated the thermodynamic hydrate inhibition performance of MEG and glycine mixture on CO_2 hydrates. They demonstrated that the highest synergistic effect could be obtained at 10 wt % of 1:1 mixture solution and the formed hydrate was dissociated with less energy than MEG. In addition, the hydrate structure did not change in the inhibitor solutions according to the results of dissociation enthalpy. The uncertainties of pressure and temperature measurements were 0.01 MPa and 0.01 ºC, respectively. Qureshi et al. [193] investigated the thermodynamic hydrate inhibition effect of doping glycine, L-alanine, and histidine with conventional THIs. The results showed that ethylene glycol and methanol synergized THI effect of amino acids at a low dosage of 1 wt %. When these amino acids were doped with 1 wt % of THIs, the equilibrium temperature shifted about 0.8 ºC. Amino acids also exhibited a synergistic effect with ionic liquids. The uncertainty of temperature measurements was 0.2 ºC. Lee et al. [131] experimentally studied KHI effect of amino acids, ionic liquids, and their synergistic effect on CH_4 hydrate formation. The onset temperature of hydrate formation for a mixture of glycine (0.5 wt %) and 1-butyl-3-methylimidazolium tetrafluoroborate ([BMIM][BF_4]) (0.5 wt %) was lower than 1.0 wt % of PVCap. The uncertainties of pressure and temperature measurements were 0.02 MPa and 0.02 ºC, respectively. In another study, Lee et al.

[128] examined the synergistic inhibitory effect of [BMIM][BF_4] and glycine on CH_4 hydrate growth and the thermodynamic phase equilibria using HP-μDSC. They found that a combination of 0.5 wt % glycine and 0.5 wt % [BMIM][BF4] had a synergism for CH_4 hydrate as a KHI. No thermodynamic synergism of them was observed on CH_4 hydrate. However, a mixture of 1.5 mol% glycine and 1.5 mol% [BMIM][BF_4] significantly reduced CH_4 hydrate growth, the final gas uptake, and the conversion of water into hydrate. The uncertainties of pressure and temperature measurements were 0.02 MPa and 0.03 ºC, respectively. Hussain and Husin [87] discussed the synergistic performance of ionic liquids and amino acids in preventing hydrate formation by COSMO-RS application. Among 91 synergistic amino acids-ionic liquids (AACILs), choline aspartate showed the best synergistic AACIL owing to its hydroxyl chain to form hydrogen bonds with water molecules. Wang et al. [280] found that a mixture of glycine and L-arginine (0.5 wt %-5.0 wt %) with 0.5 wt %-1.0 wt % of PVPK90 and VC-713 had synergistic inhibitory effects on THF hydrate formation. Additionally, the combination of 1.0 wt % VC-713 with 4.0 wt % glycine provided the best synergistic inhibition performance, in which the induction time of hydrate formation increased to 858 minutes.

3.2. Inhibition mechanism of amino acids

Since amino acids behave as zwitterions, they can make electrostatic interactions and hydrogen bonds with water molecules through their carboxylic acid and amine groups. Such electrostatic interactions decrease the activity coefficient of water and, therefore, thermodynamically inhibit the formation of gas hydrate. Additionally, improving the hydrophilicity or reducing the hydrophobicity of amino acids increase their THI activity. The mechanisms of thermodynamic and kinetic inhibitions of amino acids are totally different. The disruption of the surrounding water structure is the main kinetic inhibition mechanism of hydrophobic amino acids. The amount of perturbation has a direct relationship with the hydrophobicity of the molecule. Indeed, amino acids disrupt the hydrate cages by forming hydrogen

bonds with water molecules, whereas they inhibit the growth of gas hydrate crystals through the electrostatic interactions with the crystal surface. However, the disruption of water networks is the dominant mechanism, which was supported by X-ray diffraction data [217]. To sum up, some amino acids such as glycine and L-proline worked as good KHI as they can interact with water molecules to disrupt the hydrogen bond network of hydrate structure. However, more theoretical and experimental studies in the presence of various gas hydrate formers at different pressure-temperature conditions are still required to attain deeper insight into their inhibition properties.

4. Ionic liquids

Ionic liquids (ILs) are composed of a diversity of cations and anions, which are liquid at temperatures lower than 100 ºC or even at ambient temperature [200, 238, 244, 302]. Imidazolium, phosphonium, pyridinium, ammonium, thiazolium, and triazolium are well-known ionic liquid families [126, 235, 268]. They have several unique features such as negligible vapor pressures, high thermal stabilities, high capacities for solubilization of a variety of compounds, and a high potential for hydrogen bonding with water [7, 186, 199, 227]. They can be designed to be environmentally friendly; however, some kinds of ILs are extremely toxic [19, 25, 96, 189, 208]. ILs have been recently studied as dual-function KHI/THI inhibitors and synergists with other compounds in experimental and modeling studies [2, 17, 111, 113]. The prominent property of ILs is their dual function role in hydrate prevention, as they can retard the nucleation of gas hydrate and change the equilibrium conditions of hydrate formation simultaneously [79, 285, 294]. According to the literature, the effect of cation in the ILs structure on inhibition of gas hydrate formation was widely studied by changing the length of the alkyl chain and substituting of ammonium pyrrolidinium, imidazolium, and morpholinium ions.

THI activity of ILs mainly relies on their ability to form hydrogen bonds with free water molecules, and the inhibition efficiency depends on concentration, anions,

and cations. It has been reported that THI performance of ILs lowered in the following order of the anions where the cations are the same: $Cl^- > Br^- > I^- > BF_4^-$ [286]. Moreover, similar to conventional THIs, the inhibitory power of ILs improved as their concentration increased [147, 207, 301]. In general, ammonium, morpholinium, and piperidinium-based cations work better than imidazolium ones as THIs [172]. Xiao and Adidharma [285] examined the effect of imidazolium-based ILs on the equilibrium hydrate dissociation at 3-11 MPa and 25 ºC subcooling using a HP-μDSC. The results showed that the ILs shifted the equilibrium curve of CH_4 hydrate owing to their intense electrostatic charges and hydrogen bond with water. Meanwhile, they reduced the hydrate nucleation rate. Xiao et al. [286] reported that dialkylimidazolium halide ILs also had a dual functional inhibition effect similar to imidazolium-based ILs. The structures of imidazolium and dialkylimidazolium halide ILs are shown in Table 2 and 3, respectively.

Table 2

Symbol, chemical name, and molecular structure of imidazolium-based ILs [3]

Symbol	Chemical name	Chemical structure
EMIM-BF_4	1-ethyl-3-methylimidazolium tetrafluoroborate	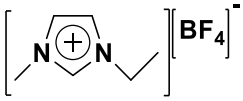
BMIM-BF_4	1-eutyl-3-methylimidazolium tetrafluoroborate	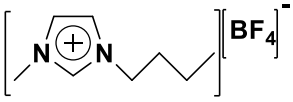
EMIM-$N(CN)_2$	1-ethyl-3-methylimidazolium dicyanamide	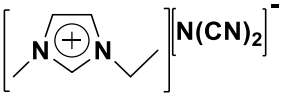
EMIM-CF_3SO_3	1-ethyl-3-methylimidazolium trifluoromethanesulfonate	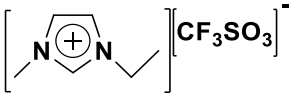
EMIM-$EtSO_4$	1-ethyl-3-methylimidazolium ethylsulfate	

Table 3

Symbol, chemical name, and molecular structure of dialkylimidazolium halide ILs [3]

Symbol	Chemical name	Chemical structure
EMIM-Cl	1-ethyl-3-methylimidazolium chloride	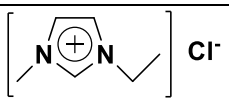
EMIM-Br	1-ethyl-3-methylimidazolium bromide	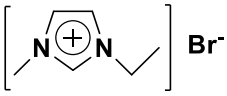
PMIM-I	1-propyl-3-methylimidazolium iodide	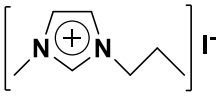
BMIM-Cl	1-butyl-3- methylimidazolium chloride	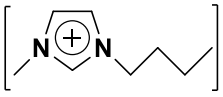
BMIM-Br	1-butyl-3- methylimidazolium bromide	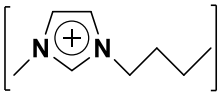
BMIM-I	1-butyl-3- methylimidazolium iodide	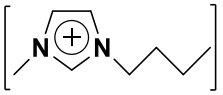

Li et al. [140, 141] determined CH_4 hydrate equilibrium conditions in presence of several dialkylimidazolium-based ILs and tetraalkylammonium-based ILs (Table 4). Their results revealed that hydroxylated cations increased the inhibitory action of dialkylimidazolium-based ILs, while the presence of the shorter alkyl in tetraalkylammonium-based ILs exhibited a better THI effect than those hydroxylated cations with the longer alkyl. The uncertainties of pressure and temperature measurements were 0.02 MPa and 0.05 ºC, respectively.

Table 4

Symbol, chemical name, and molecular structure of dialkylimidazolium-based ILs and tetraalkylammonium-based ILs [3]

Symbol	Chemical name	Chemical structure
[MMIM]-I	1,3-dimethy-imidazolium iodide	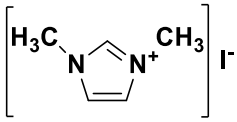
[EMIM]-I	1-ethyl-3-methy-imidazolium iodide	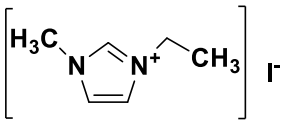
[OH-C_2MIM]-Cl	1-hydroxyethy-3-methyl-imidazolium chloride	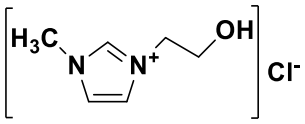
[$N_{1,1,1,1}$]-Cl	Tetramethyl-ammonium chloride	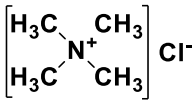
[$N_{1,1,1,\ eOH}$]-Cl	Hydroxyethyl-trimethy-ammonium chloride	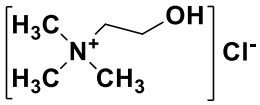

Tumba et al. [266] reported that tributylmethylphosphonium methylsulfate ([$3C_4C_1P$][$MeSO_4$]) showed an inhibitory effect on CO_2 and CH_4 hydrates, but the effect was not comparable to conventional THIs like methanol and NaCl. The effect of [OH-EMIM][BF_4], [EMIM][$EtSO_4$], [EMIM][HSO_4], [BMIM][BF_4], and [BMIM][BF_4] on CH_4 hydrate dissociation conditions at 8.75-14.25 ºC and 7-12 MPa was studied by Zare et al. [301]. They found that [OH-EMIM][BF_4] was the best THI among these five ILs. Richard and Adidharma [207] reported that, unlike NaCl or MEG, inhibitors containing 1-ethyl-3-methylimidazolium bromide (EMIM-Br) or 1-ethyl-3-methylimidazolium chloride (EMIM-Cl) showed the inhibitory effect of the inhibitors improved as the pressure increased, but the reason is unknown. Other studies also addressed the enhanced thermodynamics effect of ILs at higher pressures [101, 148, 181]. Sabil et al. [221] evaluated the performance of nine ILs as HITs (Table 5). The results showed that the effectiveness performance

decreased in the following order: [OH-EMIM][Cl] > [BMIM][HSO_4] > [OH-EMIM][Br] > [BMIM][Cl] >[BMIM][Br] > [BMIM][$N(CN)_2$] > [BMIM][CF_3SO_3] > [BMIM][CH3SO_4] > [BMIM][ClO_4]. In the presence of 0.1 wt % [OH-EMIM][Cl], the dissociation temperature of CH_4 hydrate was reduced by 1.329 ºC on average at pressures of 3.6, 5.1, 7.1, 8.6, 9.6, and 11.1 MPa. The uncertainty of pressure measurements was 0.1 MPa.

Table 5

Average reduced dissociation temperature in the presence of ILs at 0.1 wt % [3]

Ionic liquid	Average reduced temperature (ºC)
[BMIM][ClO_4]	0.37
[BMIM][CH3SO_4]	0.585
[BMIM][CF_3SO_3]	0.617
[BMIM][$N(CN)_2$]	0.663
[BMIM][Br]	0.758
[BMIM][Cl]	0.887
[OH-EMIM][Br]	0.96
[BMIM][HSO_4]	1.103
[OH-EMIM][Cl]	1.329

Lee et al. [132] synthesized a variety of pyrrolidinium- based ILs to prevent CH_4 hydrate formation (Fig. 19). The results showed that Br-based ILs offered better thermodynamic inhibition properties by inhibiting the hydrate equilibrium condition as much as 1.8 ºC at a concentration of 10 wt %. While BF_4-based ILs showed better kinetic hydrate inhibition properties. Lee et al. [129] also reported that choline chloride could function as an effective THI for CH_4 hydrate using high-pressure autoclave experiments and COSMO-RS software.

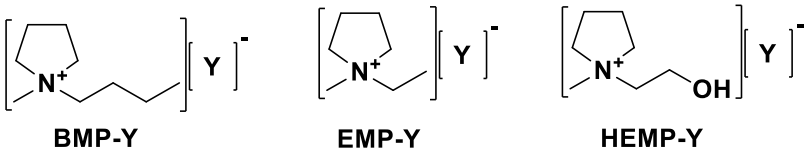

Fig. 19. Chemical Structure of pyrrolidinium- based ILs: Y indicates one of the BF_4^-, Br^-, and Cl [3]

Khan et al. [114] reported that tetraethylammonium hydroxide (TEAOH), tetramethyl ammonium chloride (TMACl), and tetrapropylammonium hydroxide (TPrAOH) at a concentration of 10 wt % showed an average suppression temperature of 1.7 ºC, 1.6 ºC, and 1.2 ºC, respectively, at 1-10 ºC and 1.80-4.20 MPa for CO_2 hydrate. The uncertainties of pressure and temperature measurements were 0.01 MPa and 0.1 ºC, respectively. They further concluded that a shorter alkyl chain provided better thermodynamic inhibition based on the study of the hydrate phase boundary of CO_2 rich mixed gas hydrate system (CO_2 (70 mol%) + CH_4(30 mol%)) in tetramethylammonium hydroxide (TMAOH), tetrabutylammonium hydroxide (TBAOH), TEAOH, and TPrAOH solutions [116]. For CH_4 rich mixed hydrate system, TMAOH was the best THI among these ILs. While TBAOH promoted hydrate formation [117]. Khan et al. [115] also showed that the phase boundary of CO_2 and CH_4 hydrates changed by 1.5 ºC and 2.3 ºC, respectively, in a solution containing 10 wt % of TMAOH. Other ammonium-based ILs were also reported as THIs on CO_2 hydrates such as tetraethyl ammonium tetrafluoroborate ($TEABF_4$) and tetra methyl ammonium tetrafluoroborate ($TMABF_4$) [77]. Gupta et al. [74] found that aromatic ILs were dominant over aliphatic ILs for CH_4 hydrate inhibition. The replacement of anion by [HSO_4] in imidazolium-based ILs improved the hydrate inhibition property, and [BMIM][HSO_4] was the best inhibitor among all investigated ILs. Altamash et al. [5] investigated three alkylammonium-based protic ILs for CH_4 hydrate inhibition. Their results demonstrated that at a concentration of 10 wt %, the suppression temperatures of [EA][Of], [DMA][Of], and [DMEA][Of] were 2.3 ºC, 2.0 ºC, and 2.1 ºC, respectively. They also concluded that the common formate anion provided the dominant inhibitory action while the effect of the

structural variation of the cation was small. The uncertainties of pressure and temperature measurements were 0.1 MPa and 0.1 ºC, respectively. Nashed et al. [170] explored the impact of 0.1 wt % ILs, namely, tetraethylammonium iodide [TEA-I], 1-methylimidazolium hydrogen sulfate [H-MIM-HSO4], 1-methyl-3-octylimidazolium chloride [MOIM-Cl], and 1-hexyl-3-methylimidazolium iodide [HMIM-I] on CH_4 hydrate formation. The results showed that the average reduced temperature was 0.37 ºC to 1.52 ºC at 5.1–11.1 MPa. Menezes et al. [37] collected CH_4 hydrate dissociation data in the presence of [BMIM][Cl] and [BMIM][Br] at 1.0 wt %, 5.0 wt %, 10.0 wt %, and 15.0 wt % and pressures from 9.6 to 10.0 MPa through high-pressure calorimetry. With this device, the small difference (~0.3 ºC) in onset values minimized the experimental uncertainty. They found that the inhibitors have both KHI and THI activities, but they accelerate hydrate growth at concentrations lower than 5 wt %. Sulaimon and Tajuddin [252] used Conductor-Like Screening Model for Real Solvents (COSMO-RS) software as a pre-screen method to assess THI power of ILs. They concluded that the hydrogen bonding energy (E_{HB}) is the main energy that directly affects the inhibition power of ILs. Their results demonstrated that increasing E_{HB} of anions enhances THI power of ILs while raising E_{HB} of cations reduces the inhibition efficiency. Moreover, they revealed that the combination of hydrogen sulfate [HSO_4] and chloride [Cl^-] as the anion provides a high E_{HB}. On the other hand, the value of E_{HB} between anion and water can be increased by incorporating the hydroxyl group into the cation structure. They suggested [OH-EMIM][HSO4]. [OHEMIM] [Cl] [EMIM][Cl][HSO4] as potential ILs for experimental tests. Qureshi et al. [194] evaluated THI effect of 3-Ethyl-1-methyl-1H-imidazol-3-ium dicyanoazanide [$C_8H_{11}N_5$] and 3-Ethyl-1-methyl-1H-imidazol-3-ium methane-sulfonate [$C_7H_{14}N_2O_3S$] on CH_4 hydrate formation in pure water and Qatar seawater solutions. Although both ILs showed poor THI effect in pure water, they worked as THIs and KHIs in the Qatar seawater solution. The sample [$C_8H_{11}N_5$] demonstrated higher THI activity than [$C_7H_{14}N_2O_3S$] by providing a maximum temperature shift of 1 ºC at 5 wt %. The KHI effect of

[$C_8H_{11}N_5$] was also better than [$C_7H_{14}N_2O_3S$] in both pure water and Qatar seawater media. However, the studied ILs did not show a comparable THI effect to methanol. The higher THI effect of ILa in Qatar seawater suggests that the presence of Mg^{2+}, Cl^-, SO_4^{2-}, and Na^+ and ions in the seawater enhance its efficiency as synergistic. The uncertainties of pressure and temperature measurements were 0.1 MPa and 0.01 ºC, respectively. Five new ILs (Fig. 20), namely tetraalkylammonium acetate (TMAA), choline octanoate (Ch-Oct), choline iso-butyrate (Ch-iB), choline butyrate (Ch-But), and choline hexanoate (Ch-Hex) were developed as green THIs for CH_4 hydrate formation by Tariq et al [264]. They also reported that TMAA and Ch-Oct were the best THI and KHI among the five investigated ILs. However, TMAA Ch-But, and Ch-Oct worked as hydrate promoters at elevated pressures and 1 wt %. They proposed that a slight change in ILs structure provides different character for the samples including, kinetic inhibition, hydrate promotion, thermodynamic inhibition, and surfactant/anti-agglomerate.

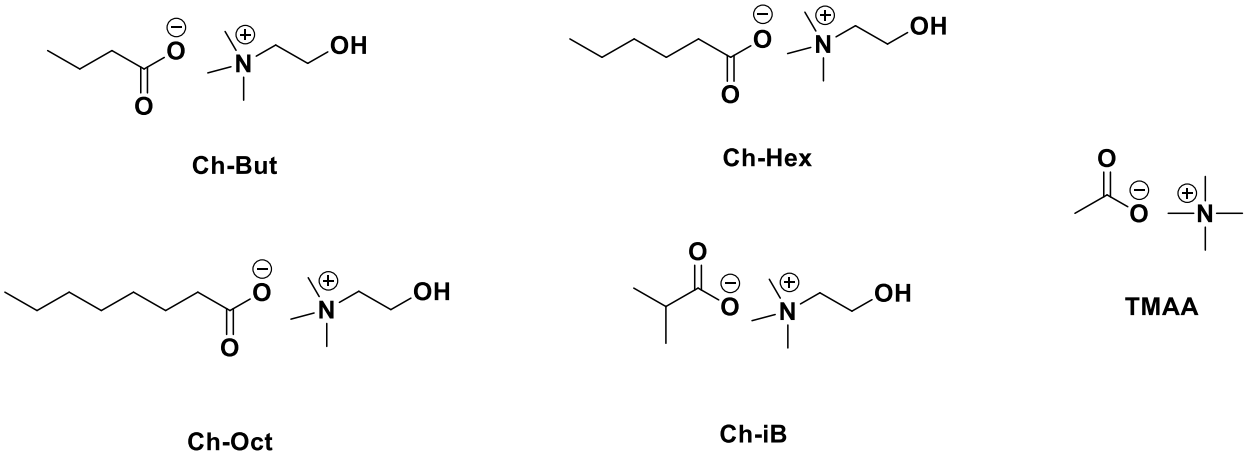

Fig. 20. Chemical structure of ILs based on tetramethylammonium and choline [3]

In contrast to experimental data on ILs as THIs, few studies have been performed on KHI activity of ILs. Most available KHI studies have been reported for CH_4 hydrate formation, yet some studies were documented on natural gas and CO_2 hydrates. Various parameters, such as induction time, rate of hydrate formation, and total gas consumed have been used to determine KHI power of ILs by different research groups. However, KHI data cannot be compared with the different

resources as the induction time is mostly used for the kinetic studies. Specifications of apparatus, method, stirring, driving force, and impurities in the sample are the main factors that significantly affect KHI data of any system. Therefore, nucleation and induction time of hydrate formation are stochastic phenomena and can only be compared with pure water data of the same system. Kim et al. [121] developed pyrrolidinium cation-based ILs as effective inhibitor for CH_4 hydrate formation. They observed that the induction time of CH_4 hydrate formation with N-(2-hydroxyethyl)-N-methylpyrrolidinium tetrafluoroborate ([HEMP][BF4]) was longer than that of PVP, PVCap, and N-ethyl-N-methylimidazolium tetrafluoroborate ([EMIM][BF4]) at concentrations of 0.1 wt % and 1 wt %. Rasoolzadeh et al. [198] reported that BMIM-BF_4, BMIMDCA, and TEACl increased the induction time of CH_4 hydrate formation, and they further proposed a three-parameter semi-empirical model to predict the data. Their model can be used for cooling rate of 1 ºC/h, ILs concentrations up to 20 wt %, and pressures lower than 8 MPa. The proposed model has an acceptable accuracy compared to the experimental data. The uncertainties of pressure and temperature measurements were 0.01 MPa and 0.1 ºC, respectively. Lee et al. [133] synthesized 1-hydroxyethyl-1-methylmorpholinium tetrafluoroborate (HEMM-BF_4) and 1-hydroxyethyl-1-methylmorpholinium chloride (HEMM-Cl) for CH_4 hydrate formation. They found that HEMM-BF_4 had a kinetic inhibitory effect on CH_4 hydrate formation. The KHI activity of HEMM-BF_4 can be related to the role of BF_4^- as a mobile pseudoguest because it cannot insert into the hydrate cage due to its charge imbalance. In contrast, HEMM-Cl acted as a promoter. They proposed that the rigid hydrate host framework can be distorted in the presence of HEMM-Cl via the hydrogen bonds of water molecules with the ions at the surface. This enhances the penetration of methane or inclusion into the growing clathrate hydrate structures and promotes hydrate formation. Nashed et al. [171] investigated the hydrate inhibition performance of nine ILs using a high-pressure micro differential scanning calorimeter. Their results demonstrated that [OH-EMIM][Br], [BMIM][CH_3SO_4], and [BMIM][CF_3SO_3]

delayed hydrate formation at 0.01 wt % higher than PVP. Khan et al. [118] reported that the relative inhibition power of TBAOH is much stronger than that of PVP on mixed gas hydrate (50 mol%-50 mol% CO_2-CH_4). However, similar to the TBAB ionic liquid [8], TBAOH was found to be a thermodynamic promoter for the gas hydrate. Interestingly, it was shown that for ammonium hydroxide ILs, their THI effect reduced with the alkyl chain due to its semi-clathratic nature along with longer alkyl chain. While the KHI performance improved with the increased alkyl chain in terms of the enhancement of hydrophobicity (Fig. 21), which also explains why TBAOH can act as both a thermodynamic promoter and a kinetic inhibitor. Therefore, to attain satisfactory hydrate inhibition performance of ammonium based ILs, the effect of the alkyl chain length on the thermodynamic and kinetic characteristics of hydrate formation needs to be further studied.

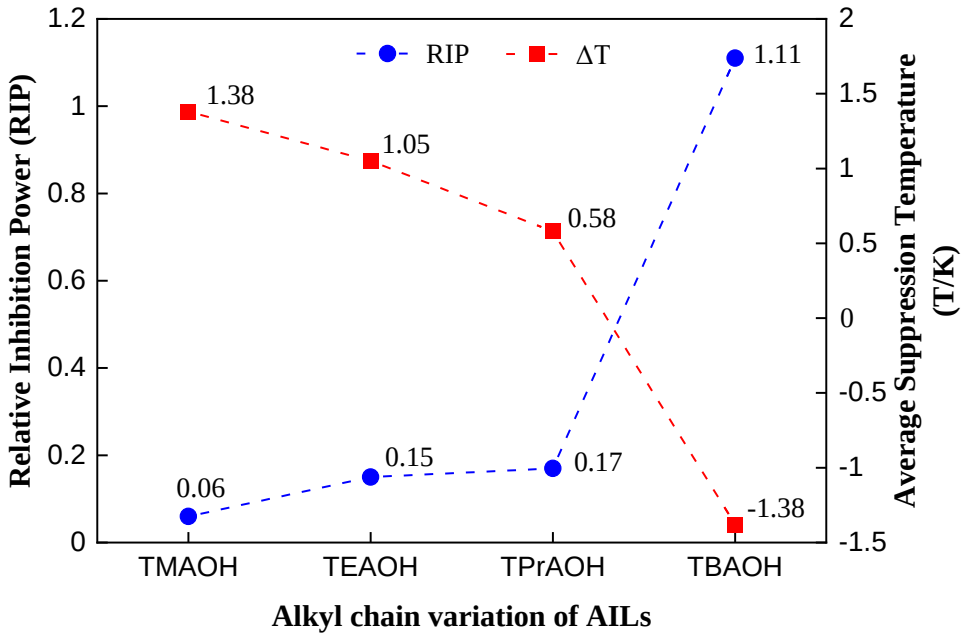

Fig. 21 Effect of alkyl chain variation on RIP and suppression temperature of ammonium hydroxide ILs [3]

Khan et al. [119] introduced TMACl as a dual THI-KHI inhibitor for CO2 and CH4 hydrates. At 10 wt%, TMACl reduced equilibrium temperatures by 1.60°C and 1.42°C for CO2 and CH4 hydrates, respectively, without participating in the hydrate structure. Moreover, TMACl significantly increased the induction time of CO_2 and CH_4 hydrates and decreased the rate of hydrate formation as an effective KHI. In another study, Moujdin et al. [163] evaluated the dual-function activity of TMACl on mixed CO_2-CH_4 hydrate formation. Their results indicated that the inhibitor worked as THI and KHI simultaneously for a mixture of 70% CO_2-30% CH_4. A maximum shift of 1.46 ºC in the hydrate equilibrium curve was obtained in a solution containing 10 wt % of TMACl due to its improved hydrogen bonding ability. Furthermore, the ionic liquid retarded the formation of hydrate up to 1.5 folds compared to pure water at 4 ºC for a mixture of 70% CO2-30% CH_4 which was comparable to PVP. Nazari and Ahmadi [173] studied THI power of 1-butyl-3-metylimidazolium methyl sulfate, [Bmim][MS], and 1-butyl-3-metylimidazolium tetrafluoroborate, [Bmim][BF_4], on CH_4 hydrate formation. They observed that the investigated ILs worked as dual THI and KHI. [Bmim][MS] showed better THI activity by shifting 3 ºC the hydrate equilibrium temperature at 10.5 MPa. While [Bmim][BF_4] acted as good KHI by increasing 2.8 times the induction time at 10.5 MPa and 4.8 times at 11.0 MPa owing to its high value of charge density. Sulaimon et al. [251] synthesized three kinds of 1-alkyl-3-methylimidazolium dihydrogen phosphate as new gas hydrate inhibitors for CH_4 hydrate. Among them, EMIMDHP with the shortest alkyl chain performed best as either THI or KHI. At the same concentration, its THI effect was slightly lower than ethylene glycol, and the KHI performance was comparable to PVP. Nazari et al. [174] studied KHI activity of [BMIM][HSO_4], [BMIM][$MeSO_4$], and [BMIM][BF_4] on the formation of CH_4 hydrate (Fig. 21). All ILs acted as dual THI and KHI inhibitors. [BMIM][BF4] was the best KHI, increasing CH4 hydrate induction time by 2.8 and 4.8 times compared to pure water at 10.5 MPa and 11.0 MPa, respectively. Measurement uncertainties were ±0.07 MPa and ±0.2°C.

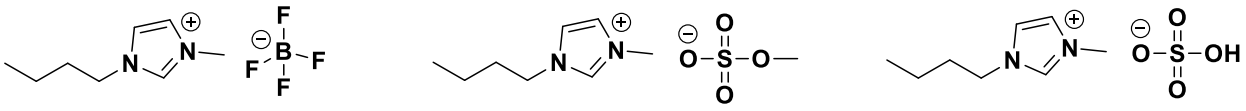

[BMIM][BF_4] [BMIM][$MeSO_4$] [BMIM][HSO_4]

Fig. 22. Chemical structure of [BMIM][HSO_4], [BMIM][$MeSO_4$], and [BMIM][BF_4] [3]

Romero-Martínez et al. [209] synthesized pyridinium-based ionic liquid type surfactant (C_{12}PyBr) by microwave-assisted reaction as green KHI to prevent CH_4 hydrate formation. They showed that a solution containing 0.1 wt % of C_{12}PyBr inhibited CH_4 hydrate formation at a subcooling of 11.2 ºC, which was better than Inhibex 101TM at the same concentration. Nakarit et al. [169] introduced the first cationic homopolymer based on tributylammoniumethylacrylate bromide (PTBAEABr) as a good KHI to inhibit natural gas and THF hydrates (Fig. 23). PTBAEABr showed subcooling temperatures of 10.2 ºC and 11.8 ºC for natural gas hydrate formation at 0.25 wt % and 0.5 wt %, respectively. PTBAEABr also worked as a good synergist with PVCap (0.25 wt %) and provided a maximum subcooling temperature of 14.3 ºC at 0.25 wt %. Additionally, the inhibition effect of PTBAEABr on THF hydrate formation was higher than tetrabutylammonium bromide (TBAB) at 0.2 wt %. The uncertainties of pressure and temperature measurements were 0.1 MPa and 0.05 ºC, respectively.

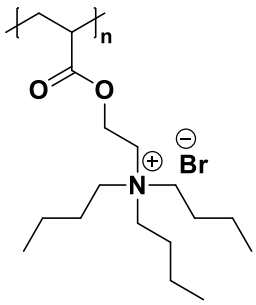

Fig. 23. Chemical structure of PTBAEABr [3]

There are also attempts to prepare a deep eutectic solvent (DES) such as choline chloride and urea-based DES to inhibit hydrate formation due to their intense hydrogen bond formation capability [197]. DES is a new type of green solvents

because of their biodegradable and non-toxic properties. Micro differential scanning calorimeter experiments showed that the induction time of CH_4 hydrate delayed up to 24.3% in the solution containing 0.1 wt % of DES. In another study, Zu Khoo et al. [314] developed reline deep eutectic solvent as THI and KHI for CH_4 hydrate formation. Reline was derived from choline chloride and urea. At 3.07 MPa, CH_4 hydrate dissociation temperature in a solution containing 10.43 wt % of reline was lower than pure water by 2.2 ºC. Additionally, reline effectively hindered the nucleation of CH_4 hydrate crystals for more than 48 h. The uncertainties of pressure and temperature measurements were 0.1 MPa and 0.01 ºC, respectively.

4.1. Synergistic inhibition effect of ILs

Villano and Kelland [272] found that the imidazolium-based ionic liquids (EMIM-BF_4 and BMIM-BF_4) showed poor KHI performance on natural gas hydrate formation at 8.5–9.0 MPa and 10.5 ºC subcooling in comparison with Luvicap 55W and RE 5131 HIO. However, they had a good synergistic effect on the performance of hyperbranched poly (ester amide)s and vinyl lactam polymers. It appears that the presence of a butyl group helps BMIM-BF_4 to exhibit a better synergistic effect than EMIM-BF_4 which has an ethyl group. It is speculated that a butyl group has a stronger Van der Waals interaction with the surface of the SII hydrate (in the Open $5^{12}6^4$ large cages) than an ethyl group, leading to stronger adsorption on the hydrate surface and stronger crystal growth inhibition. Kang et al. [98, 99] identified the synergism potential of HEMP-BF_4 with PVCap in inhibiting CH_4 and natural gas hydrates using solid-state ^{13}C NMR spectroscopy and microscopic Raman spectra (natural gas hydrate only). It was found that the addition of HEMP-BF_4 further delayed the induction time and hydrate growth. They showed that the best inhibition effect could be obtained with ILs containing a hydroxyl group through the formation of hydrogen bonds between water molecules and ILs. Lee et al. [134] investigated the synergism effect of ILs containing BF_4^- and polymeric KHIs on natural gas hydrate formation. The results showed that the combination of 1-hexyl-1-

methylpyrrolidinium tetrafluoroborate (HMP-BF_4) and PVCap significantly inhibited natural gas hydrate formation, even under higher pressures. It is inferred that the evident synergism arose from the inhibition of methane-containing 5^{12} cage formation by the IL. Lee et al. [130] found that [BMIM][BF_4] prevented the filling of small (5^{12}) cages by CH_4 molecules, while glycine had an impact on large ($5^{12}6^2$) cages of sI hydrates. Moreover, they observed that the kinetic inhibition effect of 0.5 wt % glycine and 0.5 wt % [BMIM][BF_4] mixture was better than 1 wt % PVCap. The uncertainties of pressure and temperature measurements were 0.02 MPa and 0.02 ºC, respectively. Additionally, the time-dependent Raman spectra revealed that the cage-specific inhibition of [BMIM][BF_4] and glycine is responsible for the resulting synergism effect, thus reducing the growth rate of CH_4 hydrate [131]. Long et al. [148] presented a synergetic effect for [Emim][NO_3] and [Emim][Cl] mixture at 0.05 wt % and 0.1 wt %. Their mixtures of the two ILs prevented CH_4 hydrate formation more effectively than each of single ILs. Hussain and Husin [87] investigated 91 synergistic formulations of amino acids and ILs with combinations of ionic liquids as cations and amino acids as anions using COSMO-RS software. The results indicated that the combination of amino acids and ILs had the potential as an alternative for traditional THIs and KHIs. Based on COSMO-RS software, Masri et al. [157] demonstrated that amino acid-based ILs worked as THI and KHI because of four oxygen atoms in their anions and cyano group in the 1-(3-cyanopropyl)-3-methyl-imidazolium cation. They proposed that THI properties of amino acid-based ionic liquids can be affected by the polarity of the inhibitor. While the hydrogen-bonding acceptor value of amino acid-based ionic liquids influenced its KHI activity. Literature reveals that the inhibition effect of ILs on thermodynamic conditions of gas hydrate formation is more dominant than the kinetics formation. Generally, ILs showed a considerable KHI and THI effect; however, most of these studies have been performed for CO_2 and CH_4 hydrates. Therefore, more experimental and computational studies are required to investigate the inhibition effect of ILs on natural gas hydrate formation as it is the most common gas hydrate

former in the pipelines. The synergism effect of vinyl caprolactam and PEO on THI and KHI activity of 1-methyl-1-propylpyrrolidinium chloride [PMPy][Cl] and 1-methyl-1- propylpyrrolidinium triflate [PMPy][triflate] was investigated by Qureshi et al [192]. The results showed that adding synergists improved KHI and THI effects of the studied ILs.

4.2. Inhibition mechanism of ILs

The interference of water activity on the stabilized hydrate cavities through hydrogen bonds is the main inhibition mechanism of ILs [22, 265], which is strongly affected by the IL moieties, molecular structure, cation, anion, and sizes of ILs. The behaviors of anions and cations have a key role in the inhibition mechanism of ILs. The perturbation of hydrate structure and mitigation of gas hydrate formation can be improved by increasing the hydrogen bonding affinity and electronegativity of anions [17, 22]. The inhibition power of ILs decrease in the presence of larger anions because they poorly interact with the hydrate structure. Using protic ILs and decreasing chain lengths or molecular weights of cations increase their solvation activity and the hydrogen-bonding interactions, providing higher inhibition efficiency of ILs. While aprotic ILs with long alkyl chain lead to lower THI performance because of their high hydrophobicity [11, 257]. Additionally, the rate of cation/anion movement in the bulk solution and/or towards the hydrate surface is a key parameter for the inhibition efficiency of ILs [261]. The hydrogen bonding of anion with water strongly affects IL-water interactions, thus smaller anions provide higher THI performance. Therefore, the increment of the alkyl chain in the structure of ILs decreases their THI activity and increases KHI performance.

5. Protein and peptides

Poikilothermic animals, such as fishes, insects, and plants can preserve themselves from freezing by antifreeze proteins (AFPs) and antifreeze Glycopeptides (AFGPs) [82]. For decades, researchers have been investigated the structural properties of both AFPs and AFGPs. Although about 67% alanine (Ala) can be found in both type I AFP and AFGP, they are structurally different. The secondary common amino acid in the AFGP structure is threonine (Thr), which is organized into 4-55 repetitive tripeptide blocks as Ala-Ala-Thr. In addition, after several threonines, proline (Pro) replaces Ala in some AFGP types [298]. AFGPs consist of eight distinctive glycopeptides with different molecular weights between 2.6 and 34 kDa [162]. As shown in Fig. 24, in the typical structure of AFGP, repeated Ala-Ala-Thr units to which a β-D-galactosyl-(1 → 3)-α-N acetyl-D-galactosamine is attached at the threonine side chains [158, 269].

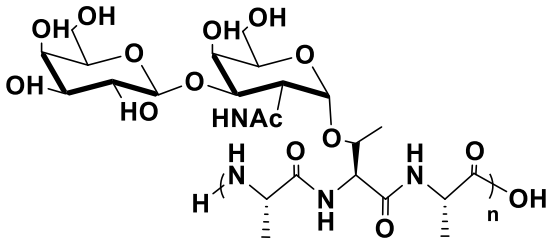

Fig. 24. Structure of a natural AFGP (n = 4–55) [3]

When it comes to AFPs, they are classified essentially into types I to III [38, 39, 72, 298] with different structures. Duman and DeVries [44], as well as Hew and Yip [83] were the first to discover type I AFPs. The winter flounder seems to be the species that have been examined the most, and like the AFGPs, they are high in Ala (~65 mol %). Type 1 AFPs have various structures containing primary, secondary, tertiary, and genetic engineering structures [298]. The primary structure of the protein is entirely α-helical (Fig. 25a) [293]. Compared to type I, the AFP structures differ among organisms and may not comprise equally spaced Thr (Fig. 2b). Besides, the type II AFPs (Fig. 25b) is found in sea raven [245], insects [183], and spruce budworm [80]. The fold of the Ca^{2+} dependent lectin family has been detected in the type II

fish AFP of the sea raven [73]. Likewise, ocean pout and eel pout from both the antarctic and arctic have type III AFP (Fig. 25b) [81, 226]. The AFP structure of the eel-pout type III has a distinctive fold made up of tiny β-sheets [249]. No single amino acid is dominant among the 62–66 residues in these proteins. Types II and III of AFPs have numerous structures, including primary and higher-level structures [298].

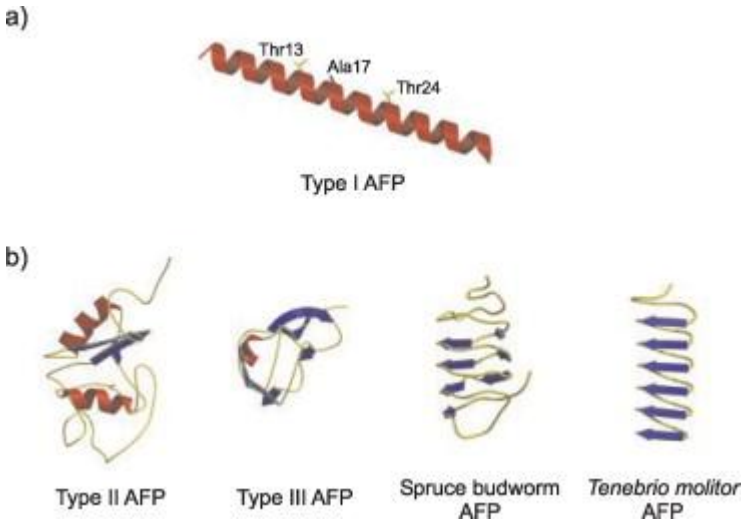

Fig. 25. Structure of winter flounder type I AFP (a). The changed residues have been shown as yellow (Thr13/Thr24) or blue (Ala17) sticks, with the wild-type protein highlighted. The identified constructions of numerous AFPs (b) [72]

On the other hand, antifreeze proteins can be divided into three other types based on their affinity for ice. They adsorb onto the ice surface and reduce the freezing point but do not affect its melting point. Thermal hysteresis (TH) is the term for the temperature differential that can be measured. Hence, antifreeze proteins have been classified as 1) low-TH AFPs, 2) moderate-TH AFPs, and 3) overactive AFPs with varying degrees of TH, which have been found in freeze-tolerant plants (containing perennial ryegrass, Lolium perenne), some freeze-intolerant fish (such as the ocean pout), and certain insects (including the beetle Tenebrio Molitor), respectively [175, 222]. Indeed, they can connect with embryonic crystals and limit their growth process within a specific temperature range, reducing the freezing point of bodily fluid in a non-colligative way [298]. The adsorption-inhibitory hypothesis

proposes that the inhibition ability is derived from the Kelvin effect, generated mostly by the adsorption of AFPs on the ice surface [201]. Lin et al. [143] developed a detailed computational model for glycine-rich AFPs (6.5 kDa) found in snow fleas (sfAFP). They considered AFP's circular dichroism spectra, disulfide bonds, and tripeptide repeat pattern discontinuities. The 81-residue polypeptide was arranged in the model as a bundle of six short polyproline type II helices linked (by one exception) via proline-containing turns. Intra-molecular interaction between the helices, enhanced with regularly spaced twists and disulfide linkages, stabilized the sfAFPs. This modeled protein, like many AFPs, was amphipathic with a predicted hydrophobic ice-binding side. In Fig. 26, the completed reduced structure of sfAFP can be seen in the stereo.

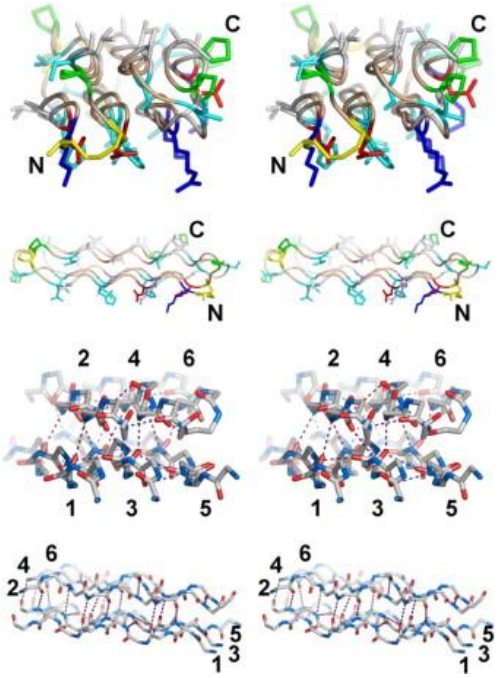

Fig. 26. Stereo views of sfAFP structure shown as tube backbone plus side groups (upper panels). Residues are color-coded: negatively/positively charged (red/blue), prolines (green), glycines (tan), cysteines (yellow), uncharged polar (cyan), and hydrophobic (white). C- and N-termini are labeled. Lower panels show the repetitious backbone with intra-segment hydrogen bonding (dotted lines) and segments labeled 1–6. Blue and red atoms represent nitrogen and oxygen, respectively. Only helices are depicted; loops are omitted [143].

Given the features of the mentioned organisms, AFPs and AFGPs can be used as efficient additives in preventing the growth of hydrate crystals, which leads to their introduction as environmentally friendly KHIs [6, 102, 278]. Zeng et al. [303, 304] reported the first application of antifreeze proteins, active fragments thereof, mimetics of these antifreeze proteins, and active fragments thereof as clathrate hydrate inhibitors, which could reduce the rate of clathrate hydrates reforming after melting. They investigated the effect of two types of antifreeze proteins, including insect AFP (CfAFP) and fish (wfAFP) AFP on THF hydrate formation. The inhibition effect of AFPs was also compared with PVP. They discovered that wfAFP and CfAFP were more effective than PVP in changing the growth morphology of the THF hydrate crystal to limit hydrate formation. Surprisingly, both AFPs demonstrated the potential to prevent the "memory effect," in which hydrate crystallization proceeds more rapidly after the first production. Their group [276] subsequently used quartz crystal microbalance-dissipation (QSM-D) assessments to explore the differences in hydrate recrystallization and better understand the interaction mechanism between AFP and hydrate. They found a relationship between the inhibitory mechanism and heterogeneous nucleation, in which antifreeze proteins operate in the heterogeneous nucleation region and suppress memory effects. Besides, Al-Adel et al. [3] performed kinetic studies in the presence of type I AFPs on the methane-water cell to determine the effectiveness of the AFPs as KHIs, particularly their impact on the hydrate growth time. Under identical temperature, pressure, and weight percent conditions, they compared the results to those obtained using a traditional polymer as a KHI, N-vinylpyrrolidone-co-N-vinylcaprolactam [poly(VP/VC)]. They also conducted a set of tests with poly (VP/VC) to investigate the concentration impact on hydrate growth inhibition. The results demonstrated that APFs could inhibit the rapid reformation of hydrate crystals. Researchers believed these inhibitors, known as ice-structuring proteins (ISPs), had a greater impact than simply acting as an antifreeze. Jensen et al. [93] studied the effect of two type III ISPs, including ocean pout and mealworm Tenebrio

Molitor on the growth of CH_4 hydrate formation and evaluated the hysteresis freezing points (HFP) of the various solutions. According to the findings of this study, in the presence of a sufficiently high concentration of ISP, the profile of nonlinear growth would initially emerge, attributable to the inhibitor adsorption on the surface of growing hydrate crystals because ISP could limit the surface area available for growth. A linear growth profile occurred when ISPs were no longer present for the absorption on the hydrate surface. The linear development duration, however, was inhibited based on the initial concentration of the ice-structuring proteins. It should be mentioned that Tenebrio Molitor was a more effective KHI than the other type III ISP and PVP.

Most of past research has focused on the inhibitory effect of AFP on hydrate growth after the nucleation step. Ohono et al. [179] performed a statistical investigation on hydrate nucleation to better understand the inhibitory effect of AFPs (all three categories of TH ice activity and two synthetic inhibitors) on a natural gas hydrate. They discovered that the nucleation inhibition process by KHIs is time-dependent and AFPs significantly affect nucleation. They stated that the inhibitory actions required for nucleation and growth differ in the mechanisms. Furthermore, the effect of AFP on cubic sII hydrate and hexagonal ice in protein interactions with the surfaces of the two crystals is not always the same. According to the work of Gordienko et al. [71], AFPs have the potential to adjust sII THF hydrate crystal morphologies via attaching to the hydrate surface and limiting growth in a manner similar to PVP. They further examined the effects of various AFPs on hydrate nucleation and the hydrate growth rates of the sII natural gas. They employed clones from the perennial grass, Lolium perenne (Lp), having lower TH and type III AFP from the ocean pout fish with higher activity. They then encode these AFPs, either with or without a green fluorescent protein (GFP). The formation and growth rate of sII gas mixture hydrate in presence of AFPs at high pressure indicated that AFPs outperform PVP as hydrate inhibitors. Fig. 27 shows the AFPs adsorption on THF hydrate.

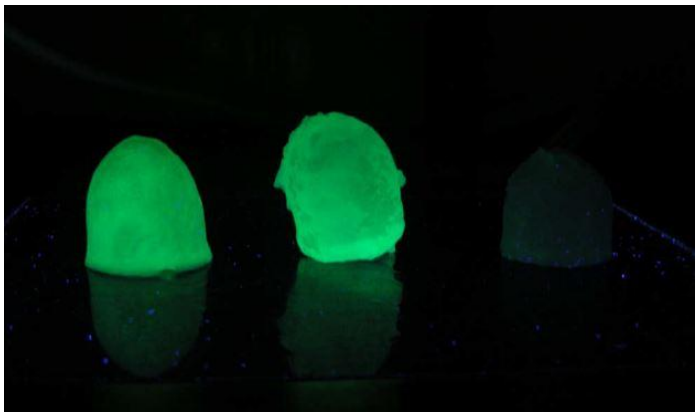

Fig. 27. The AFPs adsorption on THF hydrate. After just being produced in samples containing LpAFP-GFP (center) and type III AFP-GFP (left), typical THF hydrate polycrystals fluoresce and turn green under UV light. The THF hydrate crystals produced in GFP control samples showed no fluorescence (right). The sizes of the samples ranged from 3 to 3.5 cm [71]

In another study, Myran et al. [167] evaluated the inhibition effect of LpAFP-GFPs on natural gas hydrate formation, containing CH_4 93%, C_2H_6 5%, and C_3H_8 2%. LpAFP-GFPs included wild-type protein and compact threonine to a bulky tyrosine at the 43rd (i.e., T43Y) and 53rd (i.e., T53Y) residue. Furthermore, the polycrystal adsorption of a model clathrate such as THF hydrate was considered. It has been suggested that the relatively 'flat' ice binding faces (IBF) interact with the ice embryo surface when the AFPs adsorb to ice. They pinned it and prevented subsequent growth at the equilibrium temperature. Indeed, they created the steric mutations on the manufactured LpAFP-GFP to specify the main faces for hydrate binding. Mutagenesis to obtain further substitutions was successful. In addition, Jensen et al. [31] tested three various experimental methods to find the hydrate induction time of sI (methane) and sII (natural gas). They found that the hydrate formation rate increases by adding heptane and salt to the cell as an ordinary model for light crude and seawater. They added the type III ISP found in the ocean pout to check the possibility of its KHI activity. The results demonstrated that the ISP was better than PVCap for both sI and sII. They suggested that ISPs can be a favorable candidate as green KHIs.

In the following, Daraboina et al. [31–33] carried out three different and parallel investigations on chemical H1W85281 and PVP along with biological type III AFPs or I on multicomponent natural gas ($CH_4/C_2H_6/C_3H_8$) hydrate formation and decomposition. Firstly, they evaluated the hydrate formation in high-pressure differential scanning calorimetry [32]. They indicated that all the inhibitors remarkably reduced the hydrate formation and delayed hydrate nucleation. They observed multiple and complex melting peaks of hydrate formation with chemical inhibitors, including H1W85281 and PVP, which changed with later reformation cycles. In contrast, the type III AFP resulted in a single and less stable hydrate peak, which stayed reproducible and consistent via multiple cycles. Secondly, they tested a newly stirred reactor to study the hydrate decomposition and inhibition in presence of the additives [33]. They recorded the fastest growth rate for PVP, with the slowest growth (by a ratio of 2.2) and highest induction times (by a ratio of 33.6) for HIW8581. Moreover, comparing the growth rate and induction time, type I AFP presented more applicability than either type III AFP or PVP. The hydrate two-stage decomposition for H1W85281 and PVP was indicative of heterogeneous crystals. Furthermore, the decomposed hydrate with either AFP type was the same as no KHI controls but quicker. Consequently, they checked the compositional and structural changes of formed hydrate using Powder X-ray diffraction (PXRD), nuclear magnetic resonance (NMR) spectroscopy, and Raman spectroscopy [31]. They showed that sI was present in H1W85281 and PVP solutions. However, using AFP-III, a fairly homogeneous sII appeared with weaker proof of sI. They demonstrated that both types of inhibitors could reduce big cage methane occupancy by~25%. They stated that the big cage of CH_4 guests could be substituted with ethane when the chemical inhibitors were used. However, about 10 percent of the big cages were not fully filled in the case of AFP-III. Moreover, Daraboina et al. [34] determined the efficiency of magnetic resonance imaging (MRI) test to check out the utility of biological (type I and III AFPs) and chemical (H1W85281) inhibitors on hydrate growth or nucleation of mixed natural gas ($CH_4/C_2H_6/C_3H_8$) at the microscopic and

local scales. In addition, they compared the results with the macroscopic size data achieved via more-common gas uptake tests applying a stirred cell. They demonstrated that MRI could be an effective device for evaluating and visualizing of KHIs in natural gas hydrate formation. The MRI results revealed that AFP-I was more effective in lowering growth of hydrate than AFP-III. Reyes et al. [204] reported the synthesis and applicability of the pseudo-polypeptides series, poly(N-alkylglycine)s, as KHIs with different lengths and alkyl side chains for the first time. They used polymers with identical molecular weights to compare the performance in the multi-rocking cell at high pressure of natural gas blend with sII. They also determined that the best polymer was poly(N-propylglycine). Figure 6 depicts the structure of applied pseudo-polypeptides. The best performance was achieved by poly(N-propylglycine) with a molecular weight of 2.2 kDa, even better than PVCap. Go et al. developed three dipeptides (Gly-Gly, Ala-Gly, and Ala-Ala,) as green KHIs for inhibition of CH_4 hydrate formation [68]. The results of high-pressure autoclave and μ-DSC showed that all dipeptides inhibited CH_4 hydrate formation. Among them, Ala-Gly ranked as the most effective, and its inhibition efficiency was close to that of PVCap at 1 wt %. Additionally, the MD simulations revealed that the *N*-termini of the dipeptides were the critical components for preventing the CH_4 hydrate. Sharifi et al. [231] evaluated the efficiency of two different types of AFP as biological KHIs under possible conditions of subsea pipeline. They provided saline water, liquid hydrocarbon, and a multi-component gas mixture with great driving forces proper for hydrate formation. Type I AFP not only reduced induction time like commercial KHIs, but also the hydrate growth rate decreased significantly in exerting mentioned situations. Additionally, the dissociation of gas hydrate took longer. They reported that AFP III was better than I without reducing nucleation time under the same conditions. Perfeldt et al. [187] tested an insect AFP from the longhorn beetle, *Rhagium mordax* (RmAFP1) as the most powerful protein for freezing inhibition. They stated that it could inhibit CH_4 hydrate similar to PVP at 0.277 wt %. They also compared the efficiency of noted AFP with the amino acids

L-threonine, L-valine, and BSA protein. The amino acids or proteins did not inhibit hydrate formation in general. Thus, they proved the proficiency of RmAFP1 as a modern green KHI. Sharifi et al [232] evaluated two different AFPs, including type I and III, as green KHIs via two identical high-pressure cells (a device involving two crystallizers and a micro differential scanning calorimeter) in saline water. They indicated that the inhibitory action of AFP I was reduced in saline solution in comparison with AFP III. Adding the AFPs could initially adjust the gas hydrate growth, but it only reached the value when the crystal growth rate accelerated quickly. They found that the melting point was delayed with hydrate formation, and subsequently, the hydrate decomposition was prolonged using AFPs. Walker et al. [277] reviewed AFPs as gas hydrate inhibitors. They provided a complete description of the AFPs types and introduced more practical AFPs for important structures for hydrate formation and various hydrate formers, including natural gas, CH_4, and CO_2. They reported that the AFP adsorption on the surface of gas hydrate is distinct from commercial KHIs according to gas enclathration analysis, making them more useful in some field applications. Reyes et al. [205] synthesized a wide range of poly(β-peptoid)s, including poly(N-alkyl-β-alanine) copolymers and homopolymers with different N-alkyl replacements. For the first time, they investigated poly(β-peptoid) activity as an eco-friendly KHI. They utilized a mixture of natural gas in rocking cells with high pressure to raise gas hydrate formation with sII. Using the structure-activity relationship, they confirmed that in the case of water-soluble polymers, the availability of bigger aliphatic side groups significantly improves kinetic inhibition. Fig. 28 illustrates the structure of applied poly(β-peptoids).

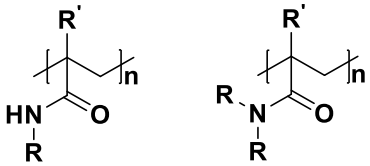

Fig. 28. Poly(N-alkyl(meth)acrylamide)s and poly(N,N-dialkyl (meth)acrylamide)s, in which RRN = cyclic imines, R = alkyl, and R′ = H or CH_3 [3]

Daraboina et al. [35] employed a HP-μDSC to study the formation and dissociation of CH_4 hydrate along with hyperactive RmAFP and Luvicap Bio. They utilized a structured capillary dispersion technique, which improved their capacity to determine the influence of the inhibitors in a limited quantity. They discovered that Luvicap Bio (relative strength in comparison with buffer: 13.45 ºC) was more effective as a nucleation inhibitor than RmAFP (9 ºC). Nevertheless, the addition of RmAFP not only delayed hydrate nucleation, but also dramatically decreased the amount of hydrate generated (20–30% following nucleation). Luvicap Bio, unlike RmAFP, increased the quantity of hydrate generated following nucleation. As a result, RmAFP can be used as a natural KHI in the oil and gas pipelines. Moreover, Sharifi et al. [233] assessed the effect of various concentrations of type III AFP, PVCap, and Luvicap Bio on the dissociation of propane hydrate using a HP-μDSC. Surprisingly, hydrates generated by the mentioned KHIs could be dissociated at temperatures other than those suggested by hydrate equilibrium predictions, even at higher temperatures. Unexpectedly, increasing the inhibitor amount reduced the quantity of gas hydrate dissociation at the equilibrium temperature. These findings suggest that because hydrate remediation with KHIs necessitates greater melting points, removing hydrates under these conditions consumes more energy. Zhou and Ferreira [312] investigated the influence of AFPs on the rate of CO_2 hydrate formation in a heat exchanger with a coil. They compared their results to those found with other additives such as poly[VP/VC]. The studied AFPs had a concentration of 0.001 wt %. They claimed that the presence of AFPs had just a minor effect on the solution's supercooling degree. Type-III AFPs greatly reduced the gas dissolution rate into the solution, as seen by the reduced solution density rise rate. Similarly, they employed a crystal growth model to estimate the impact of AFP on the rate of CO_2 migration from the bulk to the crystalline phase. The results showed that the presence of AFPs lowered the hydrate formation rate by roughly 35% corresponding to a reduction of around 21% in the mass transfer coefficient. Voets [274] provided a comprehensive review of recent achievements in IBPs and synthetic equivalents.

They highlighted the considerable insight into IBP operating as a platform for experience and understanding the development of low-cost, bio-inspired mimics via scalable techniques. They also described recent achievements in applying IBPs and related analogs to ice-templating techniques, cryopreservation improvement, gas hydrate prevention, and other advancements. Kelland et al. [110] analyzed a variety of easily obtainable and biological protein-based compounds extracted from plant and animal sources, such as green KHIs and an AFP, utilized to form ice cream smoother. All experiments were conducted in high-pressure titanium and steel rocking cells on a sII-forming gas combination. They reported that AFP performed the best, though this was due, at least in part, to certain thermodynamic inhibition by salts and other compounds in the mixture. Several protein-based compounds (tryptones and peptones) performed better as KHIs than PVP. The uncertainties of pressure and temperature measurements were 0.2 MPa and 0.1 ºC, respectively. Udegbunam et al. [267] examined the CH_4 hydrate inhibitory activity of three different synthetic AFPs. They considered two synthetic AFPs to be extremely active in terms of ice inhibition: "Maxi", a fish AFP, and a beetle AFP (TmAFP). The final grass protein was identified as a low activity AFP (LpAFP). They discovered that "Maxi" has never been evaluated as a hydrate inhibitor before, lowered hydrate growth by order of magnitude compared to pure water. LpAFP and TmAFP showed kinetic inhibition, but not as well as 'Maxi'. Qin et al. [191] employed whey protein as a natural KHI in a transparent cell and an autoclave coupled with a particle video microscope (PVM). The pressure decreasing technique was used to determine the hydrate induction time using natural gas. They showed that whey protein has better inhibition efficiency than PVP. They discovered that as the amount of whey protein was increased, the induction time prolonged linearly until it approached about 2.5 wt %. They evaluated the practicality of whey protein in a water + oil system without and with Tween 20 as it is normally impossible to employ KHIs in situations with higher water cuts. Adding Tween 20 increased the induction time noticeably under the same working conditions, explained by protein-emulsifier interactions in

aqueous systems. Singh and Suri [243] studied the synergy effect of bovine serum albumin (BSA), casein peptone, and whey protein on the inhibition of activity of commercial KHIs. They reported that all the three proteins show good synergy effect for Luvicap 55w, PVP, PVCap, and HIOP-1800. BSA considerably improved the induction time of PVP and PVCap systems by 32% and 19%, respectively. It showed excellent synergy with HIOP-1800 and increased its induction time by 65%. Peptone from casein worked as good synergist for PVCap, and enhanced its induction time by 15%. Whey increased the induction time of HIOP-1800 solution by 15%. Mu et al. [164] studied the nucleation and dissociation of CH_4 hydrate using a monomeric streptavidin of RmAFP1 (mSA-RmAFP1) and four different amino acids, including lysine, proline, histidine, and tyrosine. They compared mSA-RmAFP1 with PVP and Luvicap Bio using a rocking cell setup. The findings revealed that 0.225 wt % of mSA-RmAFP1 inhibited the hydrate nucleation. The amino acids lysine, histidine, proline, and tyrosine had a minor inhibitory effect on the formation of CH_4 hydrate. Furthermore, under laboratory conditions, CH_4 hydrate generated in the presence of tested inhibitors showed a lower onset decomposition temperature than the non-inhibited system. In another study, Mu and Solms [165] examined the influence of mSA-RmAFP1 on the nucleation of combined natural gas hydrates in the presence of crude oil and salts. They compared the effectiveness of the inhibitor with glycine, starch, chitosan, and PVP. In diverse conditions (salt water containing 15% crude oil, salt water, and pure water), 0.225 wt % of mSA-RmAFP1 inhibited natural gas hydrate nucleation more successfully than PVP. The inhibitory capabilities of different substances are as follows: starch < chitosan < glycine < PVP < mSA-RmAFP1. Solms [248] provided an excellent reference for the description of gas hydrate and associated structures, as well as gas hydrate thermodynamic inhibition. He discussed LDHIs along with strategies for determining their effectiveness. AFPs and similar references were eventually classified as hydration inhibitors by him. He suggested the AFPs should be produced on a large scale and at a low cost and tested on realistic reservoir fluids. Han et al. [76] used the cell surface display (CSD)

technique to study the expression of AFPs on Escherichia coli an effective anchoring motif for the presentation of peptides or proteins. On the exterior surfaces of bacterial cells, they revealed monomers to hexamers of type II and III AFPs. They tested mixed natural gas formation and found that as the number of peptides bound to the cells increased, AFPs had a stronger KHI efficacy. Furthermore, they noted that independent of AFP types, the optimum KHI activity of the AFPs might be attained with higher doses of the cultures when the inducer concentration is maximized. Fig. 29 shows the arrangement of AFP represented on the surface of bacteria.

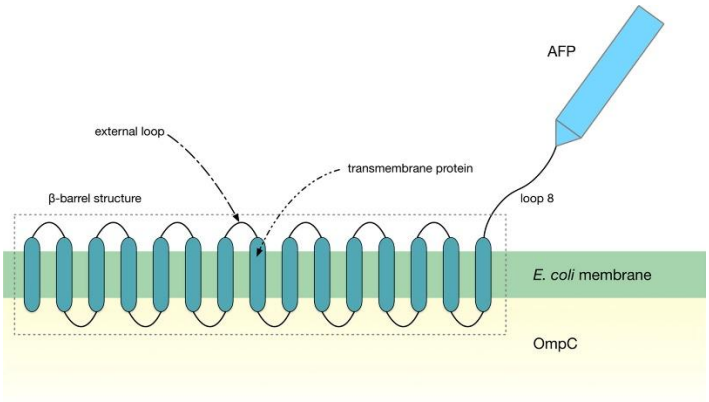

Fig. 29. The arrangement of AFP represented on the surface of bacteria [76]

Jia et al. [94] introduced a polycyclic antibacterial peptide, nisin, as a natural KHI with good biodegradability and biocompatibility. They reported that a solution containing 0.5 wt % a nisin decreased hydrate formation by 37.81% and prolonged the induction time five times at a subcooling of 10.13 ºC. Nisin maintained its inhibitory power at high temperature and low pH acid-alcohol coupling conditions, which makes it as a an applicable KHI for field applications. The adsorption of nisin molecules on the surface of hydrate crystal and the formation of hydrogen bonds with water molecules were proposed as the main inhibition mechanism of the inhibitor. The uncertainties of pressure and temperature measurements were 0.01 MPa and 0.01 ºC, respectively. Zhang et al. [305] introduced a set of alternate peptides containing glycine- N-substituted valine dipeptide repeating blocks as green KHIs. Hydroxyl, n-propyl, ethyl, and methyl groups were used as N-

substitutions. In the case of natural gas hydrate, all the mentioned polypeptides had superior KHI activity in comparison with a low molecular weight PVP. PA-Pep, a polypeptide with n-propyl groups, showed the best performance compared to PVCap at the same dosage. Fig. 30 depicts the structure of studied alternating peptides.

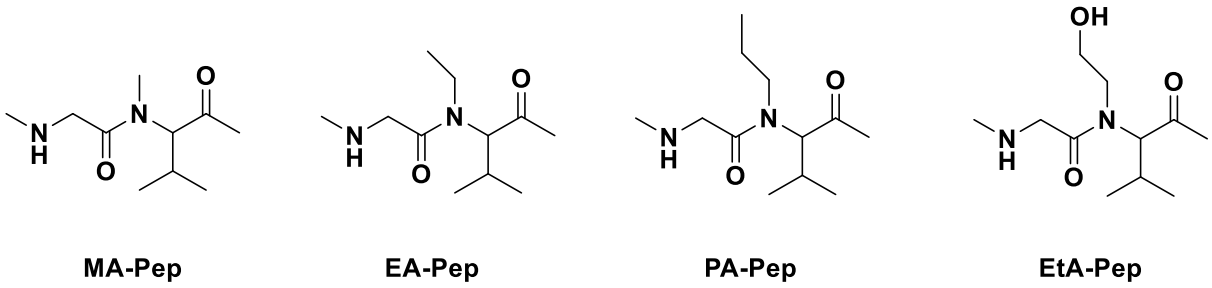

Fig. 30. Chemical structure of alternating peptides [3]

Since laboratory studies for ranking KHIs are costly and time-consuming, computer studies are useful tools for gathering preliminary data on the inhibition action of the additives before undertaking experiments. Previous research on this topic demonstrated the effectiveness of these kinds of molecular simulations. For instance, using density functional theory (DFT), CruzTorres et al. [30] investigated the potential of AFGPs to suppress clathrate-hydrate formation. To describe the inhibitor–clathrate relationship, they employed the Ala–Ala–Thr–Ala (AATA) peptide and a 5^{12}cavity, dodecahedral $(H_2O)_{20}$. AATA near water cavities creates complexes with varying cavity/peptide ratios, causing cavity deformation and elongated hydrogen bonds in dodecahedral $(H_2O)20$. AFGPs bind to the clathrate interface, preventing new water molecules from entering and inhibiting crystal formation. Complex development was linked to amide IR bands, with the amide "A" band most vulnerable to hydrogen bonding. Fig. 31 shows AATA peptide charge distribution at numbered locations, while Fig. 32 displays optimized complex geometries. Amide IR bands detected hydrogen bonds between clathrate and peptide molecules, showing red-shifts compared to isolated peptides. Larger shifts correlated with higher hydrogen bonds per peptide atom, suggesting DFT is useful for ranking KHI activity.

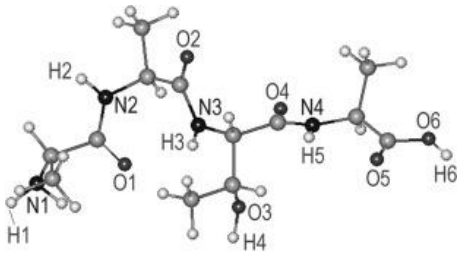

Fig. 31. Numbered sites of AATA peptide correspond to those atoms with negative or higher positive charges [30]

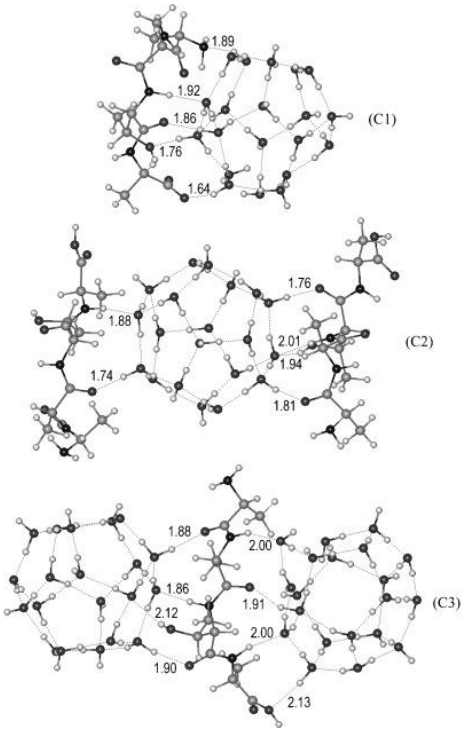

Fig. 32. Optimized geometries of the complexes caused by the AATA molecules-5^{12} cavities interactions [30]

San et al. [254] examined gas hydrate prevention using molecular modeling and developed x-ray crystallographic geometries. The interior crystalline water network of the Maxi AFP, which extends to the protein's external layer was very comparable to the {100} planes of sII gas hydrate. In silico modeling, Maxi and type I AFP binding to sII hydrates were constructed easier thanks to the crystalline structure of the water network. Also, experimental results of Maxi bound to the THF sII model hydrate supported the models. They proposed that the absorbance-inhibition and anchored clathrate water are the main mechanism for the adsorption

of inhibitors on the hydrate surface, inhibiting the formation of gas hydrate. Besides, molecular dynamics (MD) simulations were utilized by Bagherzadeh et al. [9] to identify the mechanism action of wfAFP in suppressing CH_4 hydrate formation. They discovered that the wf-AFP was bound to the CH_4 hydrate interface through the collaborative binding of a series of hydrophobic methyl chains to the vacant half-cages at the hydrate/water interface. They determined that each binding pair was made up of the methyl side group of two alanine and threonine residues located four and seven positions down in the protein sequence. Finally, Li et al. [139] simulated the alanine-rich short peptides (type I) as an efficient substitute for KHIs. They reported the design concept through MD simulation, in which at least two methyl groups docked into adjoining spaces in an ordered spatial configuration for stable hydrate adsorption, which would be critical for hydrate abatement based on the adsorption-inhibition hypothesis. They proved the process of dual methyl group docking as well as the calculation and mutation of work profiles for moving peptides from the hydrate layer to the aqueous solution. They concluded that inhibition effects and hydrate binding could be improved by correctly incorporating lysine into the peptide. Indeed, Lysine's large side chain made peptide bending easier, allowing more methyl to attach to hydration cages. Their findings may help to guide the reasonable development of eco-friendly and effective KHIs. Chen et al. [24] investigated the roles of functional groups of Tenebrio Molitor antifreeze protein (TmAFP) on inhibition of CH_4 hydrate growth. According to simulations, the adsorption of TmAFP on the hydrate growth surface occurred by trapping several functional groups, especially the methyl groups of threonine, in half hydrate cavities. Additionally, amino acids can be incorporated in half cages through the interaction of their amide groups, mainly hydrogen bonding. Surprisingly, the perturbation of surrounding water molecules was observed in the presence of TmAFP before adsorption, unlike the behavior of fish AFPs. Nevertheless, functional groups of the backbone do not work as the adsorption sites because the amino acids of this region do not match the adjacent hydrate cage. They concluded that the structure of AFPs

plays a crucial role in inhibiting CH_4 hydrate growth. Generally, AFPs show significant inhibition effect on the formation of gas hydrates under different conditions; however, most of them are too expensive substances and cannot be prepared on a large scale. In addition, more theoretical studies are still required to clarify their detailed mechanism action. Moreover, experimental investigations should be performed to assess the compatibility of AFPs with other chemicals that are injected into the oil and gas pipelines such as corrosion inhibitors.

6. Synthetic polyester and polyamide

Although the biodegradation process of amide groups is slower than ester groups, a KHI containing either of these functional groups shows more biodegradability than polyvinyl KHIs [105]. Polyesters and polyamides are high molecular weight compounds obtained by polycondensation of polybasic acids or their anhydrides with polyatomic alcohols/amines [161]. Natural polyesters (amber, wood resin, and shellac), polyamides (wool and silk), and artificial ones are well-known and have been used for various applications [78, 90, 176, 202, 271, 300]. Aliphatic polyesters are considered biodegradable materials as their ester bonds can be hydrolyzed in alkaline solutions [313]. Leinweber and Feustel [135] patented a new class of KHIs based on polyesters with a molecular weight from 0.5 to 500 kDa (more preferably from 1 to 50 kDa) as represented in Fig. 33. The final inhibitor is a product of the interaction of the compound of formula 1 with the compound of formula 2. In this case, n is 0, 1, or 2, and A is an optionally substituted C_1-C_{40} group. In the compound of formula 2, m is a number from 2 to 10 and, B is an optionally substituted C_2-C_{40} group.

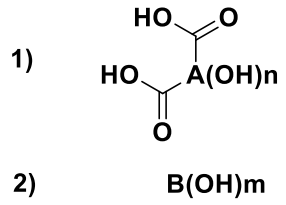

Fig. 33. Chemical structure of degradable polyesters [3]

A is preferably an alkylene radical containing 2 to 6 carbon atoms, and B is an alkylene radical containing 2 to 6 carbon atoms. m is preferably 2 to 6. They claimed that these compounds inhibit nucleation, growth of hydrates, and agglomeration of natural gas hydrate formation at 9 MPa and concentration of 0.02 to 1 wt %. Polyesters retarded the nucleation of hydrate formation in the interval from 3.5 to 4.6 h, which was higher than commercial KHI. In another patent [136], they claimed that a modified class of polyesters based on the previous patent as biodegradable KHIs. The difference is that the remaining hydroxyl groups of polyesters are further esterified with nitrogen-containing carboxylic acids with a hydrocarbon chain from C_1 to C_{20} or mixtures of these acids with fatty carboxylic acids containing from 6 to 30 carbon atoms. The molar ratio between the number of free OH-groups of the polyester complex obtained in the first step and the N-containing carboxylic acid (or mixture of acids) is from 1:0.1 to 1:1. Preferred N-containing carboxylic acids are: aspartic acid, glutamic acid, pyroglutamic acid, and aceturic acid. The study of the inhibitory properties of the final compounds was carried out similarly to the previous work [135]. Unlike the parent compounds (see previous work [135]), the described reagents more effectively inhibited hydrate formation, completely preventing this process in the interval from 10.5 to 14.2 h. These substances also exhibited anti-agglomerant properties, surpassing the commercial reagent (quaternary ammonium salt) by 2.5 to 4 times. The authors also patented [65] a class of hydrate inhibitors with improved biodegradability based on pyroglutamic or glutamic acid polyesters and alcohols containing up to 100 hydroxyl functions. The polyesters were prepared by non-catalytic or acid-catalyzed condensation of pyroglutamic or glutamic acid with an alcohol. These polyesters can inhibit nucleation, growth and/or agglomeration of natural gas hydrate formation at 5 MPa and concentrations of 0.02 to 1 wt % along with improved biodegradability. The studied reagents inhibited the process of hydrate formation in the interval from 5.9 to 8.4 h at a concentration of 0.5 wt %. Biodegradation was studied according to OECD 306 compared to commercially available PVP for 28 days. The

biodegradability of PVP was shown to be 5%, while the biodegradability of the polyesters obtained ranged from 35% to 71%, which exceeded that of the commercial inhibitor by a factor of 7 to 14. Leinweber et al. [137] claimed that a new class of biodegradable KHIs is based on substituted polyethylenimines (Fig. 34) with molecular weight preferably from 2 to 10 kDa.

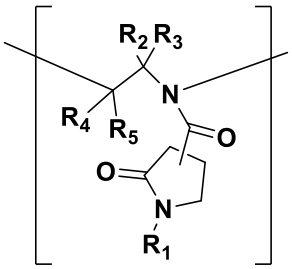

Fig. 34. Chemical structure of biodegradable substituted polyethyleneimines, where R_1 represents H, C_1-C_{30}-alkyl, C_1-C_{30}-alkenyl, or C_7-C_{30}-alkylaryl, and R_2, R_3, R_4, R_5, each independently represents H or C_1-C_6-alkyl [3]

This class of polymers can effectively inhibit nucleation, growth and/or agglomeration of gas hydrates at a concentration of 0.01 to 2 wt %. The initial oxazoles are obtained by condensing of pyroglutamic or N-alkyl-5-oxopyrrolidine 3-carboxylic acid with amino alcohols at 140 to 220 ºC, both with and without a catalyst. The inhibitory effect of the substances and their biodegradation were carried out similarly to the previous work [65]. The studied polyethyleneimines inhibited the process of natural hydrate formation in the interval from 15.0 to 25.0 h at a concentration of 0.5 wt %. Some inhibitors also exhibited anti-agglomerant properties, they were 4 times more effective than a quaternary ammonium salt. The biodegradability of obtained polyethyleneimines was in the range 30% to 72%, which exceeds this commercial inhibitor (PVP) indicator by approximately 6 to 14 times. A new class of biodegradable KHIs based on amides and esters of citric acid was described in another patent by Gonzáles and Djuve [70], as shown in Fig. 35.

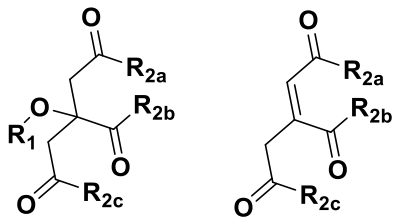

Fig. 35. Chemical structure of biodegradable citric acid derivatives as KHI [3]

In the structure of the inhibitors, R_1 represents H or acetyl, R_2 represents H, -OR_3 or -NR_4R_5, while R_3 is H, C_1 is C_6-alkyl or carbonyl derivative. R_4, and R_5 were selected from the group consisting of H, C_1-C_{18}-alkyl (preferably C_1-C_4 for better solubility), alkanol, alkoxy, cyclic/aromatic, or alkylene-containing substituents. Citric acid derivatives effectively inhibited synthetic natural gas hydrate formation at concentrations raining from 0.01 to 6 wt % at 7 MPa. It was shown that some compounds at 6 wt % concentration provided a subcooling temperature of 14.3 ºC, while Luvicap 55W showed a subcooling value of 9.7 ºC at 1 wt % concentration (subcooling for pure water was 2.5 ºC). For most of the synthesized compounds at 1 wt % concentration, this value did not exceed 5-6 ºC. Additionally, the biodegradability of the obtained citric acid derivatives was shown to be from 17% to 37%. Chua et al. [28] developed an interesting class of bifunctional inhibitors based on polyaspartamides (Fig. 36) that could simultaneously prevent natural hydrate formation and salt deposition (sI).

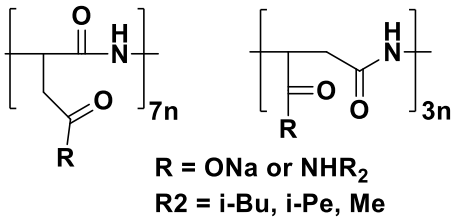

Fig. 36. Chemical structure of biodegradable polyaspartamides as KHI and SI [3]

The synthesized polyaspartamides showed a high turbidity temperature and proved to be compatible with brines containing calcium ions up to 0.2 wt %. They reported that at a concentration of 0.5 wt %, the temperature value at which hydrate formation was observed for Luvicap 55W was 12 ºC, whereas it was 18 ºC for pure

water at 7.8 MPa. The synthesized polyaspartamides inhibited the formation of gas hydrates up to a temperature of 15.3 ºC. It should be noted that the intensive growth of hydrates in the case of Luvicap 55W started at 8.4 ºC (for pure water at 16.1 ºC). However, an intensive hydrate growth was observed almost immediately after the start of reducing the pressure in the system for polyaspartamide solutions. The uncertainties of pressure and temperature measurements were 0.2 MPa and 0.1 ºC, respectively. New biodegradable KHIs based on polyesters containing amino and ammonium groups (Fig. 37) as pendant groups were claimed by Cole et al [29]. In Fig. 37, A is an acid fragment and B is an alcohol fragment. They showed that the working concentration of the inhibitors is preferably from 0.5 to 3 wt %.

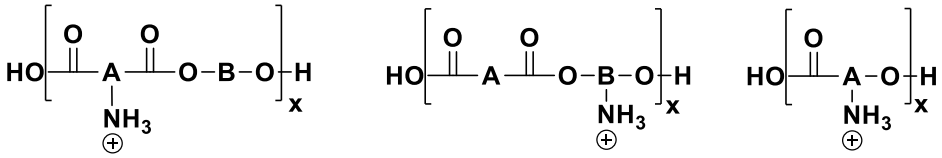

Fig. 37. Chemical structure of biodegradables KHI containing amino and ammonium groups [3]

The inhibitors were prepared by polymerizing an amino-containing dicarboxylic acid with alkylene, oxyalkylenediol or triol. A typical representative is a copolymer of aspartic acid and triethylene glycol. The maximum induction time of 24 h at 6 ºC was achieved for poly aspartic acid-MEG solution. Additionally, the studied polymers showed biodegradation values of 10% to 40%. Reyes et al. [206] introduced new poly(ester amide)s based on citric acid as biodegradable KHI as displayed in Fig. 38. The polymers with molecular weights from 3 to 10 kDa were synthesized by polycondensation reaction using tributylcitrate and ethylenediamine to form hyperbranched polyethylene citramides with NH_2-terminal groups. The amino groups were further functionalized with isopropyl, n-butyl and cyclohexyl fragments using appropriate isocyanates. The onset hydrate formation temperature of 11.6 ºC and 11.0 ºC were recorded for PVCap and PVP, respectively, at 7.6 MPa and a concentration of 0.25 wt %. The studied polymers with hydrophobic groups had the following onset hydrate formation temperature values: 10.7 ºC, 14.9 ºC, and

15.7 ºC for poly-(ethylene citramide)CONHCyHex, poly(ethylene citramide)CONHn-Bu, and poly(ethylene citramide)CONHi-Pr, respectively. An increase in the inhibitory properties of the compounds was observed with increasing hydrophobicity.

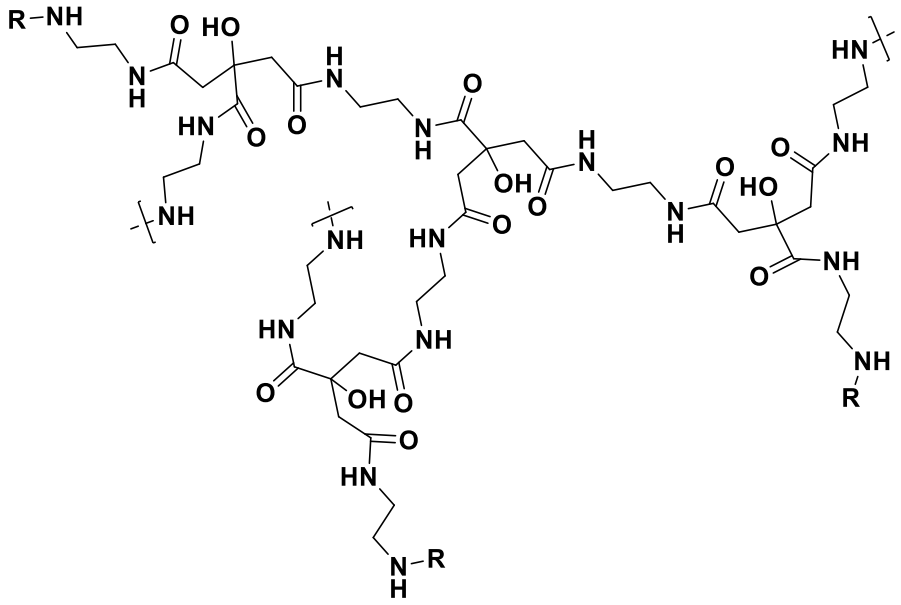

Fig. 38. Chemical structure of biodegradables poly(ester amide)s as KHI [3]

In another study, Wang et al. [281] developed new amphiphilic polyaspartamides based on L-aspartic acid (DAPA) with molecular weight from 185 kDa to 215 kDa as green KHIs (Fig. 39). They demonstrated that the synthesized compounds could inhibit THF hydrate formation (THF/water at a 1:3 volume ratio) more effectively than PVCap and PVP. In blank solution, THF hydrate was formed after 23 minutes at -5 ºC with a sharp increase in viscosity and a moderate increase in temperature. The induction times of HxA-DAPA, HpA-DAPA, OA-DAPA, PVP, and PVCap were 102, 110, 112, 79, and, 100 minutes, respectively, which signify that the induction time increased with increasing the size of the alkyl fragment at the amino group.

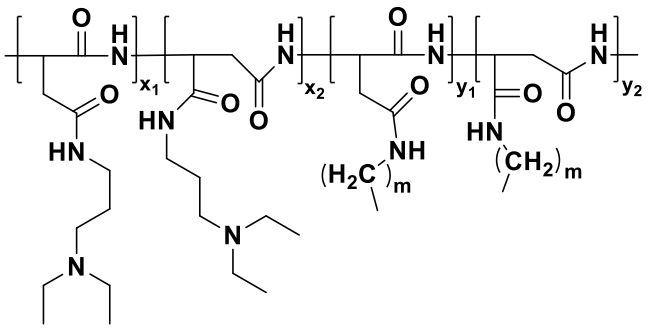

HxA = n-hexylamine (m=5)
HpA = n-heptylamine (m=6)
OA = n-octylamine (m=7)

Fig. 39. Chemical structure of amphiphilic polyaspartamides [3]

7. Grafted polymers

Another promising class of green KHIs for the prevention of gas hydrate formation is graft copolymers. It is a rather diverse class, a branched high-molecular compound whose macromolecules consist of the main chain and side branches differing in composition and/or structure [64]. This method uses of a polymer with higher biodegradability as the backbone and grafting vinylic monomers onto it. It may require some premodification of the polymer to introduce active functional groups to react with vinylic monomers. The biodegradability of the grafted polymers can be enhanced in comparison with pure PNIPMAM or PVCap. Nevertheless, the inhibition performance may be reduced because the portion of hydrate-inhibiting active groups in the grafted polymer is much smaller than the biodegradable backbone. Widmaier et al. [196] claimed a method for preparing grafted polymers based on C2-C4-polyalkylene oxides (preferably polyethylene glycol), including their block copolymers and simple esters or complex ethers and mixtures thereof. This work showed that using polyalkylene oxides with an average molecular weight of 0.3-35 kDa was preferable as KHIs. The final grafted polymers had significantly lower viscosity than their respective counterparts as well as exhibited good biodegradability according to OECD 301 A. The inhibition properties were investigated in a high-pressure autoclave under stirring. A graft polymer based on

polyethylene glycol and a mixture of vinyl acetate-N-vinylcaprolactam at a concentration of 0.45 wt % showed an induction time of 288 h at 3.0 MPa and 4 ºC. Angel et al. [158] patented a method for preparing KHIs based on grafted polymers consist of various hydrophilic or hydrophobic units. Preference is given to polyethylene glycols, polyethyleneimines, polyvinyl alcohols, polyvinylpyrrolidone, and polyvinylamine. The molecular weight of the grafted polymers should preferably be 10 to 100 kDa. It is noted that grafted polymers can also be used in combination with other suitable agents as KHIs. The patent indicated that alcohols, including methanol, isopropanol, butyl glycol, and esters, in particular partially esterified glycols, are preferably used as a solvent that have synergistic effect on gas hydrate inhibition. Solvents with a high flash point and low groundwater contamination, such as water or ethylene glycol are recommended for safety and toxicity risk reduction issues. In another patent, grafted copolymers of various polyamides and maleic anhydride with at least one side chain primarily on N-vinylcaprolactam and/or N-vinylpyrrolidone were developed as biodegradable KHIs by Reichenbach-Klinke and Neubecker [203]. Natural polyamides, especially caseins, gelatins, collagens, blood albumin, soy proteins, and oxidation products, were used as a polyamide component. The proportion of the polyamide component should preferably be in the range of 50 to 70 wt % of the weight of the copolymer. The molecular weight range of grafted copolymers was usually from 5 kDa to more than 10 kDa. Another advantageous feature of the grafted copolymers described according to the application of the invention is their solubility in water and their biodegradability. The polymers delayed the induction time of gas mixture hydrate formation up to 350 h at 0.9 wt % compared to pure water in which gas hydrate was formed after 1 h and 20 minutes. The formation of CH_4 hydrate was also studied under similar conditions. They showed that a copolymer based on hydrolyzed gelatin, maleic anhydride, and N-vinylcaprolactam inhibited the formation of CH_4 hydrate for more than 350 h. Patil et al. [182] patented sodium polyaspartate grafted with a wide range of vinyl monomers with a molecular weight of 1 to 50 kDa as

biodegradable KHI. The monomers used in the patent include (meth)acrylic acid, itaconic acid, maleic anhydride, maleic acid, methyl acrylate, methyl methacrylate, ethyl acrylate, hexyl acrylate, butyl acrylate, styrene, vinyl acetate vinylpropionate, acrylonitrile, acrylamides, methacrylamides, styrene sulfonic acid, allyl sulfonic acid, vinyl sulfonic acid, N-vinylpyrrolidone, N-vinylimidazole, N-vinylformamide, N-vinylcaprolactam, vinylpyridine, ethyloxazoline, and N-vinylacetamide. These monomers were grafted to the polymer backbone in amounts ranging from 1 to 95 wt %. Osama and Cuiyue [166] patented a new class of biodegradable KHIs based preferably on N-vinyl/(met)acrylic amides/esters as shown in Fig. 40.

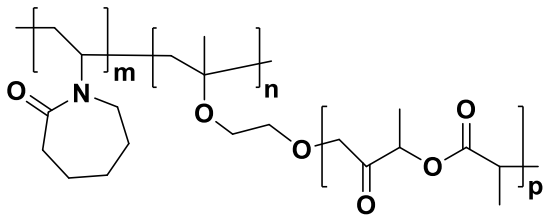

Fig. 40. Chemical structure of N-vinyl/(met)acrylic amides/esters-based KHIs [3]

Both acyclic and cyclic structures based on these monomers were described, which can be arranged in the polymer in various ways, including alternative, block, branched, linear, periodic, and/or random. They indicated that this class of copolymers inhibits hydrate formation at concentrations from 0.1 to 3 wt %. In another patent, a new class of biodegradable KHIs based on at least one ethylene unsaturated monomer, a copolymer of a natural hydroxyl-containing chain transfer agent (for example starch), or a mixture thereof (Fig. 41) was claimed by Holt and Thomaides [84]. The preferred copolymer molecular weight was <10 kDa. Ethylene unsaturated monomers include metacrylic acid, α-chloracrylic acid, α-cyanoacrylic acid, itaconic acid, crotonic acid, maleic acid, cinnamic acid, fumaric acid, vinylsulfonic acid, and vinylphosphonic acid. Without reagents, natural gas hydrate formed intensively at 16°C in 303 minutes at 7.7 MPa. With 0.5 wt% Luvicap 55W, induction time increased to 751 minutes and temperature decreased to 8.3°C. Patented compounds showed induction times of 373-550 minutes and formation temperatures of 14.8-11.7°C.

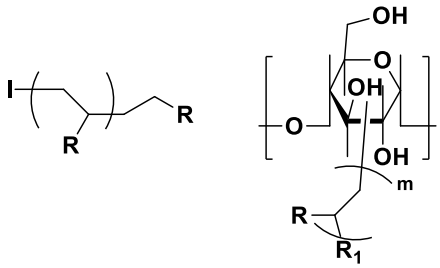

Fig. 41. Chemical structure of biodegradable KHI (A, "I" stands for a fragment of the initiator) [3]

Roosta et al. [213] developed two different series of modified polyvinyl alcohols (PVA) as new inhibitors of methane-propane hydrate growth. The authors reported that PVA is a biodegradable polymer. PVA was modified with acrylamide, acrylonitrile, and methacrylamide (Fig. 42). At 0.75 wt % concentration, the grafted copolymers PVA-g-AM, PVA-g-MAM, and PVA-g-AN reduced the hydrate growth rate from 0.75 in pure water to 0.38, 0.44, and 0.37 (mmol/min), respectively. However, their effectiveness was lower than PVP, which was equal to 0.20 (mmol/min). PVA-AM, PVA-MAM, and PVA-AN showed a competitive inhibition efficiency with PVP. For example, functionalized PVA-AM had even better performance than PVP, reducing the hydrate growth rate to 0.19 (mmol/min). Thus, the authors showed that the synthesized polymers could be ranked according to the intensity of their inhibitory properties as follows: functionalized PVA-AM > functionalized PVA-AN > functionalized PVA-MAM > PVA-g-AN > PVA-g-AM > PVA-g-MAM > PVA.

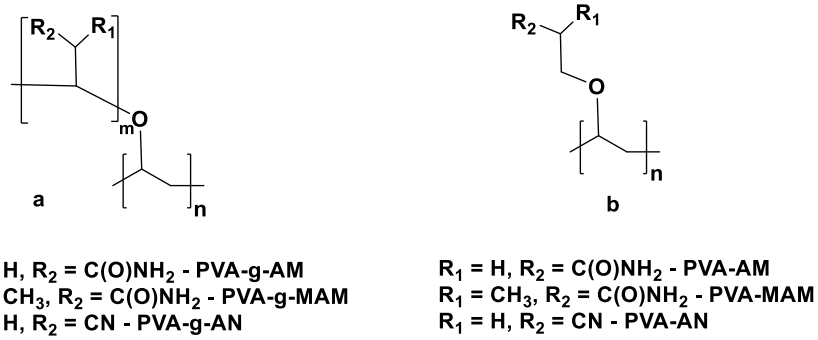

Fig. 42. Chemical structure of biodegradable KHIs based on PVA [3]

8. Miscellaneous

This section reviews several other bio-sources, such as aspartame, vegetable oils, cassava peel, and plant extract used to prepare green KHIs. Farhadian et al. [51] used castor oil to synthesize of a new class of eco-friendly KHI/AA inhibitors. They prepared several water-soluble castor-based waterborne polyurea/urethanes (CWPUUs) using the waterborne technique (Fig. 43). The gas uptake experiments demonstrated that the CWPUUs acted as high-efficiency KHIs. The onset time of CH_4 hydrate formation was delayed 26.8 and 13 times in the presence of CWPUUs with 3.2 and 6.8 kD molecular weight, respectively, compared to pure water. Additionally, CWPUUs with 3.2 and 6.8 kD molecular weight also lowered the onset temperature of hydrate formation by 6.1 and 4.7 ºC in comparison with pure water, respectively. Furthermore, during the hydrate formation the motor torque value remained constant in CWPUU solutions, suggesting that the aggregation of hydrate particles did not occur. Their findings indicate that CWPUUs have both KHI and AA properties. The uncertainties of temperature and pressure measurements were 0.1 ºC and 0.005 MPa, respectively.

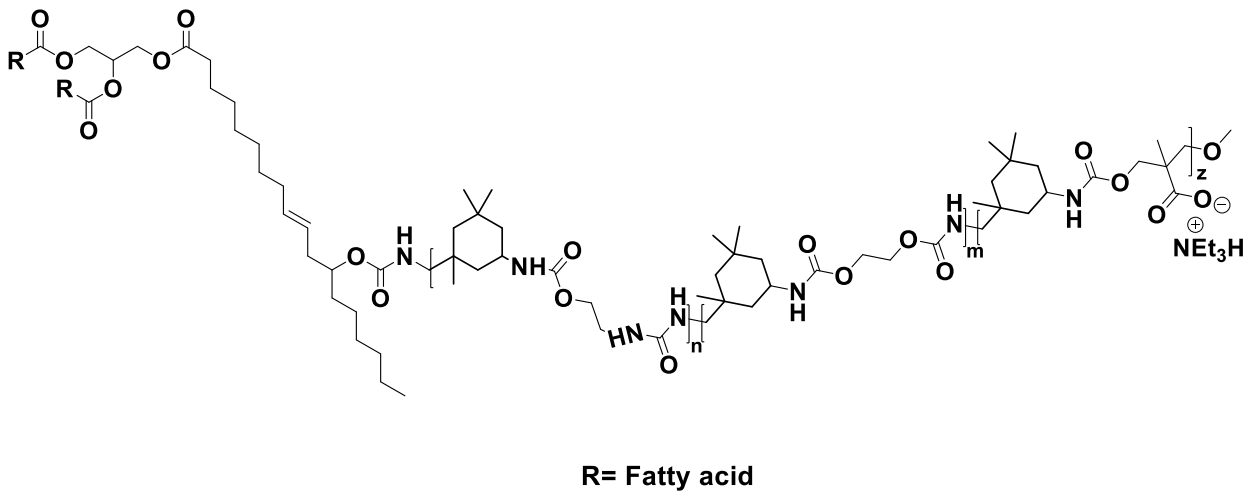

Fig. 43. Molecular structure of CWPUU [3]

Farhadian et al. [53] also developed a novel hybrid inhibition of corrosion and gas hydrate for flow assurance as incompatibility of gas hydrate and corrosion inhibitors is a serious problem inside the oil and gas pipelines. They used sunflower oil as a cheap and environmentally friendly resource for synthesizing phosphorylated waterborne polyurea/urethane (Ph-WPUU). Ph-WPUU significantly decreased the average onset temperature and retarded the induction time of hydrate nucleation. In addition, a foam-like methane-propane hydrates and the constant value of torque were observed in the presence of Ph-WPUU, which is a sign of AA property of the inhibitor. Moreover, Ph-WPUU effectively prevented corrosion of mild steel by 96% protection at 0.07 wt % concentration. Besides, the quantum chemical study showed that the triglyceride group of Ph-WPUU structure acted as an active site to interact with the surface of steel. Their results provide a bio-based strategy to design a single polymeric molecule to prevent both gas hydrate formation and corrosion. The uncertainties of temperature and pressure measurements were 0.1 ºC and 0.005 MPa, respectively.

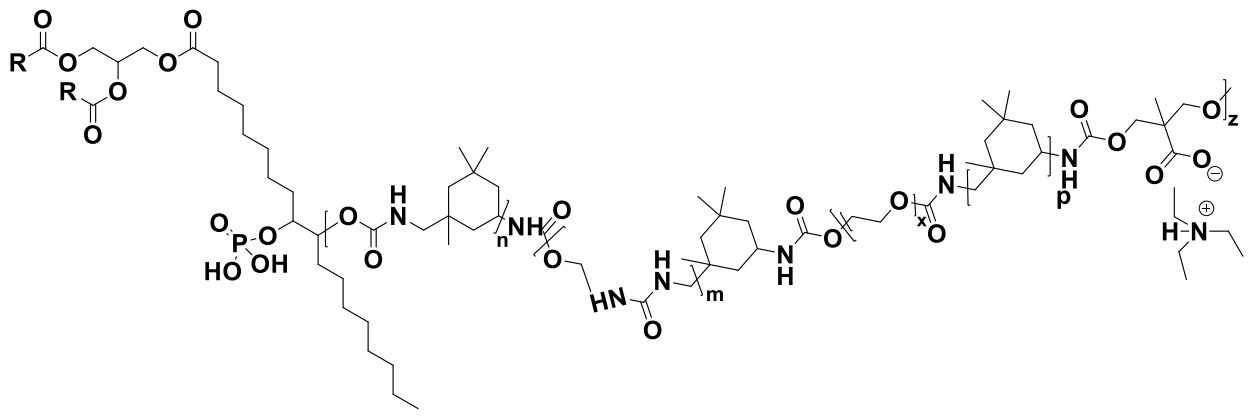

Fig. 44. Molecular structure of Ph-WPUU [3]

The inhibition effect of porcine pancreatic lipase on THF hydrate formation was investigated by Saikia et al [224]. Pancreatic lipase worked as good KHI and AA even at 0.1 wt % it showed better inhibition efficiency than PVP. The induction time was increased beyond 1440 minutes at 1.0 wt % of the inhibitor. Additionally, the

inhibitor effectively suppressed the "memory effect". Moreover, the authors reported that the inhibitor has some anti-agglomeration properties and can be used as synergists for PVP. In addition, the concentration of pancreatic lipase had a minimal effect on the rheological characteristics of the drilling fluid. They suggested that pancreatic lipase inhibited THF hydrate formation by adsorbing to the surface of hydrate crystals. Idress et al. [89] reported cassava peel as natural KHI for the inhibition of CH_4 hydrate formation. Cassava peel delayed the induction times at 4, 6, 8, and 10 MPa. The inhibition effect of cassava peel was lower than PVP at 4 and 6 MPa while at higher pressures (8 and 10 MPa) performance of the inhibitor was close to the commercial KHI. The presence of hydroxyl groups in cassava peels was confirmed by Fourier transform infrared (FTIR) analysis. Therefore, they proposed that this functional group form hydrogen bonds with water molecules, which prevent hydrates formation. A class of KHIs based on polyaspartamides (Fig. 45) with acceptable biodegradability was developed by Villano et al [273] for natural gas mixture. Polyaspartamides belong to the polypeptide polymer family and contain *N*,*N*-dialkylamides or *N*-alkylamides as pendant groups. KHI with a 3:1 ratio of isobutyl/methyl pendant groups showed the best inhibition effect; however, it was relatively lower than Luvicap 55W. A 14.6 ºC subcooling was obtained in the presence of KHI with isobutyl/methyl groups and induction time increased to 1340 minutes compared to pure water (18 min). The optimum concentration of all polymers was 0.25 wt % and no significant improvement in KHI activity was observed at higher concentrations. KHI with a 3:1 ratio of iBu/Me groups showed more than 20% biodegradability after 28 days according to the OECD306 test protocol.

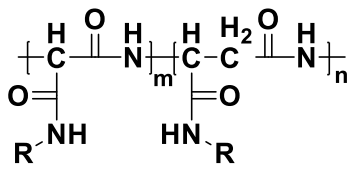

Fig. 45. Molecular structure of polyaspartamides [3]

In another study, a series of polyaspartamides based on L-aspartic acid were synthesized as green KHIs for inhibition of THF hydrate by Wang et al [281]. Their results indicated that polyaspartamide with a longer alkyl side chain (octyl) showed the best inhibition property even more than PVP and PVCap. In addition, a dynamic study of water surrounding the polyaspartamides by NMR relaxometry revealed that the inhibitors tightly bind to water molecules in the hydrate, which resulted in faster transverse relaxation times of the non-freezable water. The quantum chemical simulations also manifested that polyaspartamides-clathrate hydrate interactions were featured through short H-bonding, suggesting extreme destruction and distortion of the clathrate cages. Moreover, a high amount of non-freezable bound water per polyaspartamide repeat unit was obtained. They proposed that polyaspartamide with longer alkyl side chains effectively deforms the hydrate cages, providing better inhibition effect on the THF clathrate hydrate. Magnusson et al. [299] developed a cheap, highly biodegradable, and natural inhibitor, namely KHI530 to prevent natural gas hydrate. The inhibitor efficiently inhibited the formation of gas hydrate in both natural and methane gas systems better than low molecular weight PVP. According to isothermal experiments, gas hydrate did not form for 48h at a subcooling of 6-7 ºC in presence of 0.5 wt % of KHI530 in natural gas system. KHI530 exhibits no cloud point in the solution containing 7 wt % of KHI530 up to 95 ºC in NaCl brines or deionized water. KHI530 was fully compatible at all ratios with mono ethylene glycol (MEG) or methanol and showed a good inhibition effect in combination with MEG. They suggested that KHI530 can be considered as a stand-alone KHI for mild conditions (low subcooling), or can be used to minimize the amount of THI where the pumping capacity of the inhibitor has been reached. The anti-agglomerant activity of the active components extracted from a terrestrial plant fruit was investigated by Wang et al [282]. They extracted n-butanol-soluble, water-soluble, petroleum ether-soluble, and ethyl acetate-soluble portions by prefractionation of the plant fruit. They found that the main effective compounds were present in the ethyl acetate-soluble portion. The results of nuclear

magnetic resonance and high-resolution mass spectrum analyses confirmed that 5-(4-hydroxy-6, 7-dimethoxy-3-methylchroman-2-yl) benzene-1,2,3-triol, apigenin, eriodictyol, naringenin, and luteolin were the effective compounds for inhibition of agglomeration of gas hydrate (Fig. 46). Their results indicated that apigenin and luteolin had better AA activity than other components.

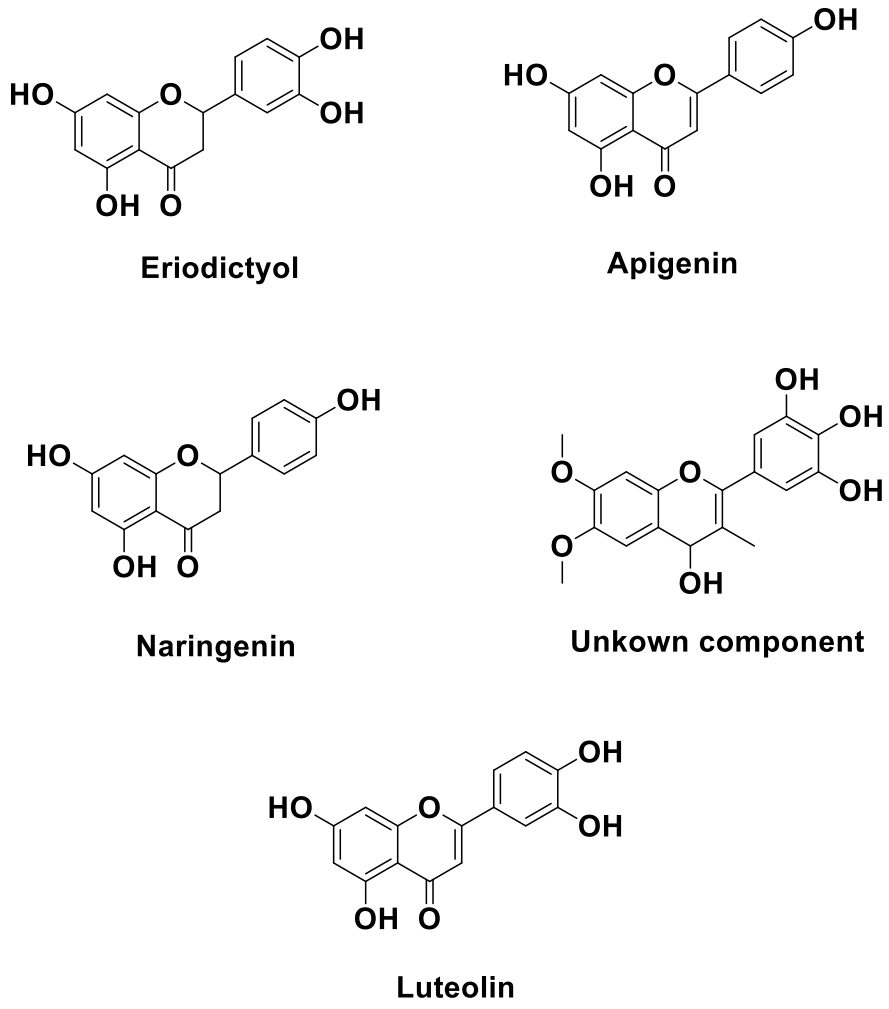

Fig. 46. Molecular structure of the main compounds in terrestrial plant fruit [3]

Elechi et al. [47] reported a laboratory evaluation of the caricaceae plant as a green gas hydrate inhibitor using a mini flow loop. Their results revealed that caricaceae plant worked better than MEG at 0.01–0.05 wt %. The inhibitor showed a maximum inhibition efficiency of 83.3%, while the efficiency value for MEG was 73.6%. In small doses, the inhibition effect of the caricaceae plant was better than MEG. The optimum concentration of caricaceae plant for desirable inhibition effect

was 0.02 wt %. Kiran et al. [122] reported natural biopowders, such as Piper betel (betel), Nelumbo nucifera (Indian lotus), and Azadirachta indica (neem), as green KHIs for CH_4 hydrate formation at 0.5 wt %. Although all investigated compounds worked as efficient THI, once the nucleation occurred, they promoted gas hydrate formation. Neem leaf showed the best result among all bio powders, followed by betel leaf. Indeed, the main inhibition effect of bio powders on CH_4 hydrate formation was detected in the nucleation step. Safranine O was introduced as a green KHI by Liu et al [144] that 0.1 wt % of the inhibitor can completely prevent CH_4 hydrate formation at a subcooling of 7.7 ºC. In both complete inhibition and slow growth regions, 0.5 wt % safranine O showed higher inhibition power than 0.5 wt % PVCap. They suggested that safranine O could be a promising substitute for KHIs in the oil and gas industries as it has a good inhibition effect, acceptable economic efficiency, and high biodegradability. The uncertainties of pressure and temperature measurements were 0.01 MPa and 0.01 ºC, respectively. Soussana et al. [250] explored the inhibition mechanism of safranine O (47) on the growth of single crystal THF hydrate using microfluidics coupled with cold stages and fluorescence microscopy. They clarified that a supramolecular lamella formed in safranine O solution, binding to the surface of THF hydrate through ordered water molecules near its methyl and amine groups, similar to some antifreeze proteins, and preventing further hydrate growth. They suggested that safranine O has a behavior similar to some antifreeze proteins.

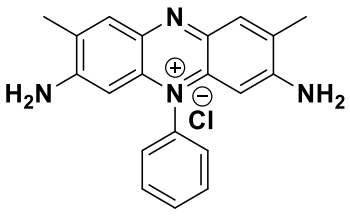

Fig. 47. Molecular structure of safranine O [3]

Magnusson et al. [155] investigated a natural polymer product under the cipher KHI530 as green KHI. The biocide THPS (tetrahydroxymethylphosphonium sulfate) was used to reduce the biodegradability of this polymer during storage,

which extended the shelf life of the product to 9 months at 22 ºC versus a few days without biocide and did not affect its KHI activity. It was shown that for synthetic natural gas and methane, the inhibition performance of KHI530 was better or comparable to PVP with a molecular weight of 8 kDa at 3.3 MPa. Wachikwu-Elechi and Ikiensikimama [275] introduced Musaceae Extract PSJ as green KHI. Their results showed that PSJ worked better than MEG at 2-5 wt %. The extract showed the best inhibition efficiency at 3 wt %. PSJ is available commercially and can be considered as effective hydrate inhibitor. Pavelyev et al. [184] developed a new class of KHIs based on water-soluble polyurethanes that showed a good inhibition effect on steel corrosion. Some of the synthesized inhibitors presented higher biodegradability than those of Luvicap 55W even without fragments of natural compounds in their composition (Fig. 48). Their results demonstrated that by increasing the hydrophobicity of the substituent at the nitrogen atom of diethanolamine, corrosion and hydrate formation inhibiting effects increase. In the case of inhibitors with N-butyl substituents, their effectiveness becomes comparable to Luvicap 55W (hydrate formation) and Armohib CI-28 (corrosion). However, in terms of biodegradation, the tert-butyl fragment was preferable to the n-butyl one.

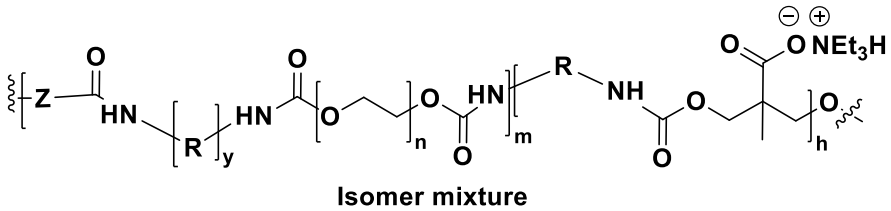

WPU-1 - Z = monoethanolamine (1x)
WPU-2 - Z = N-methyldiethanolamine (1x)
WPU-3 - Z = N-butyldiethanolamine (1x)
WPU-4 - Z = N-tert-butyldiethanolamine (1x)
WPU-5 - Z = N-methyldiethanolamine (2.5x)
WPU-6 - Z = N-butyldiethanolamine (2.5x)
WPU-7 - Z = N-tert-butyldiethanolamine (2.5x)

Z = Monoethanolamine or N-substituted diethanolamine

R=

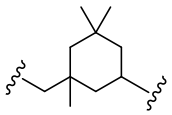

Fig. 48. Chemical structure of biodegradable water-soluble polyurethanes [3]

9. Experimental apparatus for testing of KHIs

Different experimental equipment in order to test and rank of KHIs have developed from laboratory scale to pilot scale. The stirred reactor, autoclave, (micro) differential scanning calorimetry (DSC or μ- DSC), rocking cell, batch or semi-batch crystallizers, pipe wheel, automated lag time apparatus (HPALTA), and flow loop are the most common apparatus for evaluating performance of KHIs. The goal of the research and quality of data collection are the most important factors in choosing the appropriate device. Autoclaves, stirred reactors and crystallizers are widely used in studies of gas hydrates because the agitation strength is easily adjustable and pressure and temperature can be monitored. When sampling and adding ingredients are required during the hydrate formation process the semi-batch crystallizers or autoclaves are a good option. Using the titanium and stainless steel for building the apparatus cell results in a variety of designs of the cell geometry, inner volume and pressure grading. Providing the high pressure and window to directly observe the hydrate formation process are the outstanding advantages of sapphire cells. Nowadays, there are commercial equipment with several sapphire or steel cells, which are especially beneficial for investigating AAs are now available. This leads to the multiple results in the same experimental conditions with good reproducibility and reliability. Rocking cells are particularly useful for fast screening of KHI under continuous cooling by monitoring the temperatures of hydrate formation. Compared to other types of equipment, HP-micro DSC and HPALTA needs small sample volumes (~1 mL or less), so that the sample form hydrates and then could be dissociated repeatably. The sample transparency reflected by the passing light beam in ALTA and the heat transfer measured by DSC leads to accurate and reliable diagnosis of the starting point of hydrate formation. The hydrate equilibrium cells are another class of high-pressure cell that generally gives visual observation through sapphire windows. Sealed glass ampules are less usual cells for studding the hydrate formation. They can operate collectively with NMR spectroscopy and can be used to assess the performance of selected KHIs.

Constant-cooling experiments using rocking cells have become a standard method for evaluating and ranking different gas hydrate inhibitors. Rocking cells are high-pressure apparatuses that allow for the first stage laboratory screening of KHIs. They have overtaken the use of stirred autoclaves as the preferred method for these experiments. Rocking cells offer several advantages, including more reliable statistical data about hydrate inhibition and the ability to vary different parameters to assess KHI performance. In constant-cooling experiments, the cooling rate is an important parameter to consider. The rate at which the temperature is decreased affects the formation and growth of gas hydrates. The cooling rate can be adjusted in rocking cells to study its impact on KHI performance. Constant-cooling experiments using rocking cells are a widely employed method for evaluating and ranking the performance of KHIs. The primary goal of these experiments is to assess the effectiveness of different KHIs in preventing or delaying gas hydrate formation under controlled conditions. Here's a detailed explanation of how these experiments are conducted:

1. Preparation of the rocking cell: The rocking cell is a high-pressure vessel equipped with a rocking mechanism that ensures constant agitation and mixing of the contents. The cell is thoroughly cleaned and filled with a known volume of the test fluid, which typically consists of water, hydrocarbon gas, and the KHI under investigation.

2. Pressurization: The rocking cell is pressurized with the hydrocarbon gas to a predetermined pressure, usually ranging from a few hundred to several thousand psi, depending on the desired testing conditions.

3. Constant cooling: Once the desired pressure is reached, the rocking cell is subjected to a constant cooling rate, typically ranging from 0.5°C/h to 2 ºC/h. The temperature is monitored continuously using a temperature sensor or thermocouple placed inside the cell.

4. Detection of hydrate formation: As the temperature decreases, the conditions inside the rocking cell eventually reach the hydrate formation region. The

onset of hydrate formation is typically detected by a sudden temperature increase or a visual observation of hydrate crystals.

5. Determination of KHI performance: The performance of the KHI is evaluated based on the degree of subcooling achieved before hydrate formation occurs. Subcooling is the difference between the temperature at which hydrate formation occurs in the presence of the KHI and the temperature at which hydrate formation occurs in the absence of the KHI (i.e., in pure water). A higher degree of subcooling indicates better KHI performance.

6. Comparison and ranking: By conducting constant-cooling experiments with different KHIs under identical conditions, researchers can compare their performance and rank them based on their ability to inhibit hydrate formation.

The hydrate onset temperature (T_o) refers to the temperature at which hydrates start to form under specific pressure conditions [1]. KHIs significantly influence the kinetics of hydrate formation by retarding the hydrate crystal nucleation and growth, which effectively prevents hydrates from forming even below their theoretical T_o [2]. This delay establishes a safety zone known as subcooling, allowing the system to operate without hydrate formation, even under thermodynamically favorable conditions [2,3]. The effectiveness of a KHI is measured by the subcooling temperature (ΔT), representing the difference between the system's temperature and its equilibrium hydrate formation temperature [4,5]. In other words, ΔT quantifies how much the temperature can drop below the equilibrium point without actual crystal appearance. Higher ΔT values show a greater inhibition potential [6,7]. In rocking cell experiments, pressure exhibited a linear decline attributable to gas consumption during cooling from 18.5 ºC to -0.5 ºC. T_o was identified at the point where pressure deviated from this linear trend, marking the sII hydrate nucleation and growth. Fig. 49 illustrates typical constant cooling tests for pure water and WPU-DBuA solution to determine induction time, T_o, and ΔT. As seen in Fig. 49, hydrate formation occurred after 7 hours in pure water, resulting in a low ΔT of 5.3 ºC. This indicates rapid sII hydrate formation in the absence of the inhibitor. In

contrast, the induction time increased to 18 hours with the addition of 0.5 wt % WPU-DBuA, providing a high ΔT of 15.6 ºC for the system.

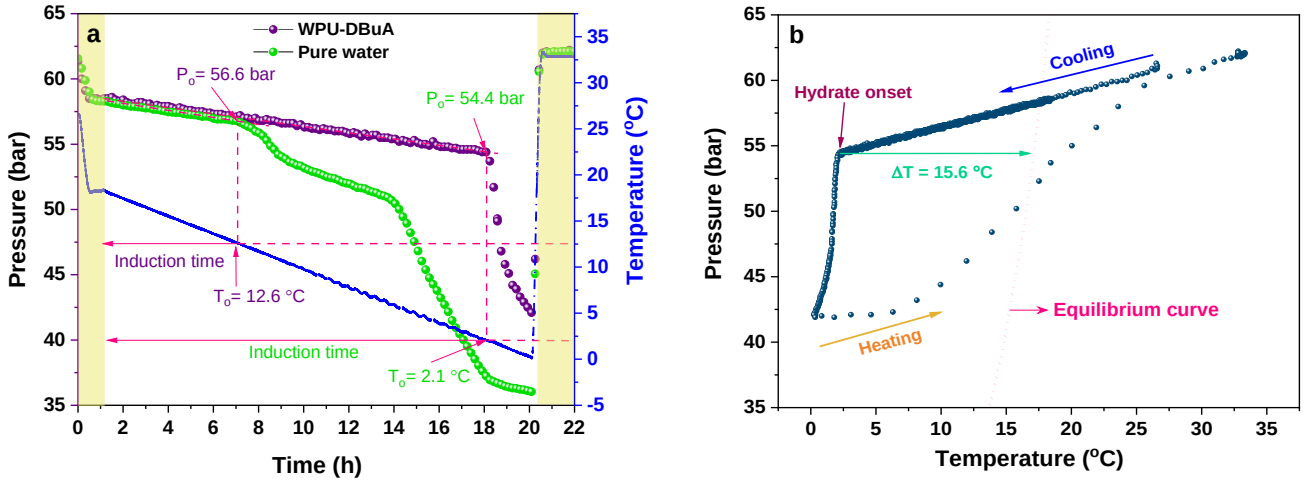

Fig. 49. Example of constant cooling test for pure water and WPU-DBuA solution (0.5 wt %). The color-filled signify pressure-temperature conditions where gas hydrates are not thermodynamically stable, while the white area aligns with the hydrate stability zone where gas hydrates can form (a). Typical pressure-temperature curve for the determination of ΔT (b) [67]

Conclusion

This report presents a systematic and comprehensive view of testing of bioresources such as ionic liquids, carbohydrate polymers, vegetable oils, amino acids, protein, and peptides as potential kinetic hydrate inhibitors since 1993. Over 270 bio-based KHIs with different gas hydrate formers were reviewed. Fruit pectin extracts are the only naturally occurring polymers that have been claimed to perform better than commercial KHI; however, further research is required to validate these findings and determine the specific composition of the extracts. A biodegradable polymer as backbone with grafted caprolactam groups looks to be one of the ideal green KHIs available when required. Polyglutamates and a naturally occurring protein-based product are two others biodegradable KHIs. In the long run, it could be feasible to develop and manufacture a powerful protein-based KHI utilizing biotechnology; however, this is presently not economically feasible due to the manufacturing costs and the scale of the KHI market. The following prospects and recommendations can be useful to illuminate the future research direction to develop efficient green KHIs.

- Most natural polymers do not have a good inhibitory function in their pure form. Therefore, they should be functionalized with active monomers to inhibit gas hydrate, and then the biodegradability of the modified polymer should also be investigated.
- Natural polymers should be hydrolyzed to reduce their molecular weight, modified with active groups in hydrate inhibition, and their inhibitory performance on the formation of gas hydrates should be investigated.
- The effect of mixed biodegradable KHIs, such as amino acids-ionic liquids, amino acids-natural polymers, ionic liquids-natural polymers, protein-ionic liquids, and their synergy with commercial KHIs on gas hydrate formation should be studied.

- Investigation of the effect of salt, water cut, and hydrocarbons on the inhibition performance of various green KHIs to simulate the real conditions of pipelines and gas fields is required.
- The inhibitory activity of green KHIs is mainly evaluated in the presence of CH_4 and CO_2 gases. More studies should be performed on natural gas systems as sII hydrate is the most common type of hydrate in pipelines.
- The effect of green KHIs on CO_2 and H_2S corrosion should be studied because some of them may have a dual inhibitory role on hydrate and corrosion, which can greatly reduce operating costs.
- The inhibition power of ionic liquids on gas hydrate formation is excellent, yet its cost limits their industrial application compared to the conventional THIs and KHIs. New synthesis methods in milder conditions should be developed for synthesis based on available materials.
- Extraction, synthesis, and modification methods of natural polymers are difficult and multi-stage; thus, simpler methods with few steps should be developed.
- Limited simulation studies have been conducted to determine the mechanism of action of green KHIs. More molecular simulation studies are needed in the face of green inhibitors under different conditions to clarify their exact inhibition mechanism. They indicate the effect of different functional groups on nucleation and hydrate growth processes.
- The source of some natural polymers varies in seasons, affecting their molecular weight and structure. More detailed studies should be carried out on different sources of natural polymers to detect the source with the highest inhibitory power.
- Some amino acids and ionic liquids significantly affect the gas hydrate formation, depending on their concentration. More research should be

performed to determine their concentration as promoters or inhibitors.

- Most studies evaluated thermodynamic inhibitory properties of ionic liquids, while their role in the kinetics of hydrate formation in different conditions should be considered in more detail.
- AFPs should be produced on a large scale as their inhibition power are sometimes close to commercial KHIs under specific conditions.

References

1. Abrahamsen E., Kelland M. A. Comparison of kinetic hydrate inhibitor performance on structure I and structure II hydrate-forming gases for a range of polymer classes // Energy & Fuels. 2018. № 1 (32). C. 342–351.

2. Aghajanloo M. [и др.]. Kinetics of methane+ hydrogen sulfide clathrate hydrate formation in the presence/absence of poly N-vinyl pyrrolidone (PVP) and L-tyrosine: Experimental study and modeling of the induction time // Chemical Engineering Science. 2022. (250). C. 117384.

3. Al-Adel S. [и др.]. The effect of biological and polymeric inhibitors on methane gas hydrate growth kinetics // Fluid Phase Equilibria. 2008. № 1 (267). C. 92–98.

4. Altamash T. [и др.]. Gas hydrates inhibition via combined biomolecules and synergistic materials at wide process conditions // Journal of Natural Gas Science and Engineering. 2017. (46). C. 873–883.

5. Altamash T. [и др.]. Cost-effective alkylammonium formate-based protic ionic liquids for methane hydrate inhibition // Journal of Natural Gas Science and Engineering. 2018. (58). C. 59–68.

6. Anselme M. J. [и др.]. A method for inhibiting gas hydrate formation // WO1993025798A1. 1993. (93). C. 25798.

7. Asiri A. M. Nanotechnology-based industrial applications of ionic liquids / A. M. Asiri, Springer, 2020.

8. Baghban A. [и др.]. Phase equilibrium modeling of semi-clathrate hydrates of seven commonly gases in the presence of TBAB ionic liquid promoter based on a low parameter connectionist technique // The Journal of supercritical fluids. 2015. (101). C. 184–192.

9. Bagherzadeh S. A. [и др.]. Why ice-binding type I antifreeze protein acts as a gas hydrate crystal inhibitor // Physical Chemistry Chemical Physics. 2015. № 15 (17). C. 9984–9990.

10. Barrett G. Chemistry and biochemistry of the amino acids / G. Barrett, Springer Science & Business Media, 2012.

11. Bavoh C. B. [и др.]. COSMO-RS: An ionic liquid prescreening tool for gas hydrate mitigation // Chinese journal of chemical engineering. 2016. № 11 (24). C. 1619–1624.

12. Bavoh C. B. [и др.]. Methane hydrate-liquid-vapour-equilibrium phase condition measurements in the presence of natural amino acids // Journal of Natural Gas Science and Engineering. 2017. (37). C. 425–434.

13. Bavoh C. B. [и др.]. Inhibition effect of amino acids on carbon dioxide hydrate // Chemical Engineering Science. 2017. (171). C. 331–339.

14. Bavoh C. B. [и др.]. The impact of amino acids on methane hydrate phase boundary and formation kinetics // The Journal of Chemical Thermodynamics. 2018. (117). C. 48–53.

15. Bavoh C. B. [и др.]. New methane hydrate phase boundary data in the presence of aqueous amino acids // Fluid Phase Equilibria. 2018. (478). C. 129–133.

16. Bavoh C. B. [и др.]. Combined inhibition effect of 1-ethyl-3-methy-limidazolium chloride+ glycine on methane hydrate IOP Publishing, 2018.C. 12060.

17. Bavoh C. B. [и др.]. Ionic liquids as gas hydrate thermodynamic inhibitors // Industrial & Engineering Chemistry Research. 2021. № 44 (60). C. 15835–15873.

18. Bharathi A. [и др.]. Experimental and modeling studies on enhancing the thermodynamic hydrate inhibition performance of monoethylene glycol via synergistic green material // Scientific reports. 2021. № 1 (11). C. 1–10.

19. Bubalo M. C. [и др.]. Toxicity mechanisms of ionic liquids // Arhiv za higijenu rada i toksikologiju. 2017. № 3 (68). C. 171–179.

20. Burla S. K., Tulluru B., Prasad P. S. R. Collective Impact of Amino Acids on Clathrate Hydrates of the CO2+ CH4 Gas Mixture // Energy & Fuels. 2022. № 18 (36). C. 10618–10626.

21. Carroll J. Natural Gas Hydrates: A Guide for Engineers / J. Carroll, 2014.

22. Castillo-Borja F., Bravo-Sánchez U. I. Molecular Dynamics simulation study of the performance of different inhibitors for methane hydrate growth // Journal of Molecular Liquids. 2021. (337). C. 116510.

23. Chen B. [и др.]. The thermodynamic inhibition study of two biological osmoprotectants on methane hydrate // The Journal of Chemical Thermodynamics. 2021. (166). C. 106671.

24. Chen C. [и др.]. The roles of functional groups of antifreeze protein in inhibition of hydrate growth // Fuel. 2022. (327). C. 125060.

25. Chen Q. [и др.]. Effect of 1-butyl-3-methylimidazolium tetrafluoroborate on the formation rate of CO2 hydrate // Journal of natural gas chemistry. 2008. № 3 (17). C. 264–267.

26. Chen Z. [и др.]. Novel core–shell and recyclable gas hydrate promoter for efficient solidified natural gas storage // Energy Conversion and Management. 2024. (301). C. 118059.

27. Chigozirim O. C., Taiwo A., Ajienka J. A. Potency of starch in hydrate inhibition in a field within Gulf of Guinea Using Aspen Hysys // Global Journal of Engineering and Technology Advances. 2021. № 1 (7). C. 91–102.

28. Chua P. C. [и др.]. Dual kinetic hydrate inhibition and scale inhibition by polyaspartamides // Energy Fuels. 2011. № 11 (25). C. 5165–5172.

29. Cole R. A., Grinrod A., Cely A. Kinetic hydrate inhibitors with pendent amino functionality // 2017.

30. Cruz-Torres A., Romero-Martínez A., Galano A. Computational Study on the Antifreeze Glycoproteins as Inhibitors of Clathrate-Hydrate Formation // ChemPhysChem. 2008. № 11 (9). C. 1630–1635.

31. Daraboina N. [и др.]. Natural Gas Hydrate Formation and Decomposition in the Presence of Kinetic Inhibitors. 3. Structural and Compositional Changes // Energy Fuels. 2011. № 10 (25). C. 4398–4404.

32. Daraboina N. [и др.]. Natural Gas Hydrate Formation and Decomposition in the Presence of Kinetic Inhibitors. 1. High Pressure Calorimetry // Energy Fuels. 2011. № 10 (25). C. 4392–4397.

33. Daraboina N. [и др.]. Natural Gas Hydrate Formation and Decomposition in the Presence of Kinetic Inhibitors . 2 . Stirred Reactor Experiments // Energy Fuels. 2011. (25). C. 4384–4391.

34. Daraboina N. [и др.]. Assessing the performance of commercial and biological gas hydrate inhibitors using nuclear magnetic resonance microscopy and a stirred autoclave // Fuel. 2013. (105). C. 630–635.

35. Daraboina N., Malmos Perfeldt C., Solms N. von Testing antifreeze protein from the longhorn beetle Rhagium mordax as a kinetic gas hydrate inhibitor using a high-pressure micro differential scanning calorimeter // Canadian Journal of Chemistry. 2015. № 9 (93). C. 1025–1030.

36. Das S. [и др.]. Experimental evaluation of Sarcosine as an eco-friendly green hydrate inhibitor for the drilling of gas hydrate bearing formations // Journal of Petroleum Science and Engineering. 2021. C. 109764.

37. Davi Éber Sánches de Menezes, Pedro de Alcântara Pessôa Filho M. D. R. F. Use of 1-butyl-3-methylimidazolium-based ionic liquids as methane hydrate inhibitors at high pressure conditions // Chemical Engineering Science. 2020. (212). C. 115323.

38. Davies P. L. [и др.]. Structure and function of antifreeze proteins // Philosophical Transactions of the Royal Society of London. Series B: Biological Sciences. 2002. № 1423 (357). C. 927–935.

39. Davies P. L., Hew C. L. Biochemistry of fish antifreeze proteins // The FASEB Journal. 1990. № 8 (4). C. 2460–2468.

40. Dirdal E. G., Kelland M. A. Alternative Lactam-Based Kinetic Hydrate Inhibitors─ Investigation of Polymers of 2-Methacrylamido-caprolactam // Energy & Fuels. 2022. № 6 (36). C. 3107–3118.

41. Dirdal E., Kelland M. A. Synthesis and Investigation of Polymers of 2-Methacrylamido-caprolactam as Kinetic Hydrate Inhibitors // Energy Fuels. 2020. № 6 (34). C. 6981–6990.

42. Dong Lee J., Wu H., Englezos P. Cationic starches as gas hydrate kinetic inhibitors // Chemical Engineering Science. 2007. № 23 (62). C. 6548–6555.

43. Dong S., Li M., Firoozabadi A. Effect of salt and water cuts on hydrate anti-agglomeration in a gas condensate system at high pressure // Fuel. 2017. № June (210). C. 713–720.

44. Duman J. G., Devries A. L. Freezing resistance in winter flounder Pseudopleuronectes americanus // Nature. 1974. № 5438 (247). C. 237–238.

45. Effendi A. D. [и др.]. Investigation on esterified pectin as natural hydrate inhibitor on methane hydrate formation // Journal of Petroleum Exploration and Production Technology. 2022. C. 1–17.

46. Effendi A. D. [и др.]. Polysaccharides from Tamarindus indica L. as natural kinetic hydrates inhibitor at high subcooling environment // Journal of Petroleum Exploration and Production Technology.

2022. C. 1–12.

47. Elechi V. U. [и др.]. Laboratory evaluation of caricaceae plant as a locally sourced surfactant for gas hydrate inhibition in a laboratory mini flow loop // Applied Petrochemical Research. 2021. № 3 (11). C. 295–303.

48. Fakhreeva A. V [и др.]. Carboxymethylcellulose sodium salt–effective “green” regent for management of calcium carbonate crystallization and nat-ural gas hydrate formation IOP Publishing, 2019.C. 12050.

49. Farhadian A. [и др.]. Accelerated methane hydrate formation by ethylene diamine tetraacetamide as an efficient promoter for methane storage without foam formation // Industrial & Engineering Chemistry Research. 2019. № 19 (58). C. 7752–7760.

50. Farhadian A. [и др.]. Waterborne Polyurethanes as a New and Promising Class of Kinetic Inhibitors for Methane Hydrate Formation // Scientific Reports. 2019. № 1 (9). C. 9797.

51. Farhadian A. [и др.]. A new class of promising biodegradable kinetic/anti-agglomerant methane hydrate inhibitors based on castor oil // Chemical Engineering Science. 2019. (206). C. 507–517.

52. Farhadian A. [и др.]. Waterborne polymers as kinetic/anti-agglomerant methane hydrate and corrosion inhibitors: a new and promising strategy for flow assurance // Journal of Natural Gas Science and Engineering. 2020. (77). C. 103235.

53. Farhadian A. [и др.]. Toward a bio-based hybrid inhibition of gas hydrate and corrosion for flow assurance // Energy. 2020. (210). C. 118549.

54. Farhadian A. [и др.]. Sulfonated chitosan as green and high cloud point kinetic methane hydrate and corrosion inhibitor: Experimental and theoretical studies // Carbohydrate Polymers. 2020. (236). C. 116035.

55. Farhadian A. [и др.]. Dual-Function Synergists Based on Glucose and Sucrose for Gas Hydrate and Corrosion Inhibition // Energy & Fuels. 2020. № 11 (34). C. 13717–13727.

56. Farhadian A. [и др.]. Inhibition Performance of Chitosan- graft-Polyacrylamide as an Environmentally Friendly and High-Cloud-Point Inhibitor of Nucleation and Growth of Methane Hydrate // Crystal Growth and Design. 2020. № 3 (20). C. 1771–1778.

57. Farhadian A. [и др.]. Renewable biosurfactants for energy-efficient storage of methane: An experimental and computational investigation // Chemical Engineering Journal. 2021. (427). C. 131723.

58. Farhadian A. [и др.]. Gas Hydrate and Corrosion Inhibition Performance of the Newly Synthesized Polyurethanes: Potential Dual Function Inhibitors // Energy & Fuels. 2021. № 7 (35). C. 6113–6124.

59. Farhadian A. [и др.]. Efficient dual-function inhibitors for prevention of gas hydrate formation and CO2/H2S corrosion inside oil and gas pipelines // Chemical Engineering Journal. 2021. (431). C. 134098.

60. Farhadian A. [и др.]. Reconsideration of the micellization theory: Promotion or inhibition of gas hydrate formation for gas storage and flow assurance applications // Chemical Engineering Journal. 2022. (427). C. 131852.

61. Farhadian A. [и др.]. Simultaneous inhibition of natural gas hydrate formation and CO2/H2S corrosion for flow assurance inside the oil and gas pipelines // Energy. 2023. (269). C. 126797.

62. Farhadian A. [и др.]. Promising kinetic gas hydrate inhibitors for developing sour gas reservoirs // Energy. 2023. (282). C. 128979.

63. Farhadian A. [и др.]. Enhanced methane hydrate formation using a newly synthesized biosurfactant: Application to solidified gas storage // Energy. 2024. (291). C. 130290.

64. Feng C. [и др.]. Well-defined graft copolymers: from controlled synthesis to multipurpose applications // Chemical Society Reviews. 2011. № 3 (40). C. 1282–1295.

65. Feustel D. L. M. Use of pyroglutamic acid esters as gas hydrate inhibitors with improved biodegradability // WO2007054226A1. 2007. № 12.

66. Fu W. [и др.]. Methane hydrate formation in a water-continuous vertical flow loop with xanthan gum // Fuel. 2020. (265). C. 116963.

67. Gnezdilov D. [и др.]. Effective prevention of structure II gas hydrate formation using the newly synthesized kinetic inhibitors // Chemical Engineering Science. 2024. (292). C. 119986.

68. Go W. [и др.]. Dipeptides as environmentally friendly CH4 hydrate inhibitors: Experimental and computational approaches // Fuel. 2022. (329). C. 125479.

69. Gong Y. [и др.]. Urea as a Green Thermodynamic Inhibitor of sII Gas Hydrates // Chemical

Engineering Journal. 2021. (429). C. 132386.

70. Gonzáles R. R., Djuve J. Hydrate Inhibitors // International (PCT) Patent No. WO2010101477A1. 2010.

71. Gordienko R. [и др.]. Towards a green hydrate inhibitor: imaging antifreeze proteins on clathrates // PLoS One. 2010. № 2 (5). C. e8953.

72. Graether S. P. [и др.]. Structure of type I antifreeze protein and mutants in supercooled water // Biophysical Journal. 2001. № 3 (81). C. 1677–1683.

73. Gronwald W. [и др.]. NMR characterization of side chain flexibility and backbone structure in the type I antifreeze protein at near freezing temperatures // Biochemistry. 1996. № 51 (35). C. 16698–16704.

74. Gupta P., Sakthivel S., Sangwai J. S. Effect of aromatic/aliphatic based ionic liquids on the phase behavior of methane hydrates: Experiments and modeling // The Journal of Chemical Thermodynamics. 2018. (117). C. 9–20.

75. Gupta P., Sangwai J. S. Formation and dissociation kinetics of methane hydrate in aqueous oilfield polymer solutions (polyacrylamide, xanthan gum, and guar gum) and their performance evaluation as low-dosage kinetic hydrate inhibitors (LDHI) // Energy & Fuels. 2019. № 7 (33). C. 6335–6349.

76. Han S. [и др.]. Efficacy of antifreeze proteins from Clupea harangues and Anarhichas minor on gas hydrate inhibition via cell surface display // Chemical Engineering Science. 2020. (215). C. 115470.

77. Haq I. U., Lal B., Zaini D. B. Experimental and modelling study of ammonium based ionic liquids in the absence and presence of methanol for CO2 hydrates // Journal of Molecular Liquids. 2022. (349). C. 118214.

78. Hearle J. W. S. A critical review of the structural mechanics of wool and hair fibres // International Journal of Biological Macromolecules. 2000. № 2 (27). C. 123–138.

79. Hertanto A., Chongwei X. Dual function gas hydrate inhibitors // WO2009114674A1. 2009.

80. Hew C. L. [и др.]. Presence of cystine-containing antifreeze proteins in the spruce bud worm, Choristoneura fumiferana // Canadian Journal of Zoology. 1983. № 10 (61). C. 2324–2328.

81. Hew C. L. [и др.]. Antifreeze polypeptides from the Newfoundland ocean pout, Macrozoarces americanus: presence of multiple and compositionally diverse components // Journal of Comparative Physiology B. 1984. № 1 (155). C. 81–88.

82. Hew C. L., Yang D. S. C. Protein interaction with ice // European Journal of Biochemistry. 1992. № 1-2 (203). C. 33–42.

83. Hew C.-L., Yip C. The synthesis of freezing-point-depressing protein of the winter flounder Pseudopleuronectusamericanus in Xenpuslaevis oocytes // Biochemical and Biophysical Research Communications. 1976. № 3 (71). C. 845–850.

84. Holt S., Thomaides J. S. Hybrid mixtures for gas hydrate inhibition applications // WO2012089654A1. 2011.

85. Hu S., Koh C. A. CH4/C2H6 gas hydrate interparticle interactions in the presence of anti-agglomerants and salinity // Fuel. 2020. (269). C. 117208.

86. Hu Y., Wang S., He Y. Interaction of amino acid functional group with water molecule on methane hydrate growth // Journal of Natural Gas Science and Engineering. 2021. (93). C. 104066.

87. Hussain H. H., Husin H. The effect of synergistic amino acids-ionic liquids in methane hydrate inhibition by COSMO-RS application // Journal of Molecular Liquids. 2021. (321). C. 114837.

88. Idress M. [и др.]. Preliminary study of natural polymer as kinetic hydrate inhibitor // Materials Today: Proceedings. 2018. № 10 (5). C. 21667–21671.

89. Idress M. [и др.]. Experimental Investigation of Methane Hydrate Induction Time in the Presence of Cassava Peel as a Hydrate Inhibitor // Energies. 2019. № 12 (12). C. 2314.

90. Ikada Y., Tsuji H. Biodegradable polyesters for medical and ecological applications // Macromolecular rapid communications. 2000. № 3 (21). C. 117–132.

91. Ishmuratov F. G. [и др.]. New “Green” polysaccharidal inhibitor of gas hydrate formation on the basis of carboxymethylcellulose sodium salt // Russian Journal of Applied Chemistry. 2018. № 4 (91). C. 653–656.

92. Ivall J. Investigations into the effects of xylomannan-based sugar compounds on methane hydrate kinetics // Master thesis. 2013.

93. Jensen L. [и др.]. Inhibition of methane hydrate formation by ice-structuring proteins // Industrial & Engineering Chemistry Research. 2010. № 4 (49). С. 1486–1492.

94. Jia Y. [и др.]. Biodegradable Organics as a Multisystem-Compatible Low-Dose Green Kinetic Hydrate Inhibitor // ACS Sustainable Chemistry & Engineering. 2022.

95. Jokandan E. F., Naeiji P., Varaminian F. The synergism of the binary and ternary solutions of polyethylene glycol, polyacrylamide and Hydroxyethyl cellulose to methane hydrate kinetic inhibitor // Journal of Natural Gas Science and Engineering. 2016. (29). С. 15–20.

96. Jordan A., Gathergood N. Biodegradation of ionic liquids–a critical review // Chemical Society Reviews. 2015. № 22 (44). С. 8200–8237.

97. Kamal M. S. [и др.]. Application of various water soluble polymers in gas hydrate inhibition // Renewable and Sustainable Energy Reviews. 2016. (60). С. 206–225.

98. Kang S.-P. [и др.]. Unusual synergy effect on methane hydrate inhibition when ionic liquid meets polymer // RSC Advances. 2013. № 43 (3). С. 19920.

99. Kang S.-P., Jung T., Lee J.-W. Macroscopic and spectroscopic identifications of the synergetic inhibition of an ionic liquid on hydrate formations // Chemical Engineering Science. 2016. (143). С. 270–275.

100. Kannan K., Punase A. D. Low-dosage, high-efficiency, and environment-friendly inhibitors: a new horizon in gas hydrates mitigation in production systems OnePetro, 2009.

101. Kazemi F. [и др.]. Experimental study and thermodynamic modeling of the stability conditions of methane clathrate hydrate in the presence of TEACl and/or BMIM-BF4 in aqueous solution // The Journal of Chemical Thermodynamics. 2019. (130). С. 95–103.

102. Kelland M. Additives for inhibiting gas hydrate formation // WO2008023989A1. 2008. С. 1557–1623.

103. Kelland M. A. History of the Development of Low Dosage Hydrate Inhibitors // Energy & Fuels. 2006. № 3 (20). С. 825–847.

104. Kelland M. A. Production chemicals for the oil and gas industry / M. A. Kelland, CRC press, 2014.

105. Kelland M. A. A Review of Kinetic Hydrate Inhibitors from an Environmental Perspective // Energy Fuels. 2018. № 12 (32). С. 12001–12012.

106. Kelland M. A. Challenges with gas hydrate formation IOP Publishing, 2019.С. 12057.

107. Kelland M. A. [и др.]. 5-Methyl-3-vinyl-2-oxazolidinone–Investigations of a New Monomer for Kinetic Hydrate Inhibitor Polymers // Energy & Fuels. 2022. № 5 (36). С. 2609–2615.

108. Kelland M. A. [и др.]. N-Vinyl Caprolactam/Maleic-Based Copolymers as Kinetic Hydrate Inhibitors: The Effect of Internal Hydrogen Bonding // Energy & Fuels. 2022. № 6 (36). С. 3088–3096.

109. Kelland M. A., Dirdal E. G., Zhang Q. High Cloud Point Polyvinylaminals as Non-Amide-Based Kinetic Gas Hydrate Inhibitors // Energy Fuels. 2020. № 7 (34). С. 8301–8307.

110. Kelland M. A., Zhang Q., Chua P. C. A study of natural proteins and partially hydrolyzed derivatives as green kinetic hydrate inhibitors // Energy & Fuels. 2018. № 9 (32). С. 9349–9357.

111. Keshavarz L. [и др.]. Experimental measurement and thermodynamic modeling of methane hydrate dissociation conditions in the presence of aqueous solution of ionic liquid // Fluid Phase Equilibria. 2013. (354). С. 312–318.

112. Keshavarz L., Ghaani M. R., English N. J. Thermodynamic evaluation of inhibitors for methane-hydrate formation // Fuel. 2022. (324). С. 124672.

113. Khan M. S. [и др.]. Experimental evaluation of a novel thermodynamic inhibitor for CH4 and CO2 hydrates // Procedia engineering. 2016. (148). С. 932–940.

114. Khan M. S. [и др.]. Thermodynamic effect of ammonium based ionic liquids on CO2 hydrates phase boundary // Journal of molecular liquids. 2017. (238). С. 533–539.

115. Khan M. S. [и др.]. Influence of tetramethylammonium hydroxide on methane and carbon dioxide gas hydrate phase equilibrium conditions // Fluid Phase Equilibria. 2017. (440). С. 1–8.

116. Khan M. S. [и др.]. Impacts of ammonium based ionic liquids alkyl chain on thermodynamic hydrate inhibition for carbon dioxide rich binary gas // Journal of Molecular Liquids. 2018. (261). С. 283–290.

117. Khan M. S. [и др.]. Experimental evaluation and thermodynamic modelling of AILs alkyl chain elongation on methane riched gas hydrate system // Fluid phase equilibria. 2018. (473). С. 300–309.

118. Khan M. S. [и др.]. Ammonium hydroxide ILs as dual-functional gas hydrate inhibitors for

binary mixed gas (carbon dioxide and methane) hydrates // Journal of Molecular Liquids. 2019. (274). C. 33–44.

119. Khan M. S. [и др.]. Tetramethyl ammonium chloride as dual functional inhibitor for methane and carbon dioxide hydrates // Fuel. 2019. (236). C. 251–263.

120. Kim K., Cho S.-G., Sa J.-H. Natural Hydrophilic Amino Acids as Environment-Friendly Gas Hydrate Inhibitors for Carbon Capture and Sequestration // ACS Sustainable Chemistry & Engineering. 2021. № 51 (9). C. 17413–17419.

121. Kim K., Kang J. W., Kang S. Tuning ionic liquids for hydrate inhibition // Chemical Communications. 2011. № 22 (47). C. 6341.

122. Kiran B. S., Prasad P. S. R. Inhibition of methane hydrates using biodegradable additives // ACS omega. 2021. № 12 (6). C. 8261–8270.

123. Koh C. A. [и др.]. Fundamentals and Applications of Gas Hydrates // Annual Review of Chemical and Biomolecular Engineering. 2011. № 1 (2). C. 237–257.

124. Koh C. A., Sloan E., Sum A. Natural Gas Hydrates in Flow Assurance / C. A. Koh, E. Sloan, A. Sum, Gulf Professional Publishing, 2011.

125. Lal B., Nashed O. Chemical Additives for Gas Hydrates / B. Lal, O. Nashed, 2020.

126. Lal B., Qasim A., Shariff A. M. Ionic Liquids in Flow Assurance / B. Lal, A. Qasim, A. M. Shariff, Springer, 2020.

127. Lee D. [и др.]. Recoverable and recyclable gas hydrate inhibitors based on magnetic nanoparticle-decorated metal–organic frameworks // Chemical Engineering Journal. 2020. (401). C. 126081.

128. Lee D. [и др.]. Inhibition synergism of glycine (an amino acid) and [BMIM][BF4](an ionic liquid) on the growth of CH4 hydrate // Chemical Engineering Journal. 2020. (393). C. 124466.

129. Lee D. [и др.]. Thermodynamic inhibition effects of an ionic liquid (choline chloride), a naturally derived substance (urea), and their mixture (deep eutectic solvent) on CH4 hydrates // Chemical Engineering Journal. 2020. (399). C. 125830.

130. Lee D., Go W., Seo Y. Experimental and computational investigation of methane hydrate inhibition in the presence of amino acids and ionic liquids // Energy. 2019. (182). C. 632–640.

131. Lee D., Go W., Seo Y. Synergistic kinetic inhibition of amino acids and ionic liquids on CH4 hydrate for flow assurance // Fuel. 2020. (263). C. 116689.

132. Lee W. [и др.]. Inhibition effect of ionic liquids and their mixtures with poly (N-vinylcaprolactam) on methane hydrate formation // Journal of Industrial and Engineering Chemistry. 2016. (38). C. 211–216.

133. Lee W. [и др.]. Kinetic promotion and inhibition of methane hydrate formation by morpholinium ionic liquids with chloride and tetrafluoroborate anions // Energy & Fuels. 2016. № 5 (30). C. 3879–3885.

134. Lee W. [и др.]. Synergetic effect of ionic liquids on the kinetic inhibition performance of poly (N-vinylcaprolactam) for natural gas hydrate formation // Energy & Fuels. 2016. № 11 (30). C. 9162–9169.

135. Leinweber D., Feustel M. Use of Polyesters in the Form of Gas Hydrate Inhibitors // 2008.

136. Leinweber D., Feustel M. Polymers and their production and use as gas hydrate inhibitors // 2011.

137. Leinweber D., Roesch A., Feustel M. Use of substituted polyethyleneimines as gas hydrate inhibitors with improved biodegradability // 2009.

138. Li B., Lu Y.-Y., Li Y.-L. A Review of Natural Gas Hydrate Formation with Amino Acids // Journal of Marine Science and Engineering. 2022. (10). C. 1134.

139. Li S. [и др.]. Design of alanine-rich short peptides as a green alternative of gas hydrate inhibitors: dual methyl group docking for efficient adsorption on the surface of gas hydrates // ACS Sustainable Chemistry & Engineering. 2020. № 10 (8). C. 4256–4266.

140. Li X.-S. [и др.]. Equilibrium hydrate formation conditions for the mixtures of CO2+ H2+ tetrabutyl ammonium bromide // Journal of chemical & engineering data. 2010. № 6 (55). C. 2180–2184.

141. Li X.-S. [и др.]. Equilibrium hydrate formation conditions for the mixtures of methane+ ionic liquids+ water // Journal of Chemical & Engineering Data. 2011. № 1 (56). C. 119–123.

142. Li Z. [и др.]. The Study on the Relationship Between the Molecular Structures of Chitosan Derivatives and Their Hydrate Inhibition Performance // Journal of Molecular Liquids. 2022. C. 120007.

143. Lin F.-H. [и др.]. Structural modeling of snow flea antifreeze protein // Biophysical journal. 2007. № 5 (92). С. 1717–1723.

144. Liu Y. [и др.]. Safranine o, an acid-resistant and environmentally friendly kinetic hydrate inhibitor // International Conference on Applied Energy. 2019.

145. Liu Y. [и др.]. Experimental study on the gas hydrates blockage and evaluation of kinetic inhibitors using a fully visual rocking cell // Journal of Natural Gas Science and Engineering. 2021. (96). С. 104331.

146. Liu Z. [и др.]. Hydrate slurry flow characteristics influenced by formation, agglomeration and deposition in a fully visual flow loop // Fuel. 2020. (277). С. 118066.

147. Long Z. [и др.]. Experimental study of methane hydrate equilibria in [EMIM]-NO3 aqueous solutions // Journal of Chemical & Engineering Data. 2015. № 9 (60). С. 2728–2732.

148. Long Z. [и др.]. Phase behavior of methane hydrate in the presence of imidazolium ionic liquids and their mixtures // Fluid Phase Equilibria. 2017. (439). С. 1–8.

149. Long Z. [и др.]. Performance of mixture of ethylene glycol and glycine in inhibiting methane hydrate formation // Journal of Natural Gas Science and Engineering. 2018. (56). С. 134–140.

150. Long Z. [и др.]. Kinetic inhibition performance of N-vinyl caprolactam/isopropylacrylamide copolymers on methane hydrate formation // Energy. 2022. (242). С. 123056.

151. Longinos S. N., Longinou D. D. Examination of different amino acids as methane-propane gas hydrate kinetic inhibitors in upstream industry // 13th Panhellenic Scientific Conference of Chemical Engineering Patras. 2022.

152. Lu Y. [и др.]. Atomistic insights into the performance of thermodynamic inhibitors in the nucleation of methane hydrate // Chemical Engineering Journal. 2021. (431). С. 133479.

153. Lubec G., Rosenthal G. A. Amino acids: chemistry, biology and medicine / G. Lubec, G. A. Rosenthal, Springer Science & Business Media, 2012.

154. Maddah M., Maddah M., Peyvandi K. Molecular dynamics simulation of methane hydrate formation in presence and absence of amino acid inhibitors // Journal of Molecular Liquids. 2018. (269). С. 721–732.

155. Magnusson C. [и др.]. As green as it gets: An abundant kinetic hydrate inhibitor from nature // Energy & fuels. 2018. № 5 (32). С. 5772–5778.

156. Mannar N. [и др.]. Thermophysical properties of aqueous lysine and its inhibition influence on methane and carbon dioxide hydrate phase boundary condition // Fluid Phase Equilibria. 2017. (454). С. 57–63.

157. Masri A. N., Sulaimon A. A. Amino acid-based ionic liquids as dual kinetic-thermodynamic methane hydrate inhibitor // Journal of Molecular Liquids. 2022. (349). С. 118481.

158. Maximilian A., Karin N., Axel S. Grafted polymers as gas hydrate inhibitors // US6867262B1. 2000.

159. Mehrabi K. [и др.]. Thermodynamic modeling of clathrate hydrate stability conditions in the presence of amino acid aqueous solution // Journal of Molecular Liquids. 2020. (313). С. 113488.

160. Mokhatab S., Wilkens R. J., Leontaritis K. J. A review of strategies for solving gas-hydrate problems in subsea pipelines // Energy Sources, Part A. 2007. № 1 (29). С. 39–45.

161. Monica F. Della, Kleij A. W. From terpenes to sustainable and functional polymers // Polymer Chemistry. 2020. № 32 (11). С. 5109–5127.

162. Morris H. R. [и др.]. Antifreeze glycoproteins from the blood of an antarctic fish. The structure of the proline-containing glycopeptides. // Journal of Biological Chemistry. 1978. № 14 (253). С. 5155–5162.

163. Moujdin I. A. [и др.]. Dual-functional gas hydrate inhibition of tetramethylammonium chloride for carbon dioxide-methane mixed gas systems // Fuel. 2021. (305). С. 121598.

164. Mu L. [и др.]. Inhibition of methane hydrate nucleation and growth by an antifreeze protein // Journal of Petroleum Science and Engineering. 2019. (183). С. 106388.

165. Mu L., Solms N. von Inhibition of natural gas hydrate in the system containing salts and crude oil // Journal of Petroleum Science and Engineering. 2020. (188). С. 106940.

166. Musa O. M., Lei C. Degradable polymer compositions and uses thereof // WO2010114761A1. 2010. С. International Patent Application WO/2010/114761.

167. Myran D. [и др.]. Genetically-engineered mutant antifreeze proteins provide insight into hydrate inhibition 2011.

168. Naeiji P., Arjomandi A., Varaminian F. Amino acids as kinetic inhibitors for tetrahydrofuran hydrate formation: experimental study and kinetic modeling // Journal of Natural Gas Science and Engineering. 2014. (21). C. 64–70.

169. Nakarit C. [и др.]. Cationic kinetic hydrate inhibitors and the effect on performance of incorporating cationic monomers into N-vinyl lactam copolymers // Chemical Engineering Science. 2013. (102). C. 424–431.

170. Nashed O. [и др.]. Experimental and modelling studies on thermodynamic methane hydrate inhibition in the presence of ionic liquids // Journal of Molecular Liquids. 2018. (249). C. 886–891.

171. Nashed O. [и др.]. Mean induction time and isothermal kinetic analysis of methane hydrate formation in water and imidazolium based ionic liquid solutions // The Journal of Chemical Thermodynamics. 2018. (117). C. 147–154.

172. Nasir Q., Suleman H., Elsheikh Y. A. A review on the role and impact of various additives as promoters/inhibitors for gas hydrate formation // Journal of Natural Gas Science and Engineering. 2020. (76). C. 103211.

173. Nazari K., Ahmadi A. N. A thermodynamic study of methane hydrate formation in the presence of (Bmim)(BF4) and (Bmim)(MS) ionic liqiuids ICGH, 2011.

174. Nazari K., Moradi M. R., Ahmadi A. N. Kinetic Modeling of Methane Hydrate Formation in the Presence of Low-Dosage Water-Soluble Ionic Liquids // Chemical Engineering & Technology. 2013. № 11 (36). C. 1915–1923.

175. Nelson J. S., Grande T. C., Wilson M. V. H. Fishes of the World / J. S. Nelson, T. C. Grande, M. V. H. Wilson, John Wiley & Sons, 2016.

176. Nguyen T. P. [и др.]. Silk fibroin-based biomaterials for biomedical applications: a review // Polymers. 2019. № 12 (11). C. 1933.

177. Ning F. [и др.]. The kinetic effects of hydrate anti-agglomerants/surfactants // Fuel. 2022. (318). C. 123566.

178. Noh H.-J. [и др.]. Fused aromatic networks as a new class of gas hydrate inhibitors // Chemical Engineering Journal. 2021. C. 133691.

179. Ohno H. [и др.]. Interaction of antifreeze proteins with hydrocarbon hydrates // Chemistry - A European Journal. 2010. № 34 (16). C. 10409–10417.

180. Omidvar M. [и др.]. Development of Highly Efficient Dual-Purpose Gas Hydrate and Corrosion Inhibitors for Flow Assurance Application: An Experimental and Computational Study // Energy & Fuels. 2023. № 2 (37). C. 1006–1021.

181. Partoon B. [и др.]. A study on thermodynamics effect of [EMIM]-Cl and [OH-C2MIM]-Cl on methane hydrate equilibrium line // Fluid Phase Equilibria. 2013. (337). C. 26–31.

182. Patil D. R. [и др.]. Method of making graft copolymers from sodium poly (aspartate) and the resulting graft copolymer // US20090326165A1. 2008.

183. Patterson J. L., Duman J. G. Purification and composition of protein antifreezes with high cysteine contents from larvae of the beetle, Tenebrio molitor // Journal of Experimental Zoology. 1982. № 3 (219). C. 381–384.

184. Pavelyev R. S. [и др.]. Performance of Waterborne Polyurethanes in Inhibition of Gas Hydrate Formation and Corrosion: Influence of Hydrophobic Fragments // Molecules. 2020. № 23 (25). C. 5664.

185. Pavelyev R. S. [и др.]. Dual Promotion–Inhibition Effects of Novel Ethylenediaminetetraacetic Acid Bisamides on Methane Hydrate Formation for Gas Storage and Flow Assurance Applications // Energy & Fuels. 2022. № 1 (36). C. 290–297.

186. Peng X. [и др.]. Separation of ionic liquids from dilute aqueous solutions using the method based on CO2 hydrates // Journal of natural gas chemistry. 2010. № 1 (19). C. 81–85.

187. Perfeldt C. M. [и др.]. Inhibition of gas hydrate nucleation and growth: efficacy of an antifreeze protein from the longhorn beetle Rhagium mordax // Energy & fuels. 2014. № 6 (28). C. 3666–3672.

188. Perrin A., Musa O. M., Steed J. W. The chemistry of low dosage clathrate hydrate inhibitors // Chemical Society Reviews. 2013. № 5 (42). C. 1996–2015.

189. Pham T. P. T., Cho C.-W., Yun Y.-S. Environmental fate and toxicity of ionic liquids: a review // Water research. 2010. № 2 (44). C. 352–372.

190. Qasim A. [и др.]. A perspective on dual purpose gas hydrate and corrosion inhibitors for

flow assurance // Journal of Petroleum Science and Engineering. 2019. (183). C. 106418–106440.

191. Qin H.-B. [и др.]. Evaluation of whey protein as a natural hydrate kinetic inhibitor // Journal of Molecular Liquids. 2019. (277). C. 490–498.

192. Qureshi M. F. [и др.]. Gas Hydrate Prevention and Flow Assurance by Using Mixtures of Ionic Liquids and Synergent Compounds: Combined Kinetics and Thermodynamic Approach // Energy Fuels. 2016. № 4 (30). C. 3541–3548.

193. Qureshi M. F., Khraisheh M., Almomani F. Doping amino acids with classical gas hydrate inhibitors to facilitate the hydrate inhibition effect at low dosages // Greenhouse Gases: Science and Technology. 2020. № 4 (10). C. 783–794.

194. Qureshi M. F., Khraisheh M., AlMomani F. Experimentally measured methane hydrate phase equilibria and ionic liquids inhibition performance in Qatar's seawater // Scientific Reports. 2020. № 1 (10). C. 1–14.

195. Rad S. A. [и др.]. Kinetic study of amino acids inhibition potential of glycine and l-leucine on the ethane hydrate formation // Journal of Natural Gas Science and Engineering. 2015. (26). C. 819–826.

196. Ralf W. [и др.]. Process for preparing graft polymers // WO2007051742A1. 2007.

197. Rasool M. H. [и др.]. A Deep Eutectic Solvent based novel drilling mud with modified rheology for hydrates inhibition in deep water drilling // Journal of Petroleum Science and Engineering. 2022. (211). C. 110151.

198. Rasoolzadeh A. [и др.]. Experimental study and modeling of methane hydrate formation induction time in the presence of ionic liquids // Journal of Molecular Liquids. 2016. (221). C. 149–155.

199. Rasoolzadeh A. [и др.]. A thermodynamic framework for determination of gas hydrate stability conditions and water activity in ionic liquid aqueous solution // Journal of Molecular Liquids. 2022. (347). C. 118358.

200. Rasoolzadeh A., Javanmardi J., Mohammadi A. H. An experimental study of the synergistic effects of BMIM-BF4, BMIM-DCA and TEACl aqueous solutions on methane hydrate formation // Petroleum Science. 2019. № 2 (16). C. 409–416.

201. Raymond J. A., DeVries A. L. Adsorption inhibition as a mechanism of freezing resistance in polar fishes. // Proceedings of the National Academy of Sciences. 1977. № 6 (74). C. 2589–2593.

202. Rehm B. H. A. Polyester synthases: natural catalysts for plastics // Biochemical Journal. 2003. № 1 (376). C. 15–33.

203. Reichenbach-Klinke R., Karin N. Graft copolymer as a gas hydrate inhibitor // WO2009083377A2. 2008.

204. Reyes F. T. [и др.]. First investigation of the kinetic hydrate inhibitor performance of poly(N-alkylglycine)s // Energy Fuels. 2014. № 11 (28). C. 6889–6896.

205. Reyes F. T. [и др.]. First investigation of the kinetic hydrate inhibition of a series of poly(β-peptoid)s on structure II gas hydrate, including the comparison of block and random copolymers // Energy Fuels. 2015. № 2 (29). C. 695–701.

206. Reyes F. T. [и др.]. Kinetic Hydrate Inhibitors: Structure-Activity Relationship Studies on a Series of Branched Poly(ethylene citramide)s with Varying Lipophilic Groups // Energy Fuels. 2015. № 8 (29). C. 4774–4782.

207. Richard A. R., Adidharma H. The performance of ionic liquids and their mixtures in inhibiting methane hydrate formation // Chemical engineering science. 2013. (87). C. 270–276.

208. Rogers R. D., Seddon K. R. Ionic liquids--solvents of the future? // Science. 2003. № 5646 (302). C. 792–793.

209. Romero-Martínez A. [и др.]. Synthesis and Evaluation of a Pyridinium-Based Ionic Liquid-Type Surfactant as a New Low-Dosage Methane Hydrate Inhibitor // Energy Fuels. 2020. № 8 (34). C. 9243–9251.

210. Roosta H. [и др.]. Inhibition properties of new amino acids for prevention of hydrate formation in carbon dioxide–water system: experimental and modeling investigations // Journal of Molecular Liquids. 2016. (215). C. 656–663.

211. Roosta H. [и др.]. Inhibition and promotion effects of modified HECs and modified starches on the growth rate of hydrate in methane-propane-water system // Journal of Molecular Liquids. 2017. (243). C. 553–563.

212. Roosta H. [и др.]. The dual effect of amino acids on the nucleation and growth rate of gas

hydrate in ethane+ water, methane+ propane+ water and methane+ THF+ water systems // Fuel. 2018. (212). C. 151–161.

213. Roosta H. [и др.]. Effects of chemical modification of PVA by acrylamide, methacrylamide and acrylonitrile on the growth rate of gas hydrate in methane-propane-water system // Journal of molecular liquids. 2018. (253). C. 259–269.

214. Sa J. [и др.]. Hydrophobic amino acids as a new class of kinetic inhibitors for gas hydrate formation // Scientific reports. 2013. C. 1–7.

215. Sa J. H. [и др.]. Gas hydrate inhibition by perturbation of liquid water structure // Scientific Reports. 2015. (5). C. 1–9.

216. Sa J.-H. [и др.]. Amino acids as natural inhibitors for hydrate formation in CO2 sequestration // Environmental science & technology. 2011. № 13 (45). C. 5885–5891.

217. Sa J.-H. [и др.]. Abnormal incorporation of amino acids into the gas hydrate crystal lattice // Physical Chemistry Chemical Physics. 2014. № 48 (16). C. 26730–26734.

218. Sa J.-H. [и др.]. Inhibition of methane and natural gas hydrate formation by altering the structure of water with amino acids // Scientific reports. 2016. (6). C. 31582.

219. Sa J.-H., Sum A. K. Promoting gas hydrate formation with ice-nucleating additives for hydrate-based applications // Applied Energy. 2019. (251). C. 113352.

220. Saberi A. [и др.]. Insights into kinetic inhibition effects of MEG, PVP, and L-tyrosine aqueous solutions on natural gas hydrate formation // Petroleum Science. 2021. № 2 (18). C. 495–508.

221. Sabil K. M. [и др.]. Experimental investigation on the dissociation conditions of methane hydrate in the presence of imidazolium-based ionic liquids // The Journal of Chemical Thermodynamics. 2015. (84). C. 7–13.

222. Sackett C. A. [и др.]. Experimental entanglement of four particles // Nature. 2000. № 6775 (404). C. 256–259.

223. Sadeh E. [и др.]. Branched sulfonated promoter: Achieving high methane uptake and foam-free gas recovery for solidified gas storage // Chemical Engineering Journal. 2024. (487). C. 150674.

224. Saikia T., Mahto V. Experimental investigations of clathrate hydrate inhibition in water based drilling fluid using green inhibitor // Journal of Petroleum Science and Engineering. 2016. (147). C. 647–653.

225. Sanatgar S. M., Peyvandi K. New edible additives as green inhibitors for preventing methane hydrate formation // Journal of Environmental Chemical Engineering. 2019. № 3 (7). C. 103172.

226. Schrag J. D. [и др.]. Primary and secondary structure of antifreeze peptides from arctic and antartic zoarcid fishes // Biochimica et Biophysica Acta (BBA)-Protein Structure and Molecular Enzymology. 1987. № 3 (915). C. 357–370.

227. Scurto A. M., Aki S. N. V. K., Brennecke J. F. Carbon dioxide induced separation of ionic liquids and water // Chemical Communications. 2003. № 5. C. 572–573.

228. Semenov A. P. [и др.]. Dimethyl sulfoxide as a novel thermodynamic inhibitor of carbon dioxide hydrate formation // Chemical Engineering Science. 2022. (255). C. 117670.

229. Shahini M. H., Ramezanzadeh B., Mohammadloo H. E. Recent advances in biopolymers/carbohydrate polymers as effective corrosion inhibitive macro-molecules: A review study from experimental and theoretical views // Journal of Molecular Liquids. 2020. C. 115110.

230. Shao Z. [и др.]. Effects of Modified Cellulose on Methane Hydrate Decomposition: Experiments and Molecular Dynamics Simulations // ACS Sustainable Chemistry & Engineering. 2021. № 29 (9). C. 9689–9697.

231. Sharifi H. [и др.]. Inhibition activity of antifreeze proteins with natural gas hydrates in saline and the light crude oil mimic, heptane // Energy & fuels. 2014. № 6 (28). C. 3712–3717.

232. Sharifi H. [и др.]. Insights into the behavior of biological clathrate hydrate inhibitors in aqueous saline solutions // Crystal Growth and Design. 2014. № 6 (14). C. 2923–2930.

233. Sharifi H., Ripmeester J., Englezos P. Recalcitrance of gas hydrate crystals formed in the presence of kinetic hydrate inhibitors // Journal of Natural Gas Science and Engineering. 2016. (35). C. 1573–1578.

234. Shen X. [и др.]. Kinetic Inhibition of CO2 Hydrate by Carboxymethylcellulose Sodium through Retarded Mass Transfer // Energy & Fuels. 2021. № 22 (35). C. 18615–18622.

235. Shen X., Zhou X., Liang D. Kinetic effects of ionic liquids on methane hydrate // Energy & Fuels. 2019. № 2 (33). C. 1422–1432.

236. Shi L. [и др.]. Effect of dodecyl dimethyl benzyl ammonium chloride on CH4 hydrate growth and agglomeration in oil-water systems // Energy. 2020. (212). C. 118746.

237. Shi L. [и др.]. Anti-agglomeration evaluation and Raman spectroscopic analysis on mixed biosurfactants for preventing CH4 hydrate blockage in n-octane+ water systems // Energy. 2021. (229). C. 120755.

238. Shiflett M. B., Scurto A. M. Ionic liquids: current state and future directions // Ionic Liquids: Current State and Future Directions. 2017. C. 1–13.

239. Silva B. L. L. D. [и др.]. Sodium alginate polymer as a kinetic inhibitor of methane hydrate formation // Journal of Materials Research and Technology. 2021. (12). C. 1999–2010.

240. Silva Ramos A. da [и др.]. Organic salts as kinetic and thermodynamic inhibitors for CO2 hydrate precipitation // Journal of Natural Gas Science and Engineering. 2020. (82). C. 103508.

241. Silva Ramos A. da [и др.]. Synthesis of new CO2 hydrate inhibitors // Journal of Natural Gas Science and Engineering. 2020. (75). C. 103166.

242. Singh A., Suri A. Enhanced Hydrate Inhibition by Plant-Based Polysaccharides as Synergists with Kinetic Hydrate Inhibitors // Energy & Fuels. 2022. № 13 (36). C. 6974–6988.

243. Singh A., Suri A. Enhanced Hydrate Inhibition Using Protein Synergists with Kinetic Hydrate Inhibitors // Energy & Fuels. 2022. № 17 (36). C. 10395–10404.

244. Singh S. K., Savoy A. W. Ionic liquids synthesis and applications: An overview // Journal of Molecular Liquids. 2020. (297). C. 112038.

245. Slaughter D. [и др.]. Antifreeze proteins from the sea raven, Hemitripterus americanus. Further evidence for diversity among fish polypeptide antifreezes. // Journal of Biological Chemistry. 1981. № 4 (256). C. 2022–2026.

246. Sloan E. D., Koh C. A. Clathrate hydrates of natural gases // CRC Press 3rd ed.; CRC Press (Taylor & Francis Group). 2008. T. 87.

247. Sloan Jr E. D. Colorado School of Mines, Golden, CO (United States). Method for controlling clathrate hydrates in fluid systems. 1995.

248. Solms N. von Antifreeze proteins and gas hydrate inhibition Springer, 2020.C. 287–306.

249. Sönnichsen F. D. [и др.]. Refined solution structure of type III antifreeze protein: hydrophobic groups may be involved in the energetics of the protein–ice interaction // Structure. 1996. № 11 (4). C. 1325–1337.

250. Soussana T. N. [и др.]. Adsorption-Inhibition of Clathrate Hydrates by Self-Assembled Nanostructures // ChemPhysChem. 2021. № 21 (22). C. 2182–2189.

251. Sulaimon A. A. [и др.]. Synthesis of dihydrogen phosphate-based ionic liquids: Experimental and COSMO-RS based investigation for methane hydrate inhibition // Journal of Molecular Liquids. 2020. (319). C. 114092.

252. Sulaimon A. A., Tajuddin M. Z. M. Application of COSMO-RS for pre-screening ionic liquids as thermodynamic gas hydrate inhibitor // Fluid Phase Equilibria. 2017. (450). C. 194–199.

253. Sun Q. [и др.]. The investigation of phase equilibria and kinetics of CH4 hydrate in the presence of bio-additives // Fluid Phase Equilibria. 2017. (452). C. 143–147.

254. Sun T., Davies P. L., Walker V. K. Structural basis for the inhibition of gas hydrates by α-helical antifreeze proteins // Biophysical journal. 2015. № 8 (109). C. 1698–1705.

255. Talaghat M. R. Intensification of the performance of kinetic inhibitors in the presence of polyethylene oxide and polypropylene oxide for simple gas hydrate formation in a flow mini-loop apparatus // Fluid phase equilibria. 2010. № 2 (289). C. 129–134.

256. Talaghat M. R. Experimental investigation of gas consumption for simple gas hydrate formation in a recirculation flow mini-loop apparatus in the presence of modified starch as a kinetic inhibitor // Journal of Natural Gas Science and Engineering. 2013. (14). C. 42–48.

257. Talaghat M. R. Enhancement of the performance of modified starch as a kinetic hydrate inhibitor in the presence of polyoxides for simple gas hydrate formation in a flow mini-loop apparatus // Journal of Natural Gas Science and Engineering. 2014. (18). C. 7–12.

258. Talaghat M. R. Experimental investigation of induction time for double gas hydrate formation in the simultaneous presence of the PVP and l-Tyrosine as kinetic inhibitors in a mini flow loop apparatus // Journal of Natural Gas Science and Engineering. 2014. (19). C. 215–220.

259. Tang C. [и др.]. Novel Biosurfactants for Effective Inhibition of Gas Hydrate Agglomeration and Corrosion in Offshore Oil and Gas Pipelines // ACS Sustainable Chemistry & Engineering. 2023. №

1 (11). C. 353–367.

260. Tang C. [и др.]. Environmentally Friendly Antiagglomerants: A Promising Solution for Gas Hydrate Plugging and Corrosion Risk Management in Oil and Gas Pipelines // Energy & Fuels. 2024. № 8 (38). C. 6738–6752.

261. Tang C., Liang D. Inhibitory effects of novel green inhibitors on gas hydrate formation // Chinese Journal of Chemical Engineering. 2019. № 9 (27). C. 2107–2117.

262. Tang C., Zhang Y., Liang D. Investigation into the Inhibition of Methane Hydrate Formation in the Presence of Hydroxy-and Esteryl-Terminated Poly (N-vinylcaprolactam) // Energy & Fuels. 2022. № 7 (36). C. 3848–3856.

263. Tariq M. [и др.]. Gas Hydrate Inhibition: A Review of the Role of Ionic Liquids // Industrial & Engineering Chemistry Research. 2014. № 46 (53). C. 17855–17868.

264. Tariq M. [и др.]. Doubly dual nature of ammonium-based ionic liquids for methane hydrates probed by rocking-rig assembly // RSC advances. 2016. № 28 (6). C. 23827–23836.

265. Tariq M. [и др.]. Experimental and DFT approach on the determination of natural gas hydrate equilibrium with the use of excess N2 and choline chloride ionic liquid as an inhibitor // Energy & Fuels. 2016. № 4 (30). C. 2821–2832.

266. Tumba K. [и др.]. Phase equilibria of methane and carbon dioxide clathrate hydrates in the presence of aqueous solutions of tributylmethylphosphonium methylsulfate ionic liquid // Journal of Chemical & Engineering Data. 2011. № 9 (56). C. 3620–3629.

267. Udegbunam L. U. [и др.]. Phase equilibria, kinetics and morphology of methane hydrate inhibited by antifreeze proteins: application of a novel 3-in-1 method // The Journal of Chemical Thermodynamics. 2018. (117). C. 155–163.

268. Ul Haq I. [и др.]. Ionic liquids for the inhibition of gas hydrates. A review // Environmental Chemistry Letters. 2022. (20). C. 2165–2188.

269. Urbańczyk M. [и др.]. Antifreeze glycopeptides: from structure and activity studies to current approaches in chemical synthesis // Amino Acids. 2017. № 2 (49). C. 209–222.

270. V.A.Dokichev, A.I.Voloshin, N.E.Nifantiev M. P. E., D.R.Kireeva, A.V.Isakov, R.N.Bakhtizin R. U. R. New «green» inhibitors of gas hydrate formation for the oil and gas industry based on polysaccharides // SOCAR Proceedings. 2021. (1). C. 033–040.

271. Vepari C., Kaplan D. L. Silk as a biomaterial // Progress in polymer science. 2007. № 8–9 (32). C. 991–1007.

272. Villano L. Del, Kelland M. A. An investigation into the kinetic hydrate inhibitor properties of two imidazolium-based ionic liquids on Structure II gas hydrate // Chemical Engineering Science. 2010. № 19 (65). C. 5366–5372.

273. Villano L. Del, Kommedal R., Kelland M. A. Class of kinetic hydrate inhibitors with good biodegradability // Energy Fuels. 2008. № 5 (22). C. 3143–3149.

274. Voets I. K. From ice-binding proteins to bio-inspired antifreeze materials // Soft Matter. 2017. № 28 (13). C. 4808–4823.

275. Wachikwu-Elechi V. U., Ikiensikimama S. S., Ajienka J. A. Musaceae Extract PSJ as Green Inhibitors in a Gas Dominated System OnePetro, 2022.

276. Walker V. K. [и др.]. The mysteries of memory effect and its elimination with antifreeze proteins 2008.

277. Walker V. K. [и др.]. Antifreeze proteins as gas hydrate inhibitors // Canadian Journal of Chemistry. 2015. № 8 (93). C. 839–849.

278. Walker V., Ripmeester J., Zeng H. Antifreeze proteins for inhibition of clathrate hydrate formation and reformation // WO2003087532A1. 2003.

279. Wan L., Zhang N., Liang D.-Q. Inhibition effects of polysaccharides for gas hydrate formation in methane–water system // Journal of Molecular Liquids. 2019. (292). C. 111435.

280. Wang J. [и др.]. Mechanisms of synergistic inhibition of hydrophilic amino acids with kinetic inhibitors on hydrate formation // Fuel. 2022. (321). C. 124012.

281. Wang Q. [и др.]. Amphiphilic Optimization Enables Polyaspartamides with Effective Kinetic Inhibition of Tetrahydrofuran Hydrate Formation: Structure–Property Relationships // ACS Sustainable Chemistry & Engineering. 2018. № 10 (6). C. 13532–13542.

282. Wang X.-Q. [и др.]. Hydrate antiagglomeration performance for the active components extracted from a terrestrial plant fruit // Energy & Fuels. 2017. № 1 (31). C. 287–298.

283. Wang Y. [и др.]. Hydrate formation management simulations with anti-agglomerants and thermodynamic inhibitors in a subsea tieback // Fuel. 2019. (252). С. 458–468.

284. Wei Ke M. A. K. Kinetic Hydrate Inhibitor Studies for Gas Hydrate Systems – A Review of Experimental Equipment and Test Methods // Energy Fuels. 2016. № 12 (30). С. 10015–10028.

285. Xiao C., Adidharma H. Dual function inhibitors for methane hydrate // Chemical Engineering Science. 2009. № 7 (64). С. 1522–1527.

286. Xiao C., Wibisono N., Adidharma H. Dialkylimidazolium halide ionic liquids as dual function inhibitors for methane hydrate // Chemical Engineering Science. 2010. № 10 (65). С. 3080–3087.

287. Xu P. [и др.]. Molecular dynamics simulation of methane hydrate growth in the presence of the natural product pectin // The journal of physical chemistry C. 2016. № 10 (120). С. 5392–5397.

288. Xu S. [и др.]. Pectin as an Extraordinary Natural Kinetic Hydrate Inhibitor // Scientific Reports. 2016. (6). С. 23220.

289. Xu S. [и др.]. Excellent synergy effect on preventing CH4 hydrate formation when glycine meets polyvinylcaprolactam // Fuel. 2017. (206). С. 19–26.

290. Xu Y., Yang M., Yang X. Chitosan as green kinetic inhibitors for gas hydrate formation // Journal of Natural Gas Chemistry. 2010. № 4 (19). С. 431–435.

291. Xu Z. [и др.]. Experiment and model investigation of D-sorbitol as a thermodynamic hydrate inhibitor for methane and carbon dioxide hydrates // Journal of Natural Gas Science and Engineering. 2021. (90). С. 103927.

292. Yánez F. [и др.]. New insights for the hydrates detection and non-conventional inhibitors evaluation 2011.С. 17–21.

293. Yang D. S. C. [и др.]. Crystal structure of an antifreeze polypeptide and its mechanistic implications // Nature. 1988. № 6170 (333). С. 232–237.

294. Yaqub S. [и др.]. Investigation of the task oriented dual function inhibitors in gas hydrate inhibition: A review // Fluid Phase Equilibria. 2018. (477). С. 40–57.

295. Yaqub S., Keong L. K. Thermodynamic and kinetic effect of biodegradable polymers on carbondioxide hydrates // Journal of Industrial and Engineering Chemistry. 2019. (79). С. 131–145.

296. Yaqub S., Mohd Shariff A. bin, Mellon N. B. Unraveling the effect of sub-cooling temperatures on the kinetic performance of biopolymers for methane hydrate // Journal of Natural Gas Science and Engineering. 2019. (65). С. 68–81.

297. Yaqub S., Murtaza M., Lal B. Towards a fundamental understanding of biopolymers and their role in gas hydrates: A review // Journal of Natural Gas Science and Engineering. 2021. (91). С. 103892.

298. Yeh Y., Feeney R. E. Antifreeze proteins: structures and mechanisms of function // Chemical reviews. 1996. № 2 (96). С. 601–618.

299. York J. D., Firoozabadi A. Comparing effectiveness of rhamnolipid biosurfactant with a quaternary ammonium salt surfactant for hydrate anti-agglomeration // Journal of Physical Chemistry B. 2008. № 3 (112). С. 845–851.

300. Zaghloul M. Y. M., Zaghloul M. M. Y., Zaghloul M. M. Y. Developments in polyester composite materials–An in-depth review on natural fibres and nano fillers // Composite Structures. 2021. (278). С. 114698.

301. Zare M. [и др.]. Experiment and thermodynamic modeling of methane hydrate equilibria in the presence of aqueous imidazolium-based ionic liquid solutions using electrolyte cubic square well equation of state // Fluid Phase Equilibria. 2013. (341). С. 61–69.

302. Zare M. [и др.]. PC-SAFT/UNIQUAC model assesses formation condition of methane hydrate in the presence of imidazolium-based ionic liquid systems // Fuel. 2020. (266). С. 116757.

303. Zeng H. [и др.]. Antifreeze proteins: Adsorption to ice, silica and gas hydrates 2005.

304. Zeng H. [и др.]. Effect of antifreeze proteins on the nucleaton, growth, and the memory effect during tetrahydrofuran clathrate hydrate formation // Journal of the American Chemical Society. 2006. № 9 (128). С. 2844–2850.

305. Zhang Q. [и др.]. Kinetic Hydrate Inhibition of Glycyl-valine-Based Alternating Peptoids with Tailor-Made N-Substituents // Energy Fuels. 2020. № 4 (34). С. 4849–4854.

306. Zhang Q., Kelland M. A. A new investigation of polymaleamides as kinetic hydrate inhibitors–Improved performance and compatibility with high salinity brines // Chemical Engineering

Science. 2021. (241). C. 116719.

307. Zhang Q., Kelland M. A., Ajiro H. Polyvinylsulfonamides as Kinetic Hydrate Inhibitors // Energy & Fuels. 2020. № 2 (34). C. 2230–2237.

308. Zhang Q., Kelland M. A., Lu H. Non-amide kinetic hydrate inhibitors: A review // Fuel. 2022. (315). C. 123179.

309. Zhang Y. [и др.]. Synthesis of Chitosan Derivatives and Their Inhibition Effects on Methane Hydrates // Energies. 2022. № 7 (15). C. 2675.

310. Zhao X. [и др.]. Experimental investigation on hydrate anti-agglomerant for oil-free systems in the production pipe of marine natural gas hydrates // Energy. 2022. (242). C. 122973.

311. Zhao Y. [и др.]. Synthesis and Application of Magnetically Recyclable Nanoparticles as Hydrate Inhibitors // Chemical Engineering Journal. 2021. (431). C. 133966.

312. Zhou H., Ferreira C. I. Effect of type-III Anti-Freeze Proteins (AFPs) on CO2 hydrate formation rate // Chemical Engineering Science. 2017. (167). C. 42–53.

313. Zohuri G. Polymer science: a comprehensive reference 2012.

314. Zu Khoo Y. [и др.]. Dual inhibition effect of reline deep eutectic solvent on methane hydrate nucleation and formation // Fuel. 2022. (328). C. 125376.